VOL. I | ISSUE 1 | 2018

OSURJ

UNIVERSITY OF OTTAWA SCIENCE UNDERGRADUATE RESEARCH JOURNAL

A BETTER RED

BRIGHTER FLUORESCENT PROTEIN USING SATURATION MUTAGENESIS

PAGE 10

ISSN 2562-2366

VOL. I | ISSUE 1 | 2018

JRSUO

JOURNAL ÉTUDIANT DE RECHERCHE SCIENTIFIQUE DE L'UNIVERSITÉ D'OTTAWA

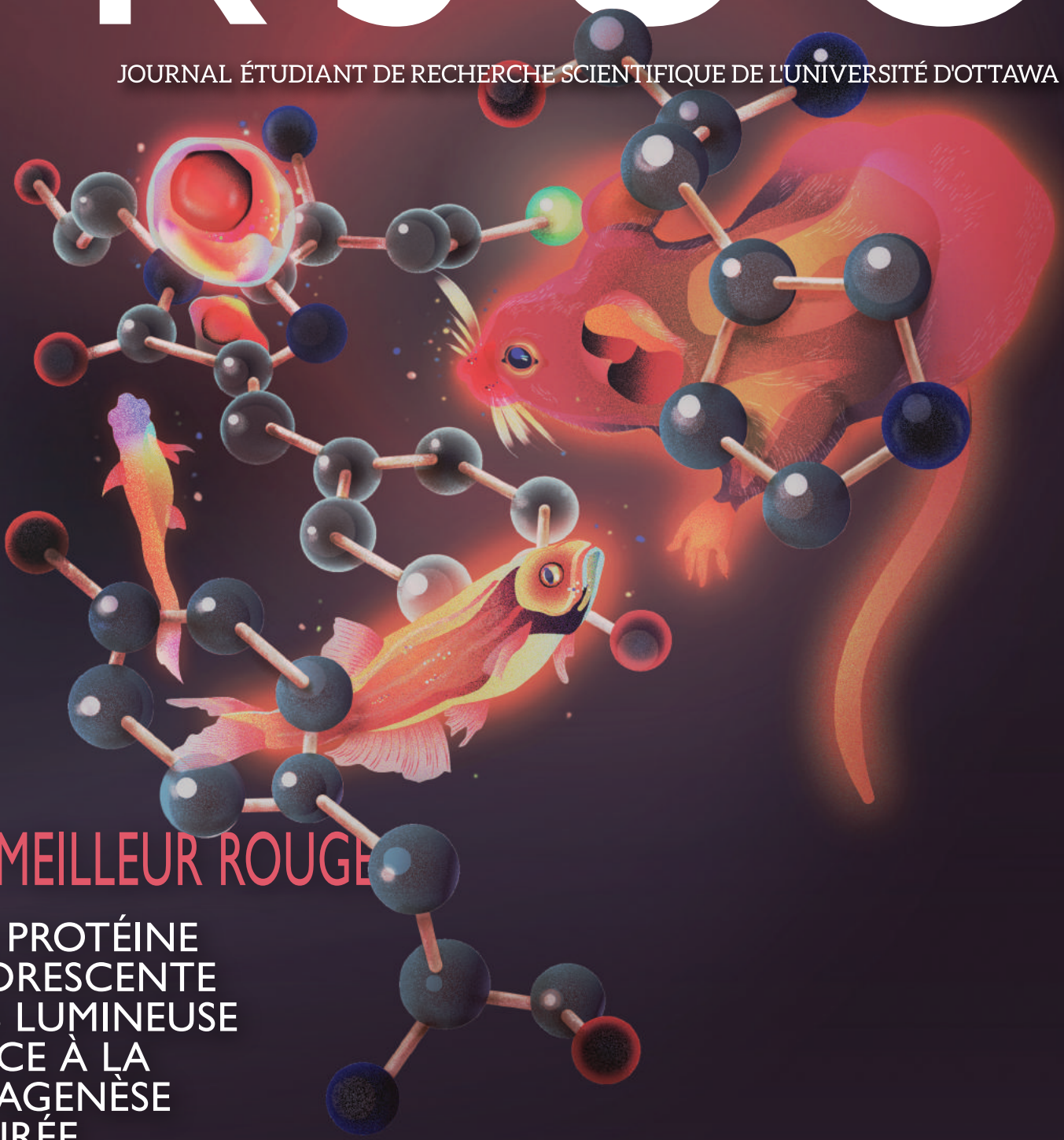

UN MEILLEUR ROUGE

UNE PROTÉINE FLUORESCENTE PLUS LUMINEUSE GRÂCE À LA MUTAGENÈSE SATURÉE

PAGE 10

ISSN 2562-2366

ON THE COVER

Triple-decker circus ring : mRojo-VHSV triple decker motif and immunofluorescent model organisms. Rattus norvegicus, HeLa cells, and Danio rerio can be used as expression systems of red fluorescent protein. The mutant triple decker consists of three motifs : the 63rd histidine (top), the chromophore (middle), and the 197th tyrosine (bottom) residue of the fluorescent protein.

SUR LA COUVERTURE

Anneau de cirque à trois étages : le motif à trois étages de mRojo-VHSV et des organismes modèles d'immunofluorescence. Rattus norvegicus, les cellules HeLa et Danio rerio peuvent être utilisés comme systèmes d'expression de la protéine fluorescente rouge. Le mutant à trois étages est constitué de 3 motifs : la 63ème histidine (en haut), le chromophore (milieu) et le 197ème résidu de tyrosine (en bas) de la protéine fluorescente.

ABOUT THE JOURNAL

About Us

Le journal étudiant de recherche scientifique de l'Université d'Ottawa (JRSUO) est une revue en ligne, académique, bilingue, non-propriétaire, multidisciplinaire et de libre accès qui est publiée et révisée par les étudiants de l'Université d'Ottawa. En plus des comités exécutif et éditorial de premier cycle dédiés, JRSUO collabore aussi avec des étudiants au doctorat, au post-doctorat et des membres de la faculté qui agissent en tant que réviseur(e)s. Ce journal publie en ligne une fois par année scolaire sur une base de publication continuelle ou roulante.

The University of Ottawa Science Undergraduate Research Journal (OSURJ) is an online, open-access, multidisciplinary, non-proprietary, bilingual academic journal that is published and reviewed by University of Ottawa students. In addition to a hardworking undergraduate executive and editorial team, OSURJ also collaborates with post-doctoral, PhD and faculty reviewers as part of a permanent review board. The journal publishes digitally once per academic year on a rolling-publishing basis.

Mission Statement

JRSUO cherche à améliorer l'expérience des étudiants en sciences de premier cycle en fournissant un moyen d'écrire, de réviser et de publier leur recherche dans un format formel et scolaire. Par l'entremise de cette initiative, JRSUO espère inspirer les étudiants de premier cycle de poursuivre de la recherche dans une discipline scientifique, ainsi que les familiariser avec le processus de publication.

OSURJ seeks to enhance the undergraduate science student experience by providing a medium to write, review and publish academic research in a formal scholarly journal format. Through this initiative, OSURJ hopes to inspire undergraduate students to continue pursuing research in the field of science.

Contact Information

Veuillez nous contacter à **osurj@uottawa.ca** si vous avez des questions ou si vous vouliez vous fixer un rendez-vous pour une séance de consultation avec nous. Pour plus de renseignements au sujet des types d'articles acceptés et les directives de soumission, veuillez visiter notre site web à **osurj.ca**.

Please contact us at **osurj@uottawa.ca** if you have any questions or would like to arrange a free consultation session with us. For more information about article types accepted and submission guidelines, please visit our website at **osurj.ca**.

EDITORIAL TEAM

TABLE OF CONTENTS

Scinapse Abstracts

FOREWORD

Dear Readers,

As one of Canada's leading research-intensive institutions and internationally as one of the top 150 universities for research in the world, it is no surprise that uOttawa's students and alumni are involved in groundbreaking research in all subdisciplines of science. Our mandate as the official University of Ottawa's Undergraduate Research Journal is to showcase such research, encourage interdisciplinary communication, and promote critical appraisal of published scientific literature. We hope that this issue inspires more University of Ottawa students to apply their passion for research by writing submitting more articles.

Thus, it is our pleasure to present the inaugural edition of the University of Ottawa Science Undergraduate Research Journal (OSURJ). This issue would not have been possible without the tireless collaboration between our dedicated editorial board and the submitting authors. These selected peer-reviewed articles and abstracts span diverse areas of scientific research, ranging from stationary black holes to the methodology behind increasing red fluorescent protein brightness.

We would like to thank our readers and sponsors for your support and readership.

Sincerely,

David Zheng and **Tanya Yeuchyk**

Editors-in-Chief

AVANT-PROPOS

Cher.e.s lecteur.rice.s,

Étant l'une des principales institutions de recherche intensive du Canada et l'une des 150 meilleures universités dans le monde en matière de recherche, il n'est pas surprenant que les étudiants et les alumni de l'Université d'Ottawa contribuent à la recherche innovatrice dans tous les domaines de la science et du génie. En tant que journal officiel de recherche scientifique de l'Université d'Ottawa, notre mission est de présenter cette même recherche, d'encourager la communication interdisciplinaire et de promouvoir l'analyse critique de la littérature scientifique publiée. Nous espérons que cette édition inspirera encore plus d'étudiants de l'Université d'Ottawa à partager leur passion pour la recherche en soumettant leurs articles.

C'est donc avec plaisir que nous vous présentons la toute première édition du Journal étudiant de recherche scientifique de l'Université d'Ottawa (JRSUO). La création de ce numéro n'aurait jamais été possible sans l'infatigable collaboration de notre très dévoué comité éditorial avec nos auteur.e.s et nos estimés conseillers de la Faculté. Ces articles et résumés de recherche ont été sélectionnés et évalués par les pairs, et ils couvrent une vaste gamme de sujets scientifiques, allant des trous noirs stationnaires à la méthodologie derrière l'augmentation de la luminosité de la protéine rouge fluorescente.

Nous voudrions remercier nos cher.e.s lecteur.rice.s ainsi que nos parrains pour leur soutien et leur lectorat.

Sincèrement,

David Zheng and **Tanya Yeuchyk**

Rédacteurs en chef

ORIGINAL RESEARCH

Increasing the brightness of red fluorescent proteins by saturation mutagenesis

Erin Nguyen[1], Antonia Pandelieva[2] and Roberto A. Chica[1,3*]

Abstract

Red fluorescent proteins (RFPs) are genetically-encoded fluorophores that are widely used for *in vivo* imaging. For all applications of RFPs, brighter variants are desired. Previously, we improved the brightness of mRojoA, a red-shifted mutant of the widely-used RFP mCherry, by designing a triple-decker motif of aromatic rings around its chromophore. This yielded the brighter variant mRojo-VHSV, which contains a triple-decker motif consisting of His and Tyr side chains that pack against the chromophore. This improved chromophore packing resulted in an approximately 3-fold brightness increase at physiological pH. However, the His side chain in the triple-decker motif of mRojo-VHSV adopted a perpendicular arrangement to the other two, which may result in a suboptimal packing arrangement. To further improve chromophore packing in mRojo-VHSV, we performed saturation mutagenesis of residues surrounding its triple-decker motif (positions 62, 97, 165, and 199). Using a microplate fluorescence screening assay, a total of 376 colonies were screened for improved brightness. The brightest mutant found, L199M, was expressed and purified, and its spectral properties were characterized in detail. We found that the quantum yield of this variant was improved by two-fold, resulting in a two-fold brightness increase compared to mRojo-VHSV as well as a 5.3-fold increase in brightness compared to mRojoA. The L199M improved variant is the basis for continued engineering with the goal of further improving the spectral properties of this family of RFPs.

Keywords: Protein engineering; Quantum yield; Bathochromic shift; Library screening; Rational design

Résumé

Les protéines rouges fluorescentes (PRF) sont des fluorophores génétiquement codés qui sont largement utilisés pour l'imagerie *in vivo*. On désire obtenir des variantes plus lumineuses pour toutes les applications des PFR. Auparavant, nous avons amélioré la brillance de mRojoA, un mutant décalé vers le rouge de la PFR populaire mCherry, par la conception d'un motif à trois étages d'anneaux aromatiques autour du chromophore. Le résultat fut une variante plus brillante, mRojo-VHSV, qui contient un motif à trois étages composé de chaînes latérales His et Tyr qui se plaquent contre le chromophore. Cet empaquetage du chromophore amélioré a abouti à une augmentation de luminosité d'environ 3 fois, au pH physiologique. Cependant, la chaîne de His dans le motif à trois étages de mRojo-VHSV a adopté un arrangement perpendiculaire aux deux autres, ce qui peut entraîner un arrangement d'empaquetage sous-optimal. Pour améliorer davantage l'empaquetage du chromophore de mRojo-VHSV, nous avons effectué la mutagenèse de saturation des résidus entourant son motif à trois étages (positions 62, 97, 165 et 199). Afin de cribler pour une luminosité améliorée, nous avons utilisé un essai de fluorescence avec microplaques. Au total, 376 colonies ont été criblées pour une luminosité améliorée. Le mutant le plus brillant, soit L199M, a été exprimé, purifié et caractérisé afin de déterminer ses propriétés spectrales détaillées. Nous avons constaté que le rendement quantique de cette variante est deux fois plus supérieur qu'initialement, résultant en une augmentation de la luminosité de deux fois par rapport à mRojo-VHSV, ainsi que d'une augmentation de la luminosité de 5,3 fois par rapport à mRojoA. La variante L199M améliorée sert comme base pour la poursuite de la recherche qui vise à améliorer davantage les propriétés spectrales de cette famille de PRF.

Mots Clés: Ingénierie des protéines; Rendement quantique; Déplacement bathochrome; Criblage de librairie; Conception rationnelle

Introduction

Red fluorescent proteins (RFPs) are members of the green fluorescent protein (GFP) superfamily of fluorescent proteins that emit light in the red and far-red regions of the visible spectrum (580–680 nm) (*2*). They differ from other members of this superfamily by the presence of an acylimine group conjugated to the standard p-hydroxybenzilideneimidazolinone chromophore of GFP, which extends the size of the chromophore π system, leading to longer emission wavelengths. The longer emission wavelengths of RFPs make them particularly useful for whole-body imaging of research model animals since cells are more transparent to red light (*3*), allowing deep tissue imaging. An additional benefit of the longer emission wavelength of RFPs is its lower energy, which reduces phototoxicity and thereby enables longer experiments (*2*). However, RFPs tend to be less bright than other members of the GFP superfamily (*4*), making it desirable to develop brighter variants through protein engineering.

Previously, we improved the brightness of mRojoA, a red-shifted and dim variant of the widely used monomeric RFP mCherry (*5*), by engineering a triple-decker motif of aromatic rings surrounding its chromophore. This resulted in a variant displaying up to 3-fold increases in brightness: mRojo-VHSV with mutations at position 16 (V), 63 (H), 143 (S) and 163 (V). Notably, the conformation of the side chain of residue His63 located directly above the chromophore resulted in a perpendicular arrangement between its aromatic ring and the phenolate group of the chromophore at a distance consistent with a weak edge-to-face -stacking interaction. (*1*)

Here, our goal was to optimize the triple-decker motif to obtain a parallel arrangement of aromatic rings and maximize packing. We hypothesized that such an arrangement would lead to an increase in the RFP brightness and a bathochromic shift in emission wavelength since it would improve the π-stacking interactions of the chromophore with nearby aromatic residues to further increase its conjugation. (*6*) Optimization of the motif was accomplished by performing saturation mutagenesis of residues S62, M97, L165 and L199, which surround the triple-decker motif in mRojo-VHSV (Figure 1). The brightest mutant found, L199M, displayed a two-fold brightness increase compared to mRojo-VHSV as well as a 5.3-fold increase in brightness compared to mRojoA, which was mostly caused by an improved quantum yield.

Results

Screening of the saturation libraries (Table 1) revealed that positions 62 and 199 are less tolerant to mutations with less than 30% of the variants displaying fluorescence above that of negative control cells containing an empty pET-11a vector. In contrast, approximately 75% of the variants from saturation libraries 97 and 165 were fluorescent, suggesting that these positions are more tolerant to mutation. However, none of the fluorescent mutants displayed a significant red shift in their emission wavelength.

Table 1: Whole cell screening assay results.

	Library[a]			
	S62X	M97X	L165X	L199X
Fluorescent[b]	12	71	70	27
Bright[c]	0	0	1	2

[a]For each library, 94 variants were screened.
[b]Variants displaying a fluorescence intensity greater than 125% that of the negative control.
[c]Variants displaying a fluorescence intensity greater than 125% that of the parent protein, mRojo-VHSV.

Three brighter variants (i.e. fluorescence intensity greater than 125% that of the mRojo-VHSV, the parent protein) were identified from the screening. The brighter mutant from library L165X was found to be L165F, while both brighter variants from the L199X library contained the same mutation (L199M). We characterized the spectral properties of mRojo-VHSV L165F and L199M and compared them with those of the mRojo-VHSV parent RFP (Table 2 and Figure 2).

The mutation L165F conserved the excitation wavelength from its parent protein, but a slight red-shift of 5 nm was observed for the emission wavelength (Figure 2, panel I). This discrepancy with the screening results is likely caused by the lower signal to noise ratio of these whole cell assays versus the *in vitro* assays using purified protein. The extinction coefficient of the L165F mutant decreased by a factor of 1.8 while the quantum yield remained unchanged, resulting in an overall brightness decrease of 1.8-fold. False positives such as this mutation are possible since the screening was done to target variants with increased brightness in whole cells. Such an increase can also be caused by a higher concentration of RFPs in the cells or a more efficient chromophore maturation. By analyzing our computational model, we hypothesize that the presence of the new phenylalanine side chain at position 165 cannot allow the H63 side chain to be in the same conformation because of steric hindrance. Interestingly, the Phe side chain introduced by the L165F mutation is located directly above the His63 side chain, making it possible to form a quadruple-decker motif with the current triple-decker motif (Figure 3). Such a motif has not yet been observed in fluorescent proteins.

The L199M mutation resulted in a 4 nm blue shift of the excitation and emission wavelengths (Figure 2,

*Correspondence: rchica@uottawa.ca
[1] Department of Chemistry and Biomolecular Sciences, University of Ottawa, 10 Marie Curie, K1N 6N5, Ottawa, Canada
Full list of author information is available at the end of the article

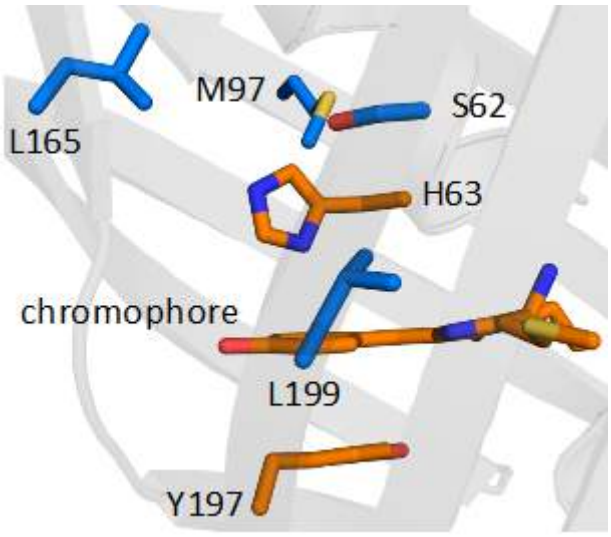

Figure 1: Model of mRojo-VHSV triple decker motif. The motif is formed by, in orange, H63 and Y197 with the chromophore in the middle, and the positions selected for saturation mutagenesis are in blue (S62, M97, L165, and L199). Model is based on PDB ID: 5H87 (*1*)

Table 2: Spectral properties of various RFPs.

RFP	λ_{ex} (nm)	λ_{em} (nm)	ϵ (mM^{-1} cm^{-1})	$\varphi \times 10^{-2}$	Brightness (% mRojo-VHSV)
mRojo-VHSV	592 ± 1	622 ± 2	117 ± 13	4.0 ± 0.4	100
mRojo-VHSV L165F	593 ± 2	627 ± 1	66 ± 8	4.1 ± 0.2	58
mRojo-VHSV L199M	588	618	118	9 ± 1	226
mRojo-VHSV FM	588 ± 1	619 ± 1	66	7.5 ± 0.3	105

Experiments were performed in triplicate (except for mRojo-VHSV L199M) from three independent proteins preparations at a pH of 7.4.

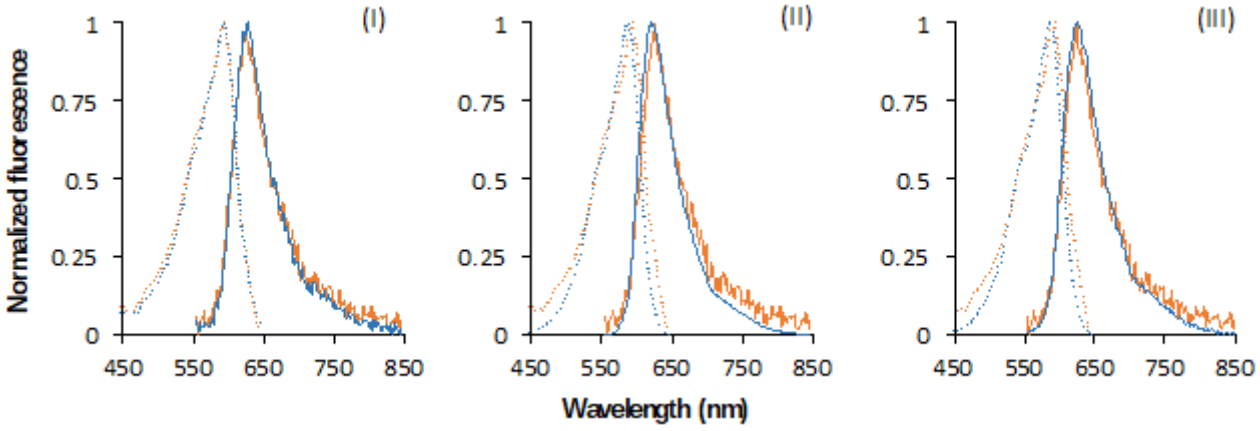

Figure 2: Fluorescence spectra. (I) mRojo-VHSV L165F, (II) mRojo-VHSV L199M, (III) mRojo-VHSV FM. mRojo-VHSV spectra are in orange while those of mutants are in blue. Excitation and emission spectra are represented as dashed and solid lines, respectively.

panel II). Contrary to the L165F mutation, the L199M mutation did not affect the extinction coefficient but increased the quantum yield by 2.3-fold. Because of this, an overall increase in brightness of the same magnitude was observed.

Since the L165F mutation causes an emission wavelength red shift while having the potential to create a

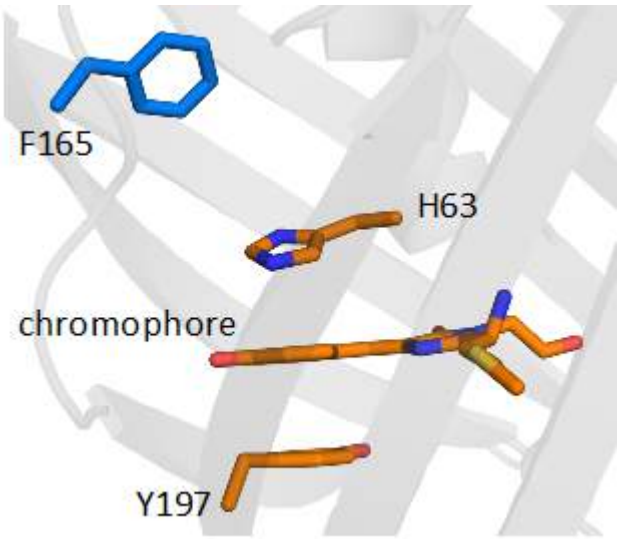

Figure 3: Computational model of the structure of mRojo-VHSV L165F. The triple-decker motif is represented in orange (H63 and Y197 with the chromophore in the middle) and the F165 residue in blue. Note the possible quadruple-decker motif. PDB ID: 5H87 (*1*).

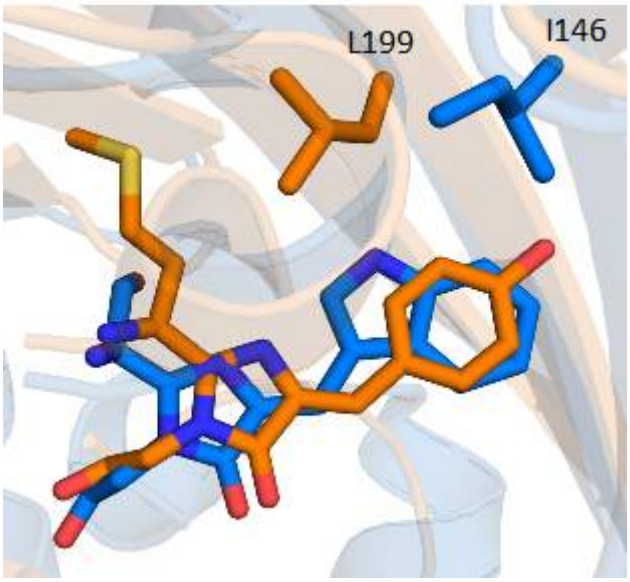

Figure 4: Overlay of the positioning of L199 in mRojo-VHSV and of I146 in mTurquoise. mRojo-VHSV is shown in orange while mTurquoise is shown in blue. PDB ID: 5H87, mRojo-VHSV (*1*) and 4AR7, mTurquoise (*7*)

quadruple-decker motif of aromatic rings, we combined it with the brightness increasing L199M mutation to create the mRojo-VHSV FM double mutant. As was observed with the L199M single mutant, excitation and emission wavelengths were blue-shifted by 4 nm. (Figure 2, panel III) In addition, the extinction coefficient of the double mutant decreased by a factor of 1.8, as in the L165F single mutant, while the quantum yield increased by a factor of 1.9. Overall, a small (5%) increase in brightness was observed. Even though the quantum yield of mRojo-VHSV FM was lower than that of the single mutant L199M, this variant can potentially form a quadruple-decker motif of aromatic rings while restoring the loss of brightness caused by the L165F mutation.

Discussion

Even though the screening results indicated that the single mutant L165F is brighter than mRojo-VHSV, spectroscopic characterization of the purified protein revealed that this was not the case. However, a small red shift of the emission wavelength was observed. This could be due to parallel π-stacking from residue H63 with the chromophore, as such an interaction was predicted by quantum mechanics to cause a similar emission red shift in GFP (*6*). However, it is unclear how this mutation decreased the extinction coefficient. A crystal structure of mRojo-VHSV L165F is required to verify the orientation of the histidine side chain relative to the chromophore.

The increase in brightness observed for the L199M mutant could result from a similar process as was seen in the mTurquoise2 cyan fluorescent protein, which displays a quantum yield increase of 10% but no change in extinction coefficient relative to its parent mTurquoise. Goedhart *et al.* observed that the single mutation I146F increased the number of van der Waals interactions with the chromophore and surrounding residues when it was introduced into mTurquoise. This improved packing led to the rigidification of a flexible strand in mTurquoise and of the chromophore, resulting in a quantum yield increase (*7*). A similar process could have happened in mRojo-VSHV L199M since L199 in mRojo-VHSV and I46 in mTurquoise occupy similar positions relative to the chromophore (Figure 4).

When combining the two mutations, we did not observe a quantum yield increase as was seen in the L199M point mutant, while the extinction coefficient was within error to that of the L165F single mutant, leading us to conclude that the mutations are not additive. The decrease in quantum yield when adding the L165F mutation to the L199M mutation could indicate that it contributes to the destabilization of the chromophore, making it more flexible. Combinatorial mutagenesis at these sites may help to identify synergistic mutations that would increase the quantum yield and overall brightness.

In conclusion, saturation mutagenesis of amino acids surrounding the triple-decker motif of mRojo-VHSV led to an increase in brightness of up to 2.3-fold from the single mutation, L199M. It was also found that the mutation L165F has the potential to form a quadruple-decker

motif which would be novel in this protein family. However, this single mutation decreased the brightness of the RFP. Combining both mutations into mRojo-VHSV FM created an RFP with the putative quadruple-decker motif while maintaining the brightness observed in mRojo-VHSV. This combined mutant could be used as a starting point in directed evolution to further increase the brightness of an RFP with a potential quadruple-decker motif.

Materials and Methods

Mutagenesis and cloning

Saturation mutagenesis was performed on the mRojo-VHSV gene by overlap extension using Vent DNA polymerase (New England BioLabs). External primers were used in combination with complementary sets of primers containing the NNS degenerate codon in individual polymerase chain reactions (PCR). The resulting overlapping fragments were agarose gel-purified (Omega Bio-tek) and recombined by overlap extension PCR. The amplicons were digested with *NdeI* and *BamHI* (New England BioLabs) and gel-purified to be ligated into a digested and dephosphorylated – via treatment with Antarctic phosphatase (New England BioLabs) – pET-11a vector (Novagen) using T4 DNA ligase (New England BioLabs). Constructs were transformed into chemically competent *E. coli* BL21-Gold(DE3) cells (Agilent). Plasmids were extracted from transformed cells using E.Z.N.A Plasmid Mini Kit I (Omega Bio-tek) and were verified by sequencing the entire reading frame.

Screening

Cells were grown in Overnight Express Instant Terrific Broth (TB) at 37°C with shaking in 96-well plates (Nunc). Following overnight expression, cells were harvested by centrifugation. Pellets were washed using phosphate-buffered saline (PBS) at pH 7.4 then left at 4°C for three days to allow for chromophore maturation. Screening of the saturation mutagenesis libraries was performed using a Tecan Infinite M1000 plate reader. The excitation spectra (with emission at 620 nm) and the emission spectra (with excitation at 535 nm) were obtained from whole cells resuspended in PBS at pH 7.4.

Protein expression and purification

E. coli BL21-Gold(DE3) cells containing the His-tagged RFP genes were inoculated and grown overnight (37°C, 200 rpm) in a Luria-Bertani (LB) broth supplemented with 100 µM of ampicillin. 10 mL of the overnight culture was transferred into 500 mL of LB broth supplemented with 100 µM of ampicillin. Cells were grown at 37°C, 200 rpm until the cultures reached an optical density at 600 nm between 0.5 and 0.7. Protein expression was induced using isopropyl -D-1-thiogalactopyranoside (IPTG) at a final concentration of 1 mM. Cells were induced overnight at 16°C with shaking at 200 rpm, then they were harvested by centrifugation. Pellets were resuspended in lysis buffer (100 mM phosphate buffer pH 8.0 supplemented with 5 mM imidazole) and lysed with an EmulsiFlex-B15 cell disruptor (Avestin). Proteins were purified by immobilized metal affinity chromatography using Profinity IMAC Ni-charged resin (Bio-rad) following the manufacturer's protocol. Eluted fractions containing the protein of interest were desalted by gel filtration using EconoPAC 10 DG columns (Bio-rad) into a buffer of 250 mM HEPES with 100 mM NaCl (pH 7.25).

Spectroscopic Characterization

Absorption, emission and excitation spectra were recorded in PBS at pH 7.4 using a Tecan Infinite M1000 plate reader. Quantum yields (φ) were determined from the integrated fluorescence intensity from excitation at 535 nm compared to samples of mCherry ($\varphi = 0.22$, (*8*)) for the range of emission from 550 to 800 nm (*9*). The molar extinction coefficients were calculated by the dynamic difference method described by Kredel et al. to take into account the presence of green chromophore. (*10*)

Competing interests
The authors declare that they have no competing interests.

Acknowledgements
RAC acknowledges an Early Research Award from the Ontario Ministry of Economic Development & Innovation, and grants from the Natural Sciences and ENgineering Research Council of Canada (NSERC), the Ontario Research Fund, and the Canada Foundation for Innovation. EN was the recipient of an Undergraduate Student Research Award from NSERC.

Author details
[1] Department of Chemistry and Biomolecular Sciences, University of Ottawa, 10 Marie Curie, K1N 6N5, Ottawa, Canada. [2]Cytokines Division, Health Canada, 70 Colombine Driveway, K1A 0K9, Ottawa, Canada. [3]Centre for Catalysis Research and Innovation, University of Ottawa, 30 Marie Curie, K1N 6N5, Ottawa, Canada.

References

1. A. T. Pandelieva, *et al.*, *ACS Chem. Biol.* **11**, 508 (2016).
2. D. M. Chudakov, M. V. Matz, S. Lukyanov, K. A. Lukyanov, *Physiol. Rev.* **90**, 1103 (2010).
3. G.-J. Kremers, S. G. Gilbert, P. J. Cranfill, M. W. Davidson, D. W. Piston, *Journal of cell science* **124**, 157 (2011).
4. K. Nienhaus, G. U. Nienhaus, *Chem Soc Rev* **43**, 1088 (2014).
5. R. A. Chica, M. M. Moore, B. D. Allen, S. L. Mayo, *Proc. Natl. Acad. Sci. U.S.A.* **107**, 20257 (2010).
6. B. L. Grigorenko, A. V. Nemukhin, I. V. Polyakov, A. I. Krylov, *J Phys Chem Lett* **4**, 1743 (2013).
7. J. Goedhart, *et al.*, *Nat Commun* **3**, 751 (2012).
8. N. C. Shaner, *et al.*, *Nat. Biotechnol.* **22**, 1567 (2004).
9. A. Williams, S. Winfield, J. Miller, *Analyst* **108**, 1067 (1983).
10. S. Kredel, *et al.*, *Chem. Biol.* **15**, 224 (2008).

ORIGINAL RESEARCH

Examining cognitive training and executive function in older adults

Meggan Porteous[1], Sheida Rabipour[1] and Patrick Davidson[1*]

Abstract
Studies have shown that cognitive functions decline with increasing age. As the population of older adults (OA) has grown, interest in cognitive training programs (CTP) has steadily expanded. The present study investigated whether CTP can lead to improvements in the performance of OA on cognitive tasks. Thirty-five adults (OA; 60-87 years) were recruited to complete 25 sessions of a CTP over five weeks, with assessments completed before and after the program. Thirty-two young adults (YA; 17-27 years) were also recruited to complete one assessment for baseline comparison with OA. During assessments, participants were evaluated using tasks of executive function, including the N-back task of working memory and Flanker task of inhibition. The response time (RT) and hit rates of YA and OA on these tasks were examined at baseline, as well as changes in OA pre- and post-training. Repeated measures analysis of variance indicated a reduction of pre- and post-training RT for the Flanker task. There was no post-training change in RT on the N-back task. While OA hit rates did not change significantly pre- and post-assessment on the Flanker task, they showed increased hit rates post-training in the N-back task. In both tasks, OA and YA hit rates and RT were significantly different, with YA demonstrating lower RT and hit rate compared to OA. Follow-up studies will determine whether other factors can also lead to improvement. Determining whether CTP can improve cognitive performance in OA can help determine the potential of such approaches to prevent or rehabilitate age-related cognitive decline.

Keywords: Cognitive training programs; Aging; Older adults; Young adults; Expectations; Working memory

Résumé
Certaines études démontrent que les fonctions cognitives diminuent avec l'âge. À mesure que la population d'adultes plus âgés (AA) augmente, on s'intéresse beaucoup plus aux programmes d'entraînement cognitif (PEC). Cette étude examine si les PEC améliorent la performance aux tâches cognitives. On a recruté trente-cinq AA (60-87 ans) qui ont dû prendre part à 25 sessions de PEC pendant cinq semaines, avec des évaluations réalisées avant et après le programme. On a également recruté trente-deux jeunes adultes (JA, 17-27 ans) afin d'avoir un groupe de base contre lequel comparer la performance. Au cours des évaluations, les participants ont été évalués en utilisant des tâches de la fonction exécutive, y compris la tâche N-back de la mémoire de travail et la tâche d'inhibition de Flanker. Le temps de réponse (TR) et les taux de succès des JA et AA pour ces tâches ont été examinés au départ, ainsi que les changements chez les AA avant et après le PEC. L'analyse de la variance des mesures répétées a indiqué une réduction du TR avant et après l'entraînement pour la tâche Flanker. Il n'y a pas eu de changement post-entraînement du TR pour la tâche N-back. Bien que les taux de succès de la performance n'aient pas changé de façon significative avant et après l'évaluation pour la tâche Flanker, ils ont montré des taux de succès accrus après l'entraînement pour la tâche N-back. Dans les deux cas, les taux de succès et les TR des JA et AA étaient significativement différents ; les JA démontraient un TR et un taux de succès inférieurs à celui des AA. Des études subséquentes seront nécessaires pour déterminer si d'autres facteurs peuvent également entraîner une amélioration. Déterminer si les PEC améliorent la performance cognitive chez les AA peut aider à déterminer le potentiel de telles approches pour prévenir ou réhabiliter le déclin cognitif lié à l'âge.

Mots Clés: Programmes d'entraînement cognitif; Vieillissement; Personnes âgées; Jeunes adultes; Attentes; Mémoire de travail

Introduction

Studies have shown that certain cognitive functions decline with increasing age (*1, 2*). With increasing life expectancy and a growing population of older adults (OA), interest in cognitive training programs is steadily expanding. Cognitive training programs may provide an effective, long-term and drug-free aid or solution to OA in need of cognitive improvements. The present study sought to investigate whether cognitive training programs can lead to improvements in the performance of OA on measures of working memory and inhibition. The authors hypothesized that young adults (YA) would perform better than OA, and that OA would demonstrate performance improvements pre- and post-training. This work was part of a larger study investigating the interactions between expectations and cognitive training on cognitive performance and other real-world outcomes in OA.

Methods

Thirty-five OA, 60-87 years of age, were recruited to complete 25 sessions of a cognitive training program over five weeks. The authors also recruited 32 YA, 17-27 years of age, to complete a single forty-minute cognitive training session and one assessment for baseline comparison with OA. The cognitive training program, a commercially-available web-based program called "Activate", comprised multiple games targeting executive functions such as spatial working memory, pattern recognition, and inhibition. The games increased in speed and difficulty depending on participants' results. YA were not required to participate in a five-week training program due to the study's interest being limited to OA data; we assessed OA before and after the program.

Participants were evaluated using tasks of executive function, including the N-back task of working memory and the Flanker task of inhibition (*3, 4*). Both working memory and inhibition were targeted in the Activate games and reflect age-related changes in cognitive function (*5*). They have been shown to decline over time, and therefore are a good indicator of cognitive training effectiveness and improvement (*6, 7*). Participants were seated at a computer, where a fixation point was presented. The researcher then randomly initiated the Flanker or the N-back task. The Flanker task was presented in four trials, each separated in time by a short break. A longer break was provided to allow participants to return to a resting state between tasks. The task required participants to indicate in which direction the center arrow pointed (right or left), while ignoring irrelevant stimuli (other arrows) surrounding the center arrow. If all the arrows pointed in the same direction, the Flanker task was considered congruent. If not, the Flanker task was incongruent. It was administered to the participants in four separate blocks, which included a random order combination of 24 left congruent trials, 24 right congruent trials, 12 left incongruent trials and 12 right incongruent trials.

The N-back task involved a zero-back, one-back, and two-back condition, generated in random order. The task required participants to respond to a specified letter in a series of varied letters. Depending on the condition, participants were instructed to respond when the target letter was shown (zero-back), when the target letter was the same as the previous letter (one-back) or when the target letter was the same as the letter two letters back (two-back). The zero-back and one-back conditions contained 202 letters each, where 98 letters were target letters requiring a response; the two-back condition contained 95 letters in total, where 55 letters were targets

For both tasks, response time (RT; i.e. how quickly the participant responded via key press in milliseconds) and hit rate (i.e. the number of correct responses out of the total number of possible responses) of YA and OA were examined at baseline, as well as post-training for OA, to examine changes in performance over the course of the training.

Results

When comparing OA pre- and post-training RT, repeated measures analysis of variance indicated a reduction of post-training RT for the congruent Flanker task ($F_{1,26} = 11.74$, $p = 0.002$, $\eta = 0.311$), more specifically for trial 1 ($T_{26} = 2.147$, $p = 0.041$, $CI[6.399, 29.453]$), trial 3 ($T_{26} = 4.494$, $p = 0.000$, $CI[15.695, 42.061]$) and trial 4 ($T_{26} = 4.174$, $p < 0.000$, $CI[10.993, 32.326]$). The incongruent Flanker task also showed a reduction of post-training RT ($F_{1,26} = 5.985$, $p = 0.021$, $\eta = 0.187$), specifically in trial 3 ($T_{26} = 3.936$, $p = 0.001$, $CI[17.489, 55.715]$). In contrast, no change was noticed in the RTs for the N-back task.

When comparing OA pre- and post-training hit rates, no significant changes were noted in the congruent and incongruent Flanker tasks. Conversely, OA hit rates did increase post-training in the N-back task ($F_{1,25} = 41.326$, $p = 0.000$, $\eta = 0.623$), notably in the one-back ($T_{25} = -4.91, p < 0.000, CI[-1.256, -0.514]$) and two-back conditions ($T_{25} = -6.548$, $p < 0.000$, $CI[-5.932, -3.093]$).

When comparing baseline data, repeated measures analysis of variance showed significant baseline RT differences between YA and OA on the congruent ($F_{3,192} = 2.181$, $p = 0.025$, $\eta = 0.047$) and incongruent Flanket tasks ($F_{3,192} = 2.616$, $p = 0.052$, $\eta = 0.039$) (Figures 1 and 2) as well as on the N-back task ($F_{2,124} = 38.124$, $p = 0.000$, $\eta = 0.381$) (Figure 3). Repeated measures

*Correspondence: patrick.davidson@uottawa.ca
[1] School of Psychology, University of Ottawa, 136 Jean-Jacques Lussier, K1N 6N5, Ottawa, Canada

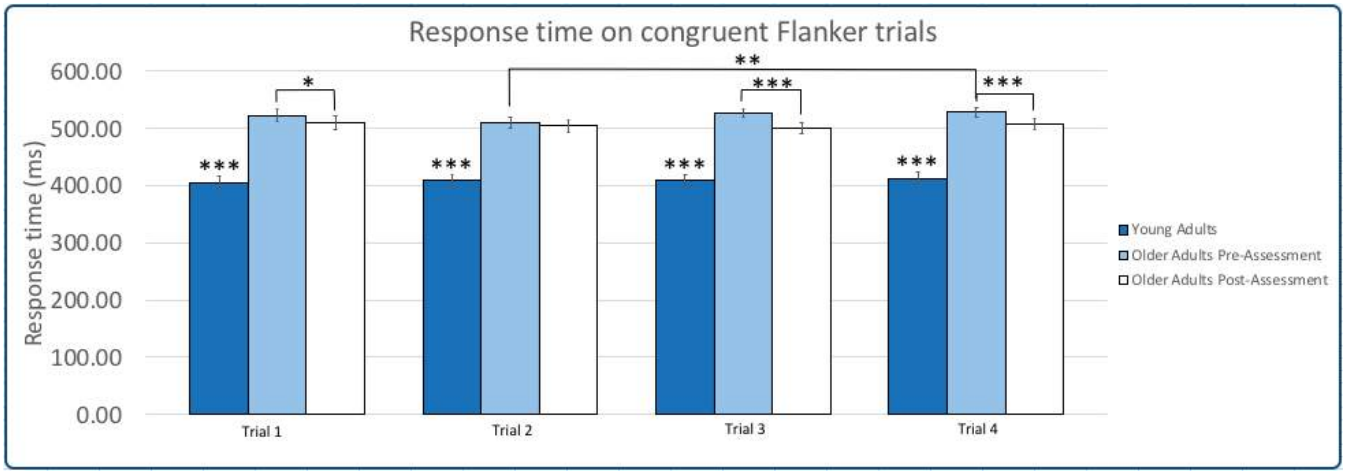

Figure 1: Response time on congruent Flanker trials. RT results of YA and OA (pre- and post-training) on the congruent Flanker trials (1-4). Statistical significance is indicated by "*", where one asterisk indicates $p < 0.05$, two asterisks indicate $p < 0.01$, and three asterisks indicate $p < 0.001$.

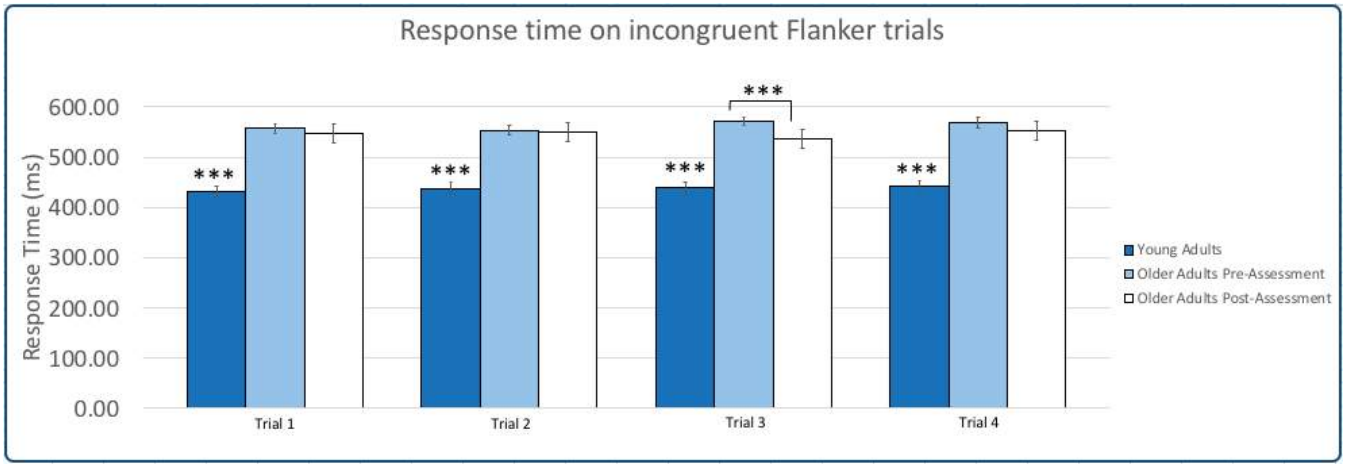

Figure 2: Response time on incongruent Flanker trials. RT results of YA and OA (pre- and post-training) on the incongruent Flanker trials (1-4). Statistical significance is indicated by "*", where one asterisk indicates $p < 0.05$, two asterisks indicate $p < 0.01$, and three asterisks indicate $p < 0.001$.

analysis of variances showed no showed no significant differences between YA and OA hit rates on either Flanker task (Figures 4 and 5). It was, however, significantly different on the N-back task ($F_{2,124} = 51.679$, $p = 0.000$, $\eta = 0.455$) (Figure 6).

Discussion

Overall, YA responded quicker than OA and were also less accurate. After training, results showed a decrease in RT for OA in both the congruent and incongruent trials of the Flanker task. This may indicate that their ability to inhibit irrelevant stimuli improved following inhibition training. However further investigation is required before any definitive conclusions can be made. This effect of time was not present for the hit rate in either the congruent or incongruent Flanker task, which indicates that while response time may be affected by cognitive training, accuracy may not be. The lack of change of accuracy in OA may be due to lack of near-transfer. *Near-transfer* refers to changes in performance caused by cognitive training programs transferring to similar tasks, as is the case with the games in cognitive training and the Flanker and N-back tasks. Near transfer may apply to the inhibition portion of the task, but not to correct answers. The N-back task of working memory showed no significant post-training change in RT, which means that OA did not become quicker after the training. They did, however, become more accurate following training, which may indicate that near-transfer applies in correct answer responses on working memory tasks, where participants are required to maintain and manipulate information before using it. YA had significantly lower RT on both the

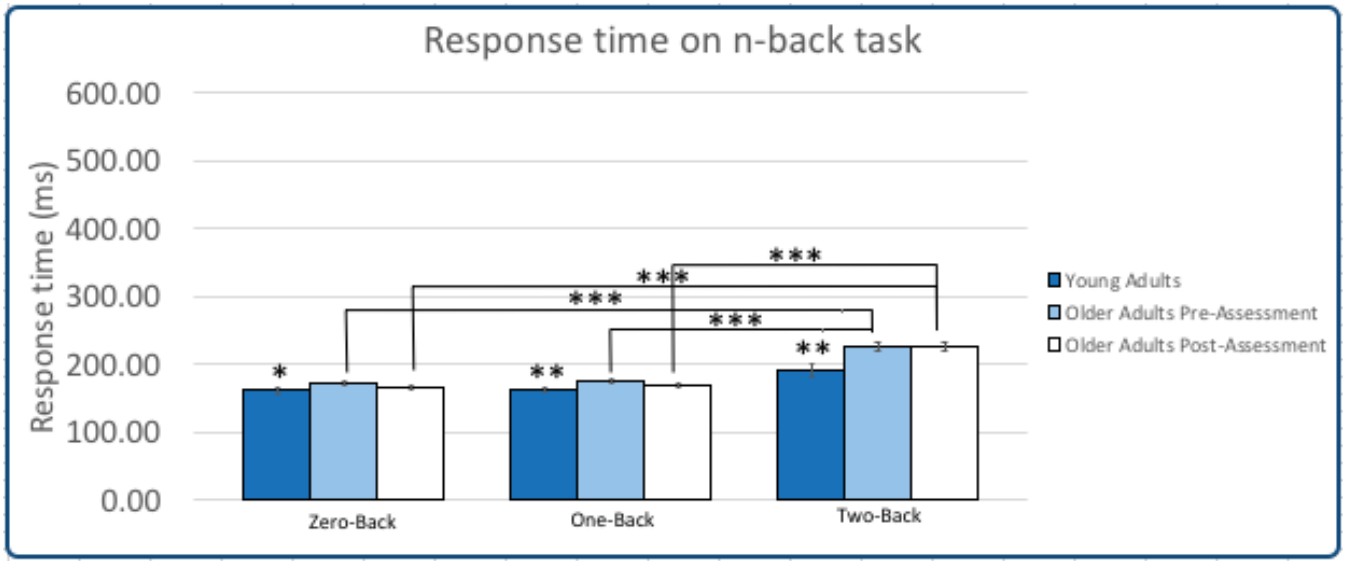

Figure 3: Response time on n-back task. RT results of YA and OA (pre- and post-training) on the n-back task (zero-, one- and two-back). Statistical significance is indicated by "*", where one asterisk indicates $p < 0.05$, two asterisks indicate $p < 0.01$, and three asterisks indicate $p < 0.001$.

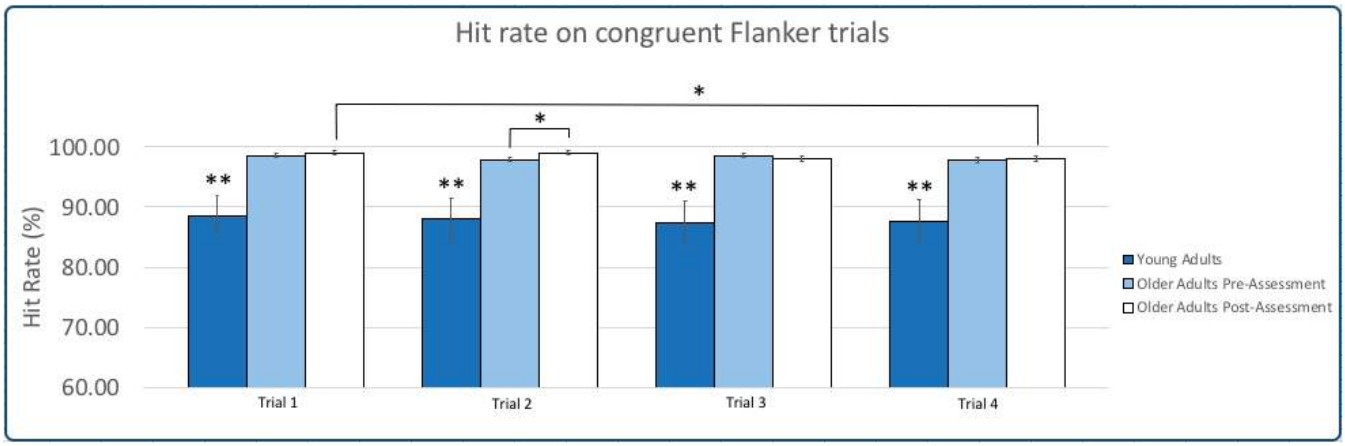

Figure 4: Hit rate on congruent Flanker trials. Hit rate results of YA and OA (pre- and post-training) on the congruent Flanker trials (1-4). Statistical significance is indicated by "*", where one asterisk indicates $p < 0.05$, two asterisks indicate $p < 0.01$, and three asterisks indicate $p < 0.001$.

congruent and incongruent Flanker task, as well as the N-back task. This might indicate that YA are quicker at identifying relevant data and responding to it, as well as maintaining and manipulating information with the purpose of using it. However, this finding could also be explained by impulsive behaviour patterns typically attributed to YA, or lack of motivation and investment in the task and subsequently, in the study. The latter interpretations are supported by the hit rate data, which indicates that while YA are quicker, they are also incorrect more often than OA. Although YA only showed a significant difference of hit rate on the N-back task, both the congruent and incongruent Flanker tasks show significant differences in one or more trials.

In summary, cognitive training may improve RT on inhibitory tasks, while also improving accuracy on memory tasks. This, while in itself not conclusive, justifies further research in the field of cognitive training and executive function. Further investigations could lead to potential discoveries regarding cognitive training in rehabilitation and preventative contexts. Such advances may help improve cognitive function in older adults and, therefore, increase independence and level of functioning. Everything considered, increased mental capabilities may enhance brain capacity longevity and allow for increased cognitive reserve in cases of problematic neuropathological diseases such as Alzheimer's disease, as well as in cases of non-pathological age-related cognitive declines.

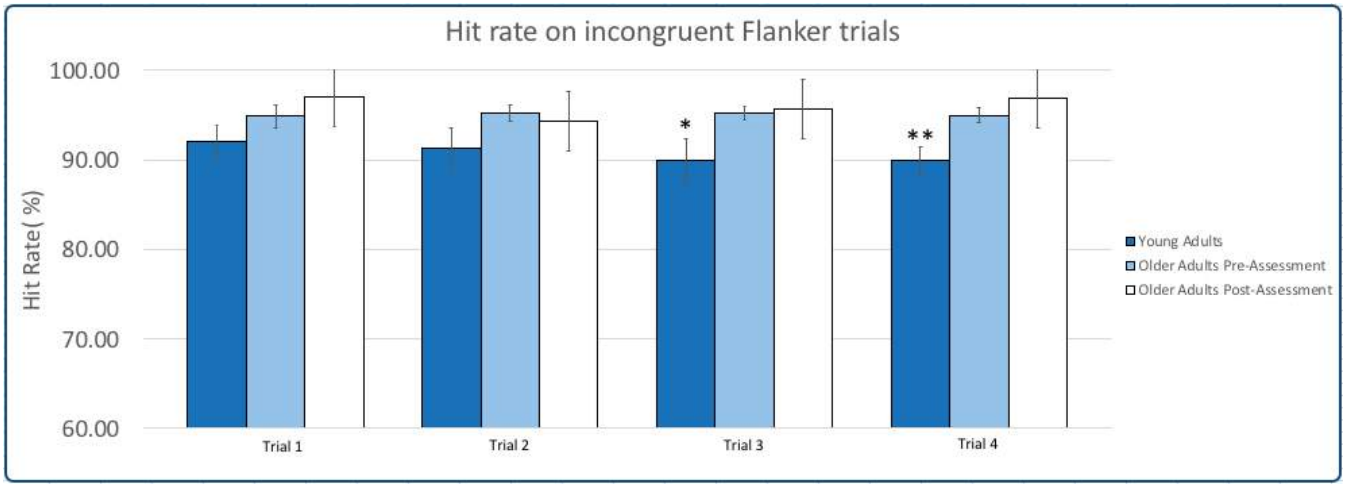

Figure 5: Hit rate on incongruent Flanker trials. Hit rate results of YA and OA (pre- and post-training) on the incongruent Flanker trials (1-4). Statistical significance is indicated by "*", where one asterisk indicates $p < 0.05$, two asterisks indicate $p < 0.01$, and three asterisks indicate $p < 0.001$.

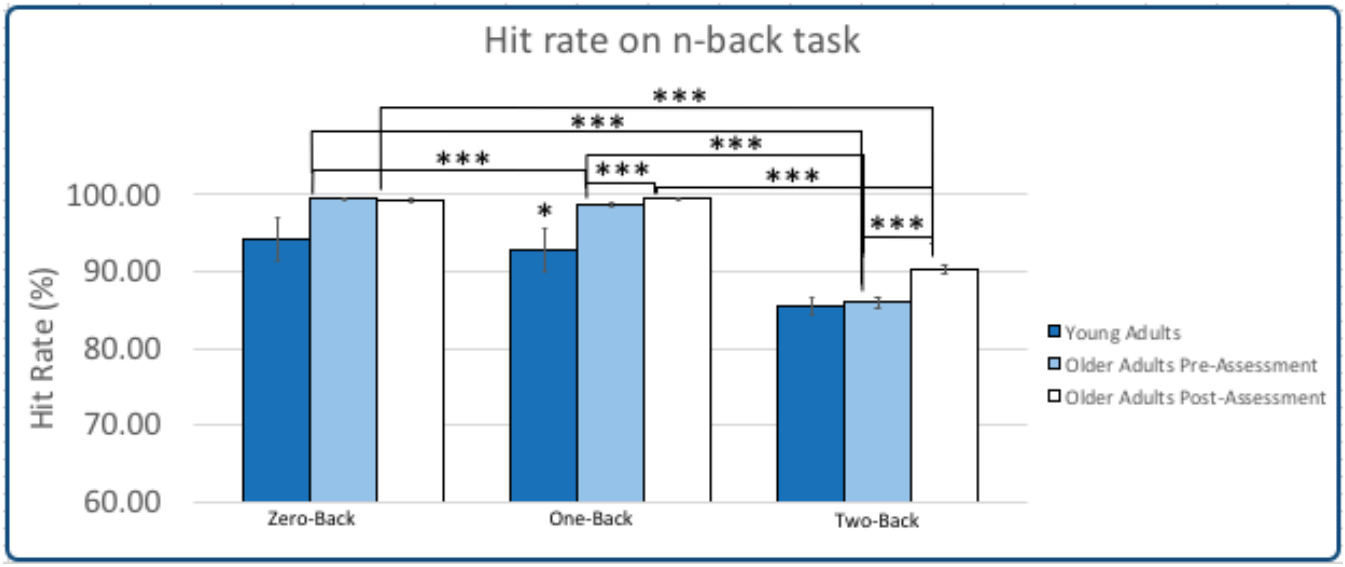

Figure 6: Hit rate on n-back task. Hit rate results of YA and OA (pre- and post-training) on the n-back task. Statistical significance is indicated by "*", where one asterisk indicates $p < 0.05$, two asterisks indicate $p < 0.01$, and three asterisks indicate $p < 0.001$.

Competing interests
The authors declare that they have no competing interests.

Acknowledgements
The authors thank the Neuropsychology lab at the University of Ottawa and its members for their help and guidance in this project. The authors also thank the Undergraduate Research Opportunity Program at the University of Ottawa for supporting this work.

Author details
[1] School of Psychology, University of Ottawa, 136 Jean-Jacques Lussier, K1N 6N5, Ottawa, Canada. [2] School of Psychology, University of Ottawa, 136 Jean-Jacques Lussier, K1N 6N5, Ottawa, Canada.

References

1. S. B. Chapman, *et al.*, *Frontiers in Human Neuroscience* **10**, 338 (2016).
2. A. L. Gooding, *et al.*, *Neuropsychol Rehabil* **26**, 810 (2016).
3. S. M. Jaeggi, M. Buschkuehl, W. J. Perrig, B. Meier, *Memory* **18**, 394 (2010).
4. C. W. Eriksen, *Visual Cognition* **2**, 101 (1995).
5. J. A. Sweeney, C. Rosano, R. A. Berman, B. Luna, *Neurobiol. Aging* **22**, 39 (2001).
6. T. Klingberg, *Trends Cogn. Sci. (Regul. Ed.)* **14**, 317 (2010).
7. A. J. Millner, A. C. Jaroszewski, H. Chamarthi, D. A. Pizzagalli, *Neuroimage* **63**, 742 (2012).

Shocking the brain to regain motor function: a non-invasive therapy for stroke patients

Michael Min Wah Leung

Abstract
Invasive treatments and its associated risks are important factors of concern when the conditions are affecting the nervous system. Transcranial direct current stimulation (tDCS) is a non-invasive technique that stimulates brain areas through the scalp and has excitatory or inhibitory neuromodulatory effects. In the context of stroke patients, recovery is often impaired from the increased inhibition of the damaged area from the unaffected hemisphere. Fujimoto *et al.* uses dual-hemisphere transcranial direct current stimulation to address this interhemispheric inhibition and demonstrates that stroke patients were able to periodically restore sensory deficits.

Keywords: Transcranial direct current stimulation; Stroke; Dual-hemisphere tDCS; Parkinson's Disease

Résumé
Les traitements invasifs et ses risques associés nécessitent une attention particulière lorsque les conditions affectent le système nerveux. La stimulation transcrânienne à courant continu (tDCS) est une technique non invasive qui stimule certaines régions du cerveau à travers la scalpe soit de façon excitatrice ou de façon neuromodulante inhibitrice. Dans le contexte de patients souffrant d'un ACV, leur rétablissement est souvent compromis à cause de l'inhibition accrue de la région endommagée de l'hémisphère non affectée. Fujimoto *et al.* utilisent une tDCS à hémisphère double afin de résoudre cette inhibition inter-hémisphérique et démontrent les déficits sensoriels ont été rétablis de façon périodique que chez les patients souffrant d'un ACV.

Mots Clés: Stimulation transcrânienne à courant direct; Accident vasculaire cérébral; tCDS à double hémisphère; La maladie de Parkinson

The preference of minimally invasive treatment to remedy various disorders and conditions is gaining popularity in patient care, emphasizing safety, recovery, and comfort. The advancements in minimally invasive treatments are essential for conditions associated with the nervous system, as high risks are normally associated with neurological medical intervention (*2*). Transcranial direct current stimulation (tDCS) is a non-invasive technique that can alter cellular activity using weak electric currents (*3*). The efficacy of tDCS depends on the method of delivery, and the trending procedure in most recent studies is by dual-hemisphere tDCS.

Dual-hemisphere tDCS makes use of interhemispheric interactions to optimize behavioral performance, in which one hemisphere is excited while the other is inhibited (*4*). This methodology of simultaneously using excitatory (anodal) and inhibitory (cathodal) signals with cathodes placed in opposite or less affected areas is well-documented (*2*–*7*). Fujimoto and colleagues have reported that a single session of dual-hemisphere tDCS over the primary and secondary somatosensory areas resulted in a transient behavioral gain in tactile discrimination with stroke patients. To support their theory, the authors compiled results from 8 applicable chronic stroke patients who all suffered a supratentorial stroke and exhibit sensory deficits with a Mini Mental Status Examination score of more than 24 points. This experiment was the first double-blind, sham-controlled experimental study for dual-hemisphere dTCS, and measured tactile discrimination via performance of both index fingers in the grating orientation task (GOT) before, during, and after dual-hemisphere tDCS over the primary and secondary somatosensory cortices (S1 and S2, respectively) (*4*).

Each patient was subject to the GOT while blindfolded and in a comfortable position. Tactile stimuli from plastic domes varying in groove widths were applied onto the

Correspondence: mleun036@uottawa.ca
Department of Cellular and Molecular Medicine, University of Ottawa, 451 Smyth Rd, K1H 8M5, Ottawa, Canada
The Ottawa Hospital Research Institute, 725 Parkdale Avenue, K1Y 4E9, Ottawa, Canada

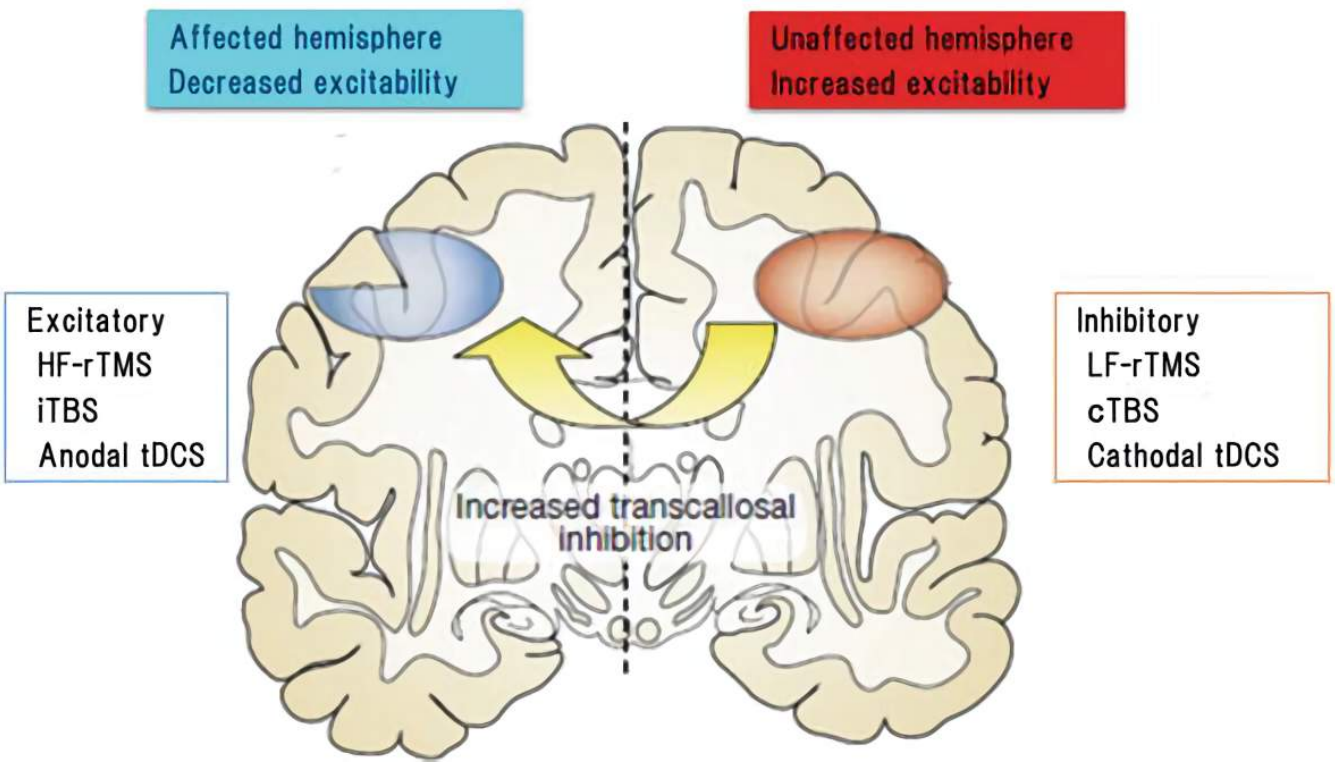

Figure 1: Interhemispheric interactions schematic from *Matsuda et al.*, 2017. (*1*)

patient's palmar side of the affected and non-affected index fingers for two seconds, and they had to differentiate the orientation of the groove (parallel or orthogonal to the axis of the index finger). The authors evaluated each patient's performance by assigning a threshold score, calculated by the finest grating spacing each patient could discern with their index finger. This experiment was repeated three times (pre-intervention, intra-intervention, and post-intervention) and was done again with the non-affected index finger. To identify the regions over the primary and secondary somatosensory cortices (S1 and S2), the researchers used magnetic resonance imaging. A verbal rating was also collected from patients in case there was any subjectivity impacting their performance.

Dual-hemisphere tDCS over the primary and secondary somatosensory cortices helped improve patient performance in the GOT. Fujimoto and colleagues claim that the behavioral gain observed was enhanced by decreased activity in the unaffected hemisphere, reducing interhemispheric inhibition during the task. Results from the GOT gathered from each patient supported their hypothesis, as the experimental stimulations in both somatosensory cortexes allowed all participants to discriminate finer crevices with their affected index finger (*4*).

Although *Fujimoto et al.* hypothesized that a single session of dual-hemisphere tDCS is more effective than single hemisphere tDCS, their current study had not shown comparable data between single hemisphere tDCS and dual-hemisphere tDCS. If single hemisphere tDCS was sufficient to elicit the same behavioral gain, then the use of dual-hemisphere tDCS was redundant. The author's original hypothesis that dual-hemisphere tDCS enhanced tactile discrimination in stroke patients in both the S1 and S2 regions was supported by their data. However, a judgment could not be made as to which somatosensory cortex was a more suitable target for tDCS due to the similar behavioral gain in S1 and S2 stimulations. Furthermore, each patient's elicited behavioral gain was of different magnitude due to the heterogeneity of each patient's stroke localization (*4*). Although the heterogeneity exhibited practicality in patients with different stroke severity and localization all benefited from tDCS, future avenues of study should explore homogenous pathologies, so conclusions could be drawn.

The future in the field of minimally invasive therapeutic treatments is expanding, with tDCS gaining popularity for its ease of use and access. Furthermore, Fujimoto and colleagues were successful in demonstrating improved somatosensory function in stroke patients via dual-hemisphere tDCS over S1 and S2. Alternative therapeutic treatments to tDCS include DBS (deep brain stimulation) and rTMS (repetitive transcranial magnetic stimulation), but tDCS remains the preferred treatment option due to a favourable safety profile, tolerability, eas-

ier applicability and cost effectiveness (*5*). Previous studies demonstrate the efficacy of tDCS to improve motor function in neurological patients suffering with sensory and motor deficits, such as cerebellar ataxia, supratentorial stroke, and Parkinson's disease (*2–7*). Future longitudinal studies could aid stroke patients with long term rehabilitation, with beneficial effects on somatosensory performance.

Competing interests

The author declares that he has no competing interests.

References

1. T. Matsuda, A. Manji, K. Amimoto, A. Inaba, Y. Wada, *Non-Invasive Brain Stimulation (TMS/tDCS) and Rehabilitation for Stroke and Parkinson's* (InTechOpen, 2017), chap. 8, pp. 121–135.
2. J. V. Rosenfeld, *Aust New Zeal J Surg* **66**, 553 (1996).
3. N. G. Pozzi, *et al.*, *Cerebellum* **13**, 109 (2014).
4. S. Fujimoto, *et al.*, *Front Neurosci* **10**, 128 (2016).
5. D. H. Benninger, *et al.*, *J. Neurol. Neurosurg. Psychiatry* **81**, 1105 (2010).
6. A. Fusco, *et al.*, *Stroke Res Treat* **2013**, 837595 (2013).
7. D. Impey, S. de la Salle, V. Knott, *Brain Cogn* **105**, 46 (2016).

The effect of context on sensory accumulation involved in decision-making

Léa Caya-Bissonnette

Abstract
The underlying processes allowing for decision-making has been a question of interest for many neuroscientists. The lateral intraparietal cortex, or LIP, was shown to accumulate context and sensory information to compute a decision variable. The following review will present the work of Kumano, Suda and Uka who studied the link between context and sensory information during decision-making. To do so, a monkey was trained to associate the color of a fixating dot to one of two tasks. The tasks consisted in either indicating the motion or the depth of the majority of the dots on a screen. The local field potential of the LIP neurons was recorded, and the researchers found a role of context during the stimulus presentation in regards to decision formation. The results have important implication for mental disorders involving malfunction in decision processes.

Keywords: Decision-making; Task-switching; Sensory accumulation

Résumé
Les processus sous-jacents permettant la prise de décision ont été une question d'intérêt pour de nombreux neuroscientifiques. On a montré que le cortex intrapariétal latéral, ou IPL, accumulait des informations contextuelles et sensorielles pour calculer une variable de décision. La revue suivante présentera le travail de Kumano, Suda et Uka qui ont étudié le lien entre le contexte et l'information sensorielle lors de la prise de décision. Pour ce faire, on a entraîné un singe afin qu'il puisse associer la couleur d'un point de fixation à l'une de deux tâches. Les tâches consistaient à indiquer le mouvement ou la profondeur de la majorité des points sur un écran. On a enregistré le potentiel de champ local des neurones IPL. D'après ceci, les chercheurs ont découvert un rôle de contexte lors de la présentation du stimulus en ce qui concerne la formation de la décision. Les résultats ont une implication importante pour certains troubles mentaux concernant un dysfonctionnement dans les processus de prise de décision.

Mots Clés: La prise de décision; Flexibilité mentale; Flexibilité

Understanding the neural basis behind decision formation in task switching performance is crucial to mapping out the extremely complex and dynamic maze that is the human brain. The impact of this understanding on the scientific community and the medical field would be significant, as decision-making is linked to some neurological diseases such as schizophrenia (*1*). Specific tasks are represented through sensory, contextual and motor components in the prefrontal neurons (*2*). However, these neurons do not seem to be independently involved in the formation of decisions. As Gold and Shadlen demonstrated, an LIP neuron also accumulates context and sensory information to compute a decision variable (*3*).

Correspondence: lcaya082@uottawa.ca
Department of Biology, University of Ottawa, 30 Marie Curie, K1N 6N5, Ottawa, Canada

Tasks involving both contextual and sensory components, such as the game "Where is Waldo?" are prevalent. The game requires the player to find a character hidden in a complex environment. Contextual components such as finding Waldo, a character wearing a striped red and white t-shirt, help the player to perform the task efficiently. Interestingly, few have looked at the potential interdependence of these two variables. Therefore, this raise an important question: would context influence the intake of sensory evidence?

The researchers Kumano, Suda, and Uka found an answer to this question by investigating if and how decision formation changes depending on context (*4*). To do so, they measured the extracellular activity of a single LIP neuron of two monkeys during task switching. The monkeys were presented with a multitude of red dots with dif-

ferent depths and directions of motion. They were then trained to indicate either the depth or the direction of the majority of the dots based on the color of a fixating point. The change in color of the fixating point represents the variation in context. In other words, even if presented with similar sensory inputs, the relevant stimulus to the task varied according to contextual components. The two tasks were randomly interwoven and were chosen for their previously established sensory representation (*5, 6*). To respond, the monkeys were required to make an eye movement, a saccade, to one of two targets. An upper target was associated with an upward motion or farther disparity of the red dot stimuli, and a lower target, which was diametrically opposite to the upper one, was associated with a downward motion or nearer disparity. Up to 128 stimuli conditions with different motion coherence and binocular correlations were recorded with their average time of reaction. To find the receptive field of the neuron, Kumano, Suda, and Uka recorded the firing rate of the LIP neuron for the upper target choice by using a memory-guided saccade task.

The researchers built a psychometric function which plotted strength of the relevant stimulus against accuracy of their choice and a chronometric function to plot strength of the relevant stimulus against time reaction. Both functions suggest that the higher the strength of the irrelevant stimulus, the less accurate and the longer the monkeys took to make a choice. More importantly, the firing rate of the relevant stimulus to the task had a shorter time of build-up than the irrelevant stimulus after stimuli onset, but both reached a common level right before saccade, meaning that the accumulation of the relevant stimulus is preferential to the irrelevant stimulus. However, the authors did not calculate the time differences between build-up onset of the relevant and irrelevant stimuli, giving no quantitative data of this preferentiality. To investigate whether this sensory accumulation occurs at the level of a single neuron, researchers Kumano, Suda, and Uka measured the sensitivity of an LIP neuron to motion coherence and to binocular correlation during both tasks (*4*). They observed a change in build-up rates related to the change in the strength of the relevant stimulus and found that most single neurons will fire for both stimuli when they are relevant. Then, they compared the sensitivity of the relevant stimulus to the irrelevant stimulus and concluded that the accumulation of the relevant feature was more prominent than the irrelevant one. This finding suggests that context does influence the preferential accumulation of a single LIP neuron. Nonetheless, some questions remain. Since the LIP neuron computes a decision variable but is not related to task error, task selection is at least partly computed elsewhere in the brain. Using electrophysiology techniques, future studies could potentially reveal the pathway leading to decision of task selection. In addition, neurological diseases such as schizophrenia underlie cognitive impairment of task switching performance, resulting in more latency and less accuracy of the saccade response (*3*). Evaluating the effect of context by measuring and comparing the sensitivity to relevant and irrelevant stimuli of a schizophrenic individual to a non-schizophrenic subject would be an interesting follow-up and could result in a major breakthrough in the field of neuropsychiatric diseases. To conclude, the preferential accumulation of LIP neurons for relevant information serves as a crucial step towards uncovering the underlying processes of decision-making.

Competing interests
The author declares that she has no competing interests.

References

1. C. Greenzang, D. S. Manoach, D. C. Goff, J. J. S. Barton, *Exp Brain Res* **181**, 493 (2007).
2. M. Siegel, T. J. Buschman, E. K. Miller, *Science* **348**, 1352 (2015).
3. J. I. Gold, M. N. Shadlen, *Annu. Rev. Neurosci.* **30**, 535 (2007).
4. H. Kumano, Y. Suda, T. Uka, *Journal of Neuroscience* **36**, 12192 (2016).
5. T. Uka, G. C. DeAngelis, *J. Neurosci.* **23**, 3515 (2003).
6. T. Uka, G. C. DeAngelis, *Neuron* **42**, 297 (2004).

Do stem cell divisions significantly contribute to cancer development?

Ryan Sandarage[1*] and Justin G. Chitpin[2†]

Abstract
Cancer is caused by uncontrolled cellular growth, yet some cancer cells may have greater roles in sustaining tumour proliferation and overcoming conventional cancer treatments. The origins of these cancer stem cells, as they are hypothesized, is widely contested. The current opinion points to extrinsic factors such as smoking, diet and sedentary lifestyle to be the primary inducer of cancer stem cells. This dogma was challenged in 2015 when Tomasetti and Vogelstein postulated that two-thirds of the variation in cancer risk could be explained by random mutations arising during DNA replication in healthy stem cells. Their "bad luck" hypothesis sparked fierce debate and controversy in the scientific community. In this point-counterpoint article, we discuss the random mutation cancer stem cell model and its implications for guiding public health through primary and secondary cancer prevention.

Keywords: Cancer; Stem cells; Driver gene mutations; Linear regression

Résumé
Le cancer est causé par une croissance cellulaire incontrôlée, pourtant certaines cellules cancéreuses peuvent jouer un rôle plus important dans le maintien de la prolifération tumorale et peuvent aider à surmonter les traitements conventionnels contre le cancer. Les origines de ces cellules souches cancéreuses, telles quelles, sont largement contestées. Actuellement, on souligne des facteurs extrinsèques tels que le tabagisme, l'alimentation et le mode de vie sédentaire comme principaux inducteurs des cellules souches cancéreuses. Ce dogme a été contesté en 2015 lorsque Tomasetti et Vogelstein ont postulé que les deux tiers de la variation du risque de cancer pouvaient être expliqués par des mutations aléatoires survenant lors de la réplication de l'ADN dans des cellules souches saines. Leur hypothèse de « malchance » a suscité de vifs débats et controverses dans la communauté scientifique. Dans cet article point-contrepoint, nous discutons du modèle de cellules souches cancéreuses à mutation aléatoire et de ses implications pour guider la santé publique à travers la prévention primaire et secondaire du cancer.

Mots Clés: Cancer; Cellules souches; Mutations génétiques directrices; Régression linéaire

Over the past decade, few articles have stimulated such scientific discourse as the origin of cancer in stem cells. While scientists are stil l working to this day to explain the biological "ground zero" for stem cell cancer, the common belief points to extrinsic factors as be the primary c ause. This paradigm was challenged in 2015 when Tomasetti and Vogelstein published "Variation in cancer risk among tissues can be explained by the nu mber of stem cell divisions" in Science (*1*). Tomasetti and Vogelstein used mathematical models to demonstrate that cancer risk corre lates more significantly with the number of stem cell divisions than environmental factors or inherited predispositions. According to their research, two-thirds of the variation in cancer risk could be explained by random mutations arising during DNA replication in healthy stem cells (*1*). Thus, their "bad luck" hypothesis sparked fierce debate and controversy in the scientific community (*1–4*).

From a deterministic standpoint, cancer discriminates against those who physically harm their bodies. This intuition is best emphasized by th e strong correlation between lung cancer and smokers inhaling carcinogens in cigarette smoke (*5–7*). While a sedu ctive argument, several confounding pieces of circumstantial evidence led Tomasetti and Vogelstein to re-think this conventional wisdom. If cancer is truly the result of grievous bodily

*Correspondence: rsand006@uottawa.ca
[1] Department of Cellular and Molecular Medicine, University of Ottawa, 451 Smyth Rd, K1H 8M5, Ottawa, Canada
Full list of author information is available at the end of the article
†Equal contributor

harm by external factors, how could cancer rates vary dramatically between different tissues in the body? For in stance, small intestinal cancers are three times less prevalent than brain tumors, yet the brain is exposed to fewer environmental mutagens than the small intestinal epithelium due to the protective blood-brain barrier (*1*). Furthermore, toxins ingested by individuals move through the gut having unimpeded interactions with intestinal cells. These anomalies led Tomasetti and Vogelstein to seek an alternative explanation for tiss ue-specific cancer risk. They postulated that random mutations in stem cell division may be responsible for causing a significant number of cancers. The more cells divide, the more opportunities there are for mutations to occur in these cells, resulting in unchecked growth and ultimately cancer.

To test this hypothesis, Tomasetti and Vogelstein developed a model to predict how the lifetime stem cell divisions (lscd) in a given tissue affects one's lifetime risk of cancer. For each tissue type, empirical estimates of the total number of stem cells and the number of times they divid ed were used to calculate the lscd. In parallel, the lifetime risks for different cancers were taken from existing literature. Linear regression anal ysis of lscd versus the lifetime risk for different cancers demonstrated that 65% of the variation in cancer risk could be explained by the number o f stem cell divisions in a healthy individual (*1*). Roughly one-third of the cancers correlated with extrinsic factors (deterministic tumors), while two-thirds correlated with the number of stem cell divisions (replicative tumors) (*1*). While elegant, Tomasetti and Vogelstein's analysis between cancer risk and cell division is unable to differentiate between the contributions of intrinsic and extrinsic factors citeWu2016. This shortcoming led to Wu *et al.*'s reply in 2016, which re-interpreted the lscd model, suggesting that extrinsic factors were indeed the dominant cancer-inducing agent (*2*).

The cornerstone of Wu *et al.*'s Nature publication, "Substantial contribution of extrinsic risk factors to cancer development" was a thought experiment where an extrinsic mutation is introduced into the environment, increasing the cancer risk by a factor of four (*2*). Whil e the lscd would change little because mutagens do not actively promote cell division, the lifetime risk of cancer would increase by a factor of four (*2*). Therefore, Tomasetti and Vogelstein's lscd model and subsequent correlation analysis would yield the same relations, whether or not m utagens were present. Using mathematical models on real-world data, Wu *et al.* consistently estimated that extrinsic factors contribute >70-9 0% in most cancers (*2*). Because of these new findings, Tomasetti and Vogelstein along with Lu Li published "Stem cell divisions, somatic m utations, cancer etiology, and cancer prevention", a follow-up article that clarified their "bad luck" hypothesis, addressing many concerns in their previous article (*3*).

It is widely accepted that cancer arises from mutations that may be hereditary, induced by environmental exposure, or the result of DNA repli cation errors (*2, 8, 9*). Yet, the scientific debate continues between Tomasetti and Wu. Tomasetti *et al.* have e xtended their analysis to include driver gene mutations classified into three categories: environmental (E), hereditary (H), and replicative (R). In most cancers, three driver gene mutations are required for tumorigenesis to occur (*3*). Using a similar thought experiment as Wu *et al.*, where exposure to an environmental mutagen causes a ten-fold increase in cancer, 90% of cancers would be preventable by simply a voiding exposure to the mutagen (*3*). However, 40% of cancers would still be attributed to R-driver gene mutations (*3*). On the surface, Tomasetti and Vogelstein's result may be surprising, but the concept of a stochastic and unpreventable cancer is n ot new. Previous research from Cancer Research UK highlighted that exposure to 14 extrinsic factors was attributed to only 42.7% of cancer in the UK in 2010 (*10*). This suggests that 57.3% of cancers could not be attributed to extrinsic factors, echoing Tomasetti and Vogelstein's fin dings.

The scientific community must consider the greater implications of these results on how it guides primary and secondary cancer effort prevent ion. Tomasetti *et al.*'s classification of deterministic and replicative tumors may better address important public health aspects of cancer prevention. Primary prevention can achieve maximum benefit by focusing on deterministic tumors through preventative measures such as smoking cessatio n to minimize lung cancer. For replicative tumors, primary prevention efforts are unlikely to be effective; focus should be placed on secondary preve ntion through early-targeted screening. Replicative tumors should not diminish the importance of primary prevention but highlight that not all cancer s can be prevented by avoiding environmental risks. Ultimately, we may never resolve the exact contribution of intrinsic and extrinsic factors to can cer; however, findings from both Tomasetti and Wu should be channeled towards quantifying cancer-causing constituents and guiding public health throu gh primary and secondary cancer prevention.

Competing interests
The authors declare that they have no competing interests.

Author details
[1] Department of Cellular and Molecular Medicine, University of Ottawa, 451 Smyth Rd, K1H 8M5, Ottawa, Canada. [2] Department of Biochemistry, Microbiology and Immunology, University of Ottawa, 451 Smyth Road, K1H 8M5, Ottawa, Canada.

References

1. C. Tomasetti, B. Vogelstein, *Science* **347**, 78 (2015).
2. S. Wu, S. Powers, W. Zhu, Y. A. Hannun, *Nature* **529**, 43 (2016).
3. C. Tomasetti, L. Li, B. Vogelstein, *Science* **355**, 1330 (2017).
4. C. Tomasetti, *et al.*, *Nature* **548**, E13 (2017).

5. M. C. Tammemagi, C. D. Berg, T. L. Riley, C. R. Cunningham, K. L. Taylor, *J. Natl. Cancer Inst.* **106**, dju084 (2014).
6. N. M. Kanodra, G. A. Silvestri, N. T. Tanner, *Cancer* **121**, 1347 (2015).
7. D. M. Burns, *Cancer* **89**, 2506 (2000).
8. O. Fletcher, F. Dudbridge, *BMC Med* **12**, 195 (2014).
9. L. A. McGuinn, *et al.*, *Environ. Res.* **112**, 230 (2012).
10. D. M. Parkin, L. Boyd, L. C. Walker, *Br. J. Cancer* **105 Suppl 2**, 77 (2011).

Chromosomal instability and aneuploidy: a conundrum in cancer evolution

Jasmin Ali

Abstract
Chromosomal instability (CIN), defined as an increased rate of gain or loss of whole chromosomes, leads to aneuploid cells, which are cells that display an abnormal number of chromosomes. Both CIN and aneuploidy are hallmarks of cancer, yet the underlying mechanisms of CIN and aneuploidy and their impact on tumourigenesis have remained poorly defined. Although multiple mechanisms have been proposed to explain the role of CIN and aneuploidy in tumourigenesis, this review focuses on three principal pathways leading to CIN: spindle assembly checkpoint defects, merotelic attachments, and cohesion defects. Here, we provide a brief overview of the current understanding of the roles of these mechanisms in CIN and aneuploidy. We also present emerging evidence that contradicts the importance of certain mechanisms in cancer evolution. A clearer understanding of these fundamental pathways could prove to be helpful in developing effective cancer therapies.

Keywords: Chromosomal instability (CIN); Aneuploidy; Cancer; Spindle assembly checkpoint (SAC); Merotelic attachment; Cohesion defect; Tumour suppressor

Résumé
L'instabilité chromosomique (INC) est définie comme étant un taux accru de gain ou de perte de chromosomes entiers, qui mène à la formation de cellules aneuploïdes, des cellules avec un nombre anormal de chromosomes. Tous deux l'INC et l'aneuploïdie sont des caractéristiques du cancer, mais leurs mécanismes sous-jacents et leur impact sur la tumourogenèse demeurent ambigus. Bien que plusieurs mécanismes aient été proposés pour expliquer le rôle de l'INC et de l'aneuploïdie dans la tumourogenèse, cet article se concentre sur trois voies principales conduisant à l'INC : les défauts de points de contrôle de l'assemblage du fuseau mitotique, les attachements mérotéliques et les défauts de cohésion. Ici, nous fournissons un bref aperçu de la compréhension actuelle des rôles de ces mécanismes impliqués dans l'INC et l'aneuploïdie. Nous présentons également des preuves émergentes qui contredisent l'importance de certains mécanismes dans l'évolution du cancer. Une meilleure compréhension de ces voies fondamentales pourrait s'avérer utile dans le développement de thérapies anticancéreuses efficaces.

Mots Clés: Instabilité chromosomique (INC); Aneuploïdie; Cancer; Point de contrôle de l'assemblage du fuseau mitotique; Attachement mérotelique; Défaut de cohésion; Suppresseur de tumeur

Introduction

In any given species, a non-cancerous cell has a defined number of chromosomes with a characteristic genome. It is essential for cells to maintain this genomic integrity during cell division to produce properly functioning daughter cells. A failure in this process can lead to chromosomal instability (CIN), a type of genomic instability, which involves a high rate of gain or loss of whole chromosomes (*1*). Consequently, daughter cells present an abnormal number of chromosomes, a state referred to as aneuploidy. Both CIN and aneuploidy are hallmarks of cancer (*2, 3*).

Over a century ago, German zoologist Theodor Boveri examined sea urchin embryos that underwent abnormal mitotic divisions. Based on his own observations as well as those previously made by David Hansemann, Boveri hypothesized that aneuploidy could cause cancer (*4*). Boveri's hypothesis became the foundation on which many of the current mechanisms have been theorized. Over the decades, the consistent presence of aneuploid cells in cancers has amplified the belief that CIN and aneuploidy induce tumourigenesis (*5*). Nevertheless, the mechanisms underlying CIN and aneuploidy and how

Correspondence: jali086@uottawa.ca
Department of Biology, University of Ottawa, 30 Marie Curie, K1N 6N5, Ottawa, Canada

they enhance tumour formation are not yet fully understood. Currently, research has been investigating some of the control mechanisms associated with CIN.

To ensure proper chromosome segregation during cell division, eukaryotes have multiple programmed checks and controls. The spindle assembly checkpoint (SAC) is one of the main control mechanisms. In mammals, the SAC consists of multiple conserved proteins that coordinate with one another to prevent aneuploidy (*6*). Accordingly, it has been observed that a problem with the SAC can lead to CIN. Moreover, when spindle fibers bind to kinetochores in a specific, but improper configuration, they can escape SAC detection. These merotelic attachments can ultimately lead to the formation of aneuploid cells (*7, 8*). Chromosomal mis-segregation can also arise when there is a flaw in the cohesin complex, which is an important regulator that ensures the correct timing of chromosome division (*9*). Overall, these regulatory processes involve the cooperation of multiple factors to ensure accurate chromosome segregation (*10*). A defect in these control mechanisms can result in CIN and aneuploidy, thereby favouring cancer progression (*11*).

In this review, we provide an overview of the roles of some of the recurring elements in these mechanisms which include the spindle assembly checkpoint, kinetochore-spindle fibre attachments, and chromosome cohesion. We briefly review how disruptions in these key constituents can cause CIN and aneuploidy. Furthermore, we present recent findings that oppose the importance of these mechanisms in tumourigenesis. We offer a possible explanation for these conflicting perspectives by exploring aneuploidy as a tumour suppressor. Future research on these paradigms may help to better explain the role of CIN and aneuploidy in tumourigenesis. A profound understanding of these mechanisms could have an important impact on the development of cancer treatments.

On the highway to CIN

Throughout eukaryotic evolution, the pathways associated with accurate chromosome transmission have remained conserved and much of the knowledge about CIN and aneuploidy has been acquired by studying model organisms, such as mice and yeast (*12*). Although multiple mechanisms have been proposed to explain CIN, here we focus on some of the main contributors: a) defects in the SAC b) merotelic attachments and c) cohesion defects.

Defective spindle assembly checkpoint

The SAC is a major regulatory pathway of the cell cycle that monitors chromosome division. The SAC ensures all chromosomes are correctly attached to the spindle before entering anaphase. Spindle microtubules attach to the kinetochores, which are protein complexes that assemble at each centromere of the chromosome (*13*). Normally, unattached kinetochores will signal the SAC to cease mitosis, preventing the loss or gain of a chromosome in a daughter cell (*14*).

On a molecular level, the SAC is comprised of multiple proteins that arrest mitosis. Some of the conserved SAC proteins include the 'mitotic-arrest deficient' (Mad) proteins Mad1, Mad2, and Mad3 and the 'budding uninhibited' by benzimidazole (Bub) proteins Bub1, BubR1, Bub3 (*14*). The mitotic checkpoint complex (MCC) is formed when Mad3/BubR1, Mad2, and Bub3 associate with Cdc20, an activator of the anaphase-promoting complex/cyclosome (APC/C). The subsequent conformational change of the APC inhibits its E3 ubiquitin ligase activity, thereby delaying the onset of anaphase (*15*). This delay allows for chromosomes to achieve the proper bipolar spindle attachment, ensuring the fidelity of chromosome segregation during mitosis (*16*).

Unsurprisingly, defective SAC components have been associated with CIN and cancer. Studies with testicular germ cell tumours showed reduced Mad2 protein expression in 6 of 8 cell lines (*17*). The identification of mutations in the *Mad2* gene in a breast cancer line and in numerous gastric cancer tumour cell lines corroborated this finding (*18*). In another case, the mutational inactivation of a human homologue of the *Bub1* gene was found in cancer cells presenting CIN (*19*). All these findings imply mitotic checkpoint defects are necessary for the progression of CIN and tumourigenesis. However, further experiments deem the relationship between SAC defects and tumourigenesis to be more intricate.

The complexity in the correlation between SAC defects and cancer development has been investigated by experiments with mice. Mouse models demonstrate that while homozygous deletion of SAC genes is lethal, mice heterozygous for the genes are viable and have an increased chromosomal mis-segregation rate (*18*). Although this finding suggests that defective SAC genes are linked with CIN, it has been observed that only some of the heterozygous mice spontaneously form tumours later in life, while other mice that are heterozygous for *Bub1*, *BubR1*, or *Bub3* remain tumour-free (*20*). Interestingly, when the two heterozygous groups are compared, both groups have similar levels of aneuploidy in spleen cells and mouse embryonic fibroblasts (*18*). Such observations put into question the association of CIN and tumourigenesis with SAC defects. Indeed, further research has demonstrated that multiple cancer cells have functional mitotic checkpoints, despite displaying CIN and aneuploidy (*21*). This indicates that a defective mitotic checkpoint may not be an integral constituent for the formation of tumours.

Merotelic attachments

In normal cellular divisions, kinetochores bind with microtubules from opposing spindles. However, merotelic

attachments occur when a single kinetochore attaches to fibers from both poles of the spindle (*10*). This kind of improper attachment is common and is usually corrected early in mitosis (*7*). Unlike other forms of attachment, merotelic attachments create kinetochore tension allowing them to bypass the mitotic checkpoint (*8*). Studies using oocytes demonstrate that merotelic attachments silence Mad2-signalling which contributes to the inactivation of the mitotic checkpoint and to chromosome missegregation in wild-type MII oocytes (*22*). When this improper attachment continues into anaphase, it can lead to the presence of lagging chromatids, which followed by cytokinesis, can give rise to aneuploid cells (*7*). To explain the frequent presence of this type of attachment, several mechanisms have been proposed, amongst which, centrosome amplification correlates strongly with CIN (*23*). Current research also demonstrates the importance of timely centrosome division, an aspect that was historically overlooked.

Because supernumerary centrosomes can form multipolar spindles, which appear in tumours, it was proposed that multipolar divisions were drivers of CIN and tumourigenesis (*24*). However, the rarity and the detrimental impact of multipolar divisions to cell proliferation led researchers to conclude that multipolar metaphases are transient (*25*). Instead, the geometry of these transient intermediates promotes merotelic attachments, and thereby increases the frequency of lagging chromosomes in bipolar anaphase, following centrosome clustering (*26*). Sure enough, a link between centrosome amplification and merotelic attachments has been observed *in vivo* (*10*). To determine if supernumerary chromosomes could lead to aneuploidy in mice, researchers isolated and analyzed epidermal cells. While not a single of the 78 control cells were aneuploid, the cells from mice with centrosome amplification showed 23 aneuploid cells out of 99 cells (*23*). Research does support the increase of aneuploid cells with supernumerary centrosomes. In humans, the presence of abnormal centrosome numbers has been observed in various malignant tumours and has more notably been abundant in high grade metastatic breast adenocarcinoma (*27*). Consequently, centrosome amplification and merotelic attachments continue to be probable mechanisms leading to CIN.

In addition to centrosome amplification, the timing of centrosome division is becoming an increasingly significant factor in understanding CIN and aneuploidy. Centrosome separation is a regulated mechanism that commences early in the cell cycle to ensure the bipolar spindle accurately divides the duplicated chromosome amongst the two daughter cells (*28*). Initial work by Silkworth and Cimini indicated that delayed centrosome separation allowed a geometry in which two spindle poles were proximal to one another, thus favouring merotelic attachments (*29*). Recent research, however, provides a contradictory observation. Studies with mice revealed overexpressed Cyclin B2 hyperactivates aurora-A-mediated Plk1, which causes accelerated centrosome separation and a recurrence of lagging chromosomes (*28*). Although this study suggests that an accelerated centrosome separation favours an increase in merotelic formation, the mechanism remains to be elucidated. Considering that both, a delay and an acceleration of centrosome division increases frequency of merotelic attachments, it emphasizes the importance of this factor in CIN.

Cohesion defects

Cohesion plays an integral role in proper genome transmission. Along with serving a purpose in DNA repair and gene expression, cohesion prevents the premature segregation by tethering sister chromatids together from S phase until the metaphase-to-anaphase transition (*30, 31*).

In a properly segregating cell, cohesion between the sister chromatids remains intact through the G2 and M phases of the cell cycle and then dissolves at anaphase onset following SAC activation (*18*). Cohesion is achieved by the evolutionarily conserved cohesin complex (*32*). In humans and mice, the complex is composed of four core subunits. The structural maintenance of chromosomes (Smc) proteins, Smc1 and Smc3, heterodimerize to form a V-shape (*9*). Another protein, Stag1-3, associates with a kleisin protein, Re8, thereby completing the cohesin complex (*33*). Defects in cohesion have been observed to cause CIN and aneuploidy.

By sequencing human homologues of genes known to cause CIN in budding yeast, Barber *et al.* were able to identify mutations in genes responsible for regulating sister chromatid cohesion (*12*). The Smc1, Smc3, and Stag3 proteins were all found to be mutated in 9 out of 132 colorectal adenocarcinomas (*12*). Although the direct relevance of these mutations to CIN remains ambiguous, research with *Stag2* cultivated a causative link between cohesion defects and CIN. The targeted inactivation of *Stag2* in numerous tumours led to defective chromatid cohesion and a rise in aneuploidy, while the targeted correction of mutant alleles resulted in enhanced chromosomal stability (*3*). Yeast and mice models concurred with these findings (*34, 35*). However, more recent studies demonstrate mixed results and dispute the role of *Stag2* in aneuploidy.

Current research with mutated cohesins in naturally-occurring human tumours indicate little to no correlation to aneuploidy (*36*). This is supported by the presence of euploid tumours in bladder cancers, despite recurrent inactivation of *Stag2* (*37*). To understand how *Stag2* mutations may affect cohesion, Kim *et al* introduced nine

tumour-derived mutations, including nonsense and missense mutations into cultured human cells (*38*). Their findings showed that only the nonsense mutations led to cohesion defects and only one of the nine mutations caused changes in chromosome counts (*38*). These observations indicate that not all tumour-derived *Stag2* mutations have a fundamental role in cohesion defects and aneuploidy. However, the mechanistic basis behind this phenomenon is presently undetermined. In the future, determining the precise functional consequences of different kinds of mutations in cohesion genes could provide insight on their impact in aneuploidy and cancer formation.

Aneuploidy: a double-edged sword

It has been commonly believed that aneuploidy plays a critical role in cancer progression. Most recently, research has implicated a novel perspective, in which aneuploidy works as a tumour suppressor. Sheltzer *et al* observed that single-chromosome gains, which consisted of the chromosomes mChr1, mChr13, mChr16, mChr19, hChr3, and hChr5, conferred the trisomic cells a reduced tumourigenicity in comparison to their euploid counterparts (*2*).

More remarkably, certain aneuploidies have both tumour-promoting and tumour-suppressing characteristics. Such an effect can be observed in Down syndrome (trisomy 21) patients. On one hand, children with Down syndrome have an elevated incidence of certain kinds of leukemia such as acute myeloid and lymphoblastic leukemia (*39*). On the other hand, they exhibit a lower risk of developing most solid tumours (*40*). Mouse models for trisomy 21 reflect such findings. Studies have shown that the gain of a third copy of the Down syndrome critical region-1 (*Dscr1*) gene was sufficient to limit the proliferation of lung tumours by decreasing tumour vascularization and increasing apoptosis of the tumour cells (*41*).

Because the expression of multiple genes is affected when an extra chromosome is gained, a proposed hypothesis is that the net effect of all gene expression alterations, some of which can be tumour-promoting or tumour-suppressing, dictates whether the aneuploidy is oncogenic or tumour-protective (*1*). This line of thought could provide insight as to why mechanisms enhance tumour formation in certain contexts, while in other circumstances, they do not appear to play a substantial role. Indeed, it has been discovered that while the surplus of the SAC genes, *Mad2* and *Bub1*, may have tumourigenic effects, the overexpression of *BubR1* can counteract defects that affect the mitotic checkpoint and/or kinetochore-microtubule attachments (*42*). Moreover, mouse embryonic fibroblasts that are trisomic exhibit impaired immortalization and less growth (*43*). A molecular understanding of such observations could be exploited in the future to advance aneuploid-specific therapies.

Concluding remarks

Although CIN and aneuploidy have been observed for over a century, research has only begun characterizing the roles of these mechanisms at the molecular level. In doing so, it is apparent that the relationship between CIN, aneuploidy, and tumourigenesis is more complex than what was previously hypothesized. In this review, we summarized literature studying how defects in the SAC, in microtubule-kinetochore attachments, and in the cohesin complex can be sources of CIN and tumourigenesis. We highlighted evidence that contradicted these findings. Lastly, to reconcile these two opposing views, we presented how aneuploidy can be both tumour-promoting and tumour-protective under certain conditions. In future work, it may be useful to revisit how SAC genes influence the expression of one another. SAC genes have been associated with multiple cellular processes. Could certain contexts cause the expression of certain SAC genes to silence the expression of others? How would this affect CIN and cancer evolution? Are centrosome amplification and centrosome division interconnected? If so, how do supernumerary centrosomes affect centrosome dynamics or vice-versa? At what point during tumourigenesis and in which environments do *Stag2* mutations occur? Further investigations into these areas could provide useful information to devise alternative strategies to combat cancer.

Competing interests

The author declares that she has no competing interests.

Acknowledgements

This was work was supported in part by NSERC grant number 000000-1999

References

1. M. Giam, G. Rancati, *Cell Div* **10**, 3 (2015).
2. J. M. Sheltzer, *et al.*, *Cancer Cell* **31**, 240 (2017).
3. D. A. Solomon, *et al.*, *Science* **333**, 1039 (2011).
4. A. J. Holland, D. W. Cleveland, *Nat. Rev. Mol. Cell Biol.* **10**, 478 (2009).
5. H. Rajagopalan, C. Lengauer, *Nature* **432**, 338 (2004).
6. F. Marchetti, S. Venkatachalam, *Cell Cycle* **9**, 58 (2010).
7. J. Gregan, S. Polakova, L. Zhang, I. M. Tolić-Nørrelykke, D. Cimini, *Trends Cell Biol.* **21**, 374 (2011).
8. A. A. Guerrero, C. Martinez-A, K. H. van Wely, *Cell Div* **5**, 13 (2010).
9. T. Gligoris, J. Lowe, *Trends Cell Biol.* **26**, 680 (2016).
10. D. J. Gordon, B. Resio, D. Pellman, *Nat. Rev. Genet.* **13**, 189 (2012).
11. K. Tanaka, T. Hirota, *Biochim. Biophys. Acta* **1866**, 64 (2016).
12. T. D. Barber, *et al.*, *Proc. Natl. Acad. Sci. U.S.A.* **105**, 3443 (2008).
13. P. Lara-Gonzalez, F. G. Westhorpe, S. S. Taylor, *Curr. Biol.* **22**, R966 (2012).
14. T. Lischetti, J. Nilsson, *Mol Cell Oncol* **2**, e970484 (2015).
15. F. Herzog, *et al.*, *Science* **323**, 1477 (2009).
16. G. J. Gorbsky, *FEBS J.* **282**, 2471 (2015).
17. M. K. Fung, *et al.*, *Biochim. Biophys. Acta* **1773**, 821 (2007).
18. S. L. Thompson, S. F. Bakhoum, D. A. Compton, *Curr. Biol.* **20**, R285 (2010).
19. D. P. Cahill, *et al.*, *Nature* **392**, 300 (1998).

20. M. E. Burkard, B. A. Weaver, *Cancer Discov* **7**, 134 (2017).
21. B. D. Vitre, D. W. Cleveland, *Curr. Opin. Cell Biol.* **24**, 809 (2012).
22. A. Kouznetsova, A. Hernandez-Hernandez, C. Hoog, *Nat Commun* **5**, 4409 (2014).
23. M. S. Levine, *et al.*, *Dev. Cell* **40**, 313 (2017).
24. A. Krämer, B. Maier, J. Bartek, *Mol Oncol* **5**, 324 (2011).
25. S. A. Godinho, D. Pellman, *Philos. Trans. R. Soc. Lond., B, Biol. Sci.* **369** (2014).
26. N. J. Ganem, S. A. Godinho, D. Pellman, *Nature* **460**, 278 (2009).
27. J. Y. Chan, *Int. J. Biol. Sci.* **7**, 1122 (2011).
28. H. J. Nam, J. M. van Deursen, *Nat. Cell Biol.* **16**, 538 (2014).
29. W. T. Silkworth, I. K. Nardi, R. Paul, A. Mogilner, D. Cimini, *Mol. Biol. Cell* **23**, 401 (2012).
30. K. Nasmyth, *Nat. Cell Biol.* **13**, 1170 (2011).
31. D. Dorsett, *Chromosoma* **116**, 1 (2007).
32. J. Gerton, *PLoS Biol.* **3**, e94 (2005).
33. J. M. Cheng, Y. X. Liu, *Int J Mol Sci* **18**, 1578 (2017).
34. S. Covo, C. M. Puccia, J. L. Argueso, D. A. Gordenin, M. A. Resnick, *Genetics* **196**, 373 (2014).
35. S. Remeseiro, *et al.*, *EMBO J.* **31**, 2076 (2012).
36. V. K. Hill, J. S. Kim, T. Waldman, *Biochim. Biophys. Acta* **1866**, 1 (2016).
37. C. Balbás-Martinez, *et al.*, *Nat. Genet.* **45**, 1464 (2013).
38. J. S. Kim, *et al.*, *PLoS Genet.* **12**, e1005865 (2016).
39. C. M. Zwaan, D. Reinhardt, J. Hitzler, P. Vyas, *Hematol. Oncol. Clin. North Am.* **24**, 19 (2010).
40. D. Nižetić, J. Groet, *Nat. Rev. Cancer* **12**, 721 (2012).
41. S. Ryeom, *et al.*, *Cancer Cell* **13**, 420 (2008).
42. D. J. Baker, *et al.*, *Nat. Cell Biol.* **15**, 96 (2013).
43. B. R. Williams, *et al.*, *Science* **322**, 703 (2008).

A spherically topological analysis of stationary black holes

Benjamin Puzantian

Abstract A black hole with zero angular momentum is said to be stationary and under certain conditions such a black hole can represented as a sphere. This review examines Hawking's topology theorem, the Schwarzschild metric, novel solutions to Einstein's equations, resonances of hyperbolic orbits around the event horizon for spherical, stationary black holes, and analyzes their importance. It is suggested, that in the spherical stationary black hole case, the Fourier analysis can be used to find the resonances due to Geometric scattering of hyperbolic orbits and thus the outgoing energy fields from the event horizon can be found more precisely; allowing for the adequate signal processing analysis to be found for such a field.

Keywords: Stationary black holes; General relativity; Fourier analysis; Hyperbolic orbits; Quasi-gravity; Geometric scattering

Résumé
Un trou noir avec un moment cinétique nul est dit stationnaire. Dans certaines conditions, un tel trou noir peut être représenté comme une sphère. Cette article examine le théorème de topologie de Hawking, la métrique de Schwarzschild, les nouvelles solutions aux équations d'Einstein, les résonances des orbites hyperboliques autour de l'horizon des événements pour les trous noirs stationnaires et sphériques, et analyse leur importance. Dans le cas du trou noir sphérique stationnaire, on suggère l'utilisation de l'analyse de Fourier pour trouver les résonances dues à la dispersion géométrique des orbites hyperboliques. Ainsi, on peut trouver les champs énergétiques sortants de l'horizon des événements de façon plus précise ; permettant l'analyse de traitement du signal adéquat pour un tel champ.

Mots Clés: Trous noirs stationnaires; Relativité générale; Analyse de Fourier; Orbites hyperboliques; Quasi-gravité; Diffusion géométrique

Introduction

In 1915, on the front lines of World War I, Schwarzschild calculated and discovered, through Einstein's equations, large masses that significantly distort the fabric of space-time that are known today as black holes. In this review, Hawking's topology theorem, and the special case of the Kerr metric of stationary black holes are examined. Furthermore, novel solutions to Einstein's equations, and resonances due to geometric scattering of hyperbolic orbits around the event horizon of stationary spherical black holes are outlined, and their hallmarks are discussed. This paper aims to offer an introductory outlook on the topology of spherical black holes. Moreover, it is argued that finding a spherical metric representing the hyperbolic behaviour of matter around the event horizons of stationary black holes will allow for adequate Fourier analysis calculations to obtain the photonic energy fields radiating away from the event horizon.

Correspondence: bpuza021@uottawa.ca
Department of Physics, University of Ottawa, 598 King Edward, K1N 6N5, Ottawa, Canada

Schwarzschild metric: a special case of the Kerr metric and null geodesics

The metric that represents the stationary axisymmetric (that is, in the well-behaved outside domain rotating case when the Killing vector that generates the stationary symmetry becomes spacelike) black hole equilibrium state can be represented by the following Kerr metric:

$$\begin{aligned} ds^2 &= (r^2 + a^2 cos^2\theta)(d\theta^2 + sin^2\phi^2) \\ &+ 2(du + asin^2\theta d\phi)(dr + asin^2\theta d\phi) \\ &- (1 - \frac{2mr}{r^2 + a^2 cos^2\theta})(du + asin^2\theta d\phi)^2 \end{aligned} \quad (1)$$

where a is a real constant, r is the radius from the event horizon, and u is the time element (*1*). When the angular momentum ma and the Schwarzschild mass m are zero, then the special case of the Kerr metric, called the Schwarzschild metric, can be seen to be:

$$\begin{aligned} ds^2 &= r^2(d\theta^2 + sin^2\theta d\phi^2) \\ &+ \frac{dr^2}{1-\frac{2m}{r}} \\ &- (1-\frac{2m}{r})dt^2 \end{aligned} \quad (2)$$

where $r = 2m$ is the location where the field becomes weak in terms of the mass (*1*).

When an outgoing null coordinate patch is analyzed, the Kerr metric at $a = 0$ becomes:

$$\begin{aligned} ds^2 &= -(1-\frac{2m}{r})du^2 + 2dudr \\ &+ r^2dudr + r^2d\theta^2 \\ &+ sin^2\theta d\phi^2 \end{aligned} \quad (3)$$

where $x^0 = u$, $x^1 = r$, $x^2 = \theta$, $x^3 = \phi$ (*1*), that is the usual spherical coordinate system.

Hawking's Topology Theorem: The Stationary Case

It has been shown that non-rotating stars of $M > M_\odot$ (solar mass) will eventually deplete all of their nuclear fuel and undertake catastrophic collapse, causing a significant distortion in the fabric of spacetime. However, if such a collapse is said to be spherically symmetric, then it can be characterized using the Schwarzschild metric (*2*). The Schwarzschild metric obeys the following characteristics:

1. The star's surface will exist inside the Schwarzschild radius $R = \frac{2G}{c^2}M$, where G is the universal gravitational constant, c is the speed of light and M is the mass of the black hole (*2*). Such a surface is said to be a closed trapped surface; that is, a space-like 2-surface such that both future directed families of null geodesics converge at each's respective future directed families of null geodesics orthogonal to it converge i.e. such a strong gravitational field that outwardly travelling light is pushed inwards will exist) (*3, 4*).
2. There exists a spacetime singularity (*2*).
3. An observer positioned outside the singularity and the Schwarzschild radius will not be able to physically observe the inside of the black hole (*2*). Therefore, physical theories inside the Schwarzschild radius are said to be unachievable (*2*). However, through the Cauchy data on the spacelike surface outside and near the Schwarzschild radius, physical theories can be predicted (*2*).

If such a collapse occurs under these conditions (*5*) and obeys the Schwarzschild metric, it must then be strongly asymptotic and thus stationary (*2*). Indeed, matter in proximity to this space obeys Maxwell's equations; therefore, the matter in this space can be described with well-behaved hyperbolic equations (*2*). Evidently, asymptotic stationary black holes will have a Killing vector tangent to the event horizon because they are invariant under the horizontal parameter transformation (*2*). Moreover, Israel (*5, 6*) showed that if the black hole is stationary, static, and is empty or contains only a Maxwell field, then the solution will have spherical symmetry. However, if the space is not empty then the solutions on the event horizons will be directed along the null generators (*2*).

A general result of Lichnerowicz (*7*) conveys that within a stationary and empty black hole there exists a region such that the Killing vector is spacelike (*2*). One can conclude that the event horizon of this space will be rotating with respect to infinity because a particle that has a trajectory along the null geodesic generator of the horizon is moving with respect to the stationary frame (or the integral curves of the Killing vector) (*2*).

Essentially, Hawking's black hole topology theorem forms the event horizon into cross sectional spheres in the case where the black hole obeys the dominant energy condition (that is the condition that allows the mass-energy of the universe can never flow at a speed faster then the speed of light and contributes to the evolution of universe) and is stationary in four dimensional asymptotically flat spacetimes (*2, 8*).

Galloway and Schoen (*9*) extended Hawking's theorem of black hole topology to higher dimensions and concluded that in higher dimensions, stationary black holes are not necessarily spherical (*7*). It was shown that the spacetime $(M^{\pi+1}, g)$ obeying the dominant energy condition also satisfies the Einstein equations:

$$R_{ab} - \frac{1}{2}Rg_{ab} = T_{ab} \quad (4)$$

if, in addition, the energy-momentum tensor T satisfies $T(X,Y) = T_{ab}X^aY^a \geq 0$ for the vectors X, Y (*7*). For dimensions $n \geq 3$, there exists a space-like hypersurface in the space-time $(M^{\pi+1}, g)$ (*7*).If the outer apparent horizon, $\sum^{n-1}$ is of positive in V^n unless $n = 3, 4$ (or Ricci flat) that is of induced metric and thus both the tensors X and $T_{ab}U^aK^b$ vanish on $\sum$ (*7*).

A special solution that exists for dimension $dim\, M = 5$ or $dim \sum = 3$ (assuming $\sum$ is orientable) is due to calculations by Schoen-Yau (*10, 11*) and Gromov-Lawson (*12, 13*). The $\sum$'s topology is a finite connected spherical sum of spaces (*7*). This sum of spherical spaces can be expressed as a connected sum of spheres by the prime decomposition theorem (*7*).

Hence, Hawking's topology theorem elegantly states that when black holes are stationary they can unquestionably be represented topologically as spheres. Such a topology can be manipulated mathematically to find the signals of the energy fields of photons nearby through Fourier analysis. The energy fields of photons will be discussed in the upcoming sections.

Solutions to Einstein's Equations in Spherical Black Holes

The theory of quasi-topological gravity has well-defined properties on spherically symmetric backgrounds (*14–19*) that allow the field equations to reduce to second order differential equations with exact solutions (*20*). If one were to maximize these symmetric spherical backgrounds, then the corresponding linearized equations of motion would suitably coincide with the Einsteinian linearized equations (*20*). While quasi-gravity is a useful theory for its avoiding the extra degrees of freedom required in Einsteinian gravity, it only becomes non-trivial in dimensions (*20*).

Where the theory of quasi-gravity is non-trivial in dimensions $n \geq 5$, the theory of Einsteinian cubic gravity is non-trivial in four dimensions, consequently allowing for static spherically symmetric solutions (*21, 22*) to be represented as:

$$ds^2 = -N^2 f dt^2 + \frac{dr^2}{f} + r^2 d \sum_{(d-2)k}^{2} \tag{5}$$

where N is a constant, and $d\sum_{(d-2)k}^{2}$ is the line element on a surface of constant scalar curvature $K = +1, 0, -1$ corresponding respectively to spherical, flat and hyperbolic topologies (*20*). The solution (4) to the Einsteinian cubic gravity in four dimensions has a Schwarzschild-like solution that is not true in higher dimensions (*21, 22*).

The general metric for all dimensions was discovered by Hennigar et al. [20]:

$$f(r) = 4\pi T(r - r_+) + \sum_{i=2}^{n} a_n (r - r_+)^n \tag{6}$$

where T is the Hawking temperature, r is the radius of the event horizon,r_+ is the outward radius from the black hole, and a_n is the usual Taylor Series expansion coefficient (*20*).

The Taylor series expansion about $f(r)$ shows the difference between the black hole's outer radius r_+ and its inner radius r. This difference characterizes the behaviour near the event horizon (*20*). Therefore, Hennigar *et al.*'s quasi-topological gravity describes gravitational fields around the event horizon of black holes and compares the numerical results as the fields are emitted. The expansion about the event horizon of a spherical and the asymptotical expansion of a flat black hole are consistent; hence, the theory was seen to be numerically accurate.

Nevertheless, Hennigar *et al.* do not assess what are the physical implication of their quasi-topological gravity theory.

Geometric Scattering and Resonances Around the Event Horizon

Geometric scattering is a popular model (*23–26*) that is used when describing the association between the resonances and a representative sphere of hyperbolic orbits in the stationary black hole case. Quasi-normal modes (resonances) (*27*) on a well-defined strip below the real axis with angular momenta l can be approximated by the "pseudo-poles" (*28*):

$$\left(\pm 1 \pm \frac{1}{2} - \frac{i}{2}(k + \frac{1}{2}) \right) \frac{(1 - 9\Lambda m^2)^{1/2}}{3^{3/2} m} \tag{7}$$

where $l = 1, 2, \ldots, k (k = 0, 1, \ldots)$ with the resonances having multiplicity $2l + 1$, Λ is the cosmological constant, and m is the mass of the black hole. Recall that the Schwarzschild stationary black hole case occurs when $\Lambda = 0$ (more specifically, when the angular momentum is zero).

The resonances of black holes can be thought of as pure tones, or more precisely; as frequencies and rates of damping of signals emitted by the black hole while in the company of perturbations (*27*). Therefore, the real part of a black hole resonance relates to the frequency of the emitted black hole signals while the imaginary part of the resonance relates to the signals' rate of decay in time (*28*). These significantly large pure tone resonance times are a property of the black hole and thus become independent of the perturbation (*28*). On the other hand, the stability of such a system under the perturbation will correspond to the distance from a reference point of the resonances (on the real axis) and thus at significantly larger distances the system will be more stable (*28*).

A hyperbolic operator to Schwarzschild black hole for the exterior of a black hole is:

$$\blacksquare g = \alpha^{-2} D_t^2 - \alpha^2 r^{-2} D_r (r^2 \alpha^2) - D_r \alpha^2 r^{-2} \Delta_w \tag{8}$$

where $\alpha = (1 - \frac{2m}{r} - \frac{1}{3}\Lambda r^2)^{1/2}$, and $D = \frac{1}{i}\partial$ and Δ_w are the positive Laplacian on the 2-surface (*28–30*). Correspondingly, particular resonances in the stationary scattering phenomena with special solutions of (8) $\blacksquare_g u = 0$, relating to the following operator on X:

$$P = \alpha^{-2} r^{-2} D_r (r^2 \alpha^2) D_r + \alpha^2 r^{-2} \Delta_w \tag{9}$$

where P is the scattering resonance operator (*28*). Through the method of the separation of variables and

the Regge-Wheeler transformation, a family of one-dimensional Schrödinger operators with potentials decaying at infinity that has some unique non-degenerate maxima can be acquired (*30*). This resulting family of one-dimensional Schrödinger operators can be represented by the Hamiltonian that is required to constitute a single hyperbolic trajectory that unfolds the trapped set from the classical flow of the black hole (*28*).

Evidently, the pure tones of black holes can be found, generally, by the Fourier analysis for hyperbolic orbits of spherical black holes. This will allow for a more rigorously general theorem of energy fields of particles being outward emitted by the stationary black holes then the manipulation of the spherical symmetry technique.

Conclusion

Hawking's topology theorem, and the special case of the Kerr metric of stationary black holes are examined. Furthermore, novel solutions to Einstein's equations, and resonances due to geometric scattering of hyperbolic orbits around the event horizon of stationary black holes are outlined and their hallmarks are discussed. On non-Euclidean space-times such as the extremely distorted Hawking topological space-time present around black holes, there do not exist theorems for the resonances on hyperbolic trajectories. Therefore, the spherical symmetry of the black hole must be manipulated order to find the resonances. Consequently, this paper suggests performing an appropriate volume transformation with a spherical Laplacian on the Schwarzschild metric such that it is then transformed into Fourier space. As a result, a theorem that describes the resonances of the hyperbolic trajectories can be found that is more exact and general then the spherical symmetry approach. In return, by applying the Fourier analysis in the spherical black hole case, a more exact theorem of the frequency that is emitted from the spherical black hole's signals under perturbations will be found. Indeed, future research using Fourier analysis will allow for the resulting frequency and decay in signal time to be articulated into a more precise theorem that describes energy fields emitted outwardly from the event horizon to infinity through signal processing in extremely distorted space-times with Hawking's topology-like geodesics.

Competing interests

The author declares that he has no competing interests.

References

1. B. Carter, *AIP Conference Proceedings* **841**, 29 (2006).
2. S. W. Hawking, *Comm. Math. Phys.* **25**, 152 (1972).
3. R. Penrose, *Phys. Rev. Lett.* **14**, 57 (1965).
4. C. DeWitt-Morette, J. Wheeler, B. S. R. Center, B. M. Institute, *Battelle Rencontres: 1967 Lectures in Mathematics and Physics* (Benjamin, 1968).
5. W. Israel, *Phys. Rev.* **164**, 1776 (1967).
6. W. Israel, *Comm. Math. Phys.* **8**, 245 (1968).
7. A. Lichnerowicz, *C. R. Acad. Sci. Paris Ser. A* .
8. S. Hawking, G. Ellis, *The Large Scale Structure of Space-Time*, Cambridge Monographs on Mathem (Cambridge University Press, 1973).
9. G. J. Galloway, R. Schoen, *Commun. Math. Phys.* **266**, 571 (2006).
10. R. Schoen, S.-T. Yau, *Annals of Mathematics* **110**, 127 (1979).
11. R. Schoen, S. T. Yau, *manuscripta mathematica* **28**, 159 (1979).
12. M. Gromov, H. B. Lawson, *Annals of Mathematics* **111**, 209 (1980).
13. M. Gromov, H. Lawson, *Publications Mathematiques de l'Institut des Hautes Etudes Scientifiques* **58**, 83 (1983).
14. J. Oliva, S. Ray, *Classical and Quantum Gravity* **27**, 225002 (2010).
15. J. Oliva, S. Ray, *Phys. Rev. D* **82**, 124030 (2010).
16. R. C. Myers, B. Robinson, *Journal of High Energy Physics* **2010**, 67 (2010).
17. R. C. Myers, M. F. Paulos, A. Sinha, *Journal of High Energy Physics* **2010**, 35 (2010).
18. A. Cisterna, L. Guajardo, M. Hassaïne, J. Oliva, *Journal of High Energy Physics* **2017**, 66 (2017).
19. A. Ghodsi, F. Najafi, *The European Physical Journal C* **77**, 559 (2017).
20. R. A. Hennigar, D. Kubizňák, R. B. Mann, *Phys. Rev. D* **95**, 104042 (2017).
21. R. A. Hennigar, R. B. Mann, *Phys. Rev. D* **95**, 064055 (2017).
22. P. Bueno, P. A. Cano, *Phys. Rev. D* **94**, 124051 (2016).
23. P. Briet, J. Combes, P. Duclos, *Journal of Mathematical Analysis and Applications* **126**, 90 (1987).
24. C. Gérard, *Mémoires de la Société Mathématique de France* **31**, 1 (1988).
25. R. R. Mazzeo, R. B. Melrose, *Journal of Functional Analysis* **75**, 260 (1987).
26. M. Zworski, *Inventiones mathematicae* **136**, 353 (1999).
27. S. Chandrasekhar, *The Mathematical Theory of Black Holes* (Springer Netherlands, Dordrecht, 1984), pp. 5–26.
28. A. S. Barreto, M. Zworski, *Math. Res. Lett.* **4**, 103 (1997).
29. S. Chandrasekhar, S. Detweiler, *Proceedings of the Royal Society of London. Series A, Mathematical and Physical Sciences* **344**, 441 (1975).
30. M.-B. A. Bachelot, Alain, *Annales de l'I.H.P. Physique théorique* **59**, 3 (1993).

Comparison of regenerative neurogenesis in response to CNS injury between adult zebrafish and mice

Kuan-En Chung

Abstract The difference between adult zebrafish and mice in their regenerative capacity following central nervous system (CNS) injury is influenced by the permissiveness of the brain microenvironment aside from the intrinsic neurogenic potential of the cell population. In adult zebrafish, glia cells largely retain their radial characteristics and neurogenic capacity, and the zebrafish brain shows full recovery after traumatic brain injury (TBI) as well as spinal cord injury (SCI). Conversely, in mice, radial glia (RG) have largely differentiated into astrocytes. Excluding certain brain regions, following TBI, reactive astrocytes that show the potential to become neural stem cells (NSCs) *in vitro* remain strictly non-neurogenic *in vivo* due to the presence of inhibitory factors in the microenvironment. Combined with prolonged inflammation and gliosis, injury to the CNS eventually results in formation of a glial scar further impeding regeneration. However in rodents, suppression of neurogenesis may be a protection mechanism against possible detrimental side-effects of neurogenesis in the long term.

Keywords: Regeneration; Adult neurogenesis; Zebrafish; Mouse; Traumatic brain injury; Spinal cord injury

Résumé
La différence entre le poisson zèbre adulte et les souris quant à leur capacité de régénération après une lésion du système nerveux central (SNC) est influencée par la permissivité du microenvironnement du cerveau, mis à part le potentiel neurogène intrinsèque de la population cellulaire. Chez le poisson zèbre adulte, les cellules gliales conservent en grande partie leurs caractéristiques radiales et leur capacité neurogène. De plus, le cerveau du poisson zèbre démontre un rétablissement complet après une lésion cérébrale traumatique (LCT) et une lésion de la moelle épinière (LME). Inversement, chez les souris, les cellules gliales se différencient en astrocytes. En excluant certaines régions du cerveau, après une LCT, les astrocytes réactifs qui ont le potentiel de devenir des cellules souches neurales (CSN) *in vitro* demeurent strictement non-neurogènes *in vivo*, en raison de facteurs inhibiteurs présents dans le microenvironnement. Combinée avec une inflammation prolongée et une gliose, une lésion du SNC aboutit finalement à la formation d'une cicatrice gliale qui entrave encore la régénération. Cependant, chez les rongeurs, la suppression de la neurogenèse peut constituer un mécanisme de protection contre les effets éventuels de la neurogenèse à long terme.

Mots Clés: Régénération; Neurogenèse adulte; Poisson zèbre; Souris; Lésion cérébrale traumatique; Lésion de la moelle épinière

Introduction

The adult zebrafish has an excellent ability to regenerate its CNS following TBI. TBI is characterized by physical injury to the brain that is not the result of a natural disease, in contrast to non-TBI such as neural degeneration due to stroke. Whereas mammals lack the capacity to do so save for a few areas such as the hippocampus (*1*).

Since regenerative capacities differ even across teleost and mammalian species, this review focuses on the comparison between zebrafish and mice specifically. It investigates the conserved molecular mechanisms regarding neurogenesis and neural stem cell (NSC) response following injury to the CNS, and reflects on the reasons of these differences from an evolutionary standpoint.

Correspondence: kchun091@uottawa.ca
Department of Biology, University of Ottawa, 30 Marie Curie, K1N 6N5, Ottawa, Canada

Regeneration in adult zebrafish CNS

Under physiological conditions, there is widespread neurogenesis in the zebrafish brain (*2*). While glial fibrillary acidic protein-positive (GFAP+) RG cells that reside in the ventricular zone (VZ) are a major NSC component (*3*), many other neuronal progenitors do not show GFAP or radial characteristics. For instance, neuroepithelial (NE) cells dominate the stem cell population for cerebellar regeneration (*4*). Even neurogenesis pathways show considerable heterogeneity: two distinct modes of neurogenesis, dorsal and ventral have been found in the zebrafish respectively in the dorsal and ventral forebrain. The dorsal stem cell niche is dominated by RG, while the ventral stem cell niche mainly has an NE population and shows more dependence on Fgf signalling (*5*). While previous research has suggested similarities between certain ventral stem cells of the zebrafish and the progenitors of the mammalian SVZ (*6*), the role of Fgf in the latter is less defined.

The well-known outcome in adult zebrafish following TBI is reactive neurogenesis and complete regeneration, yet only the response in the dorsal telencephalic NSC niche has been characterized to date. In response to injury, telencephalic RG cells proliferate and generate neuroblasts that migrate to the lesion site. Major responding RG cells express the *her4.1* gene, a target of Notch signaling, and they are thought to act directly as neuronal progenitors without undergoing dedifferentiation to a less specialized cellular state (*7*). The entire process is initiated by an acute inflammatory response and reactive gliosis that subsides within a few days: up-regulation of the M2 macrophage secretes anti-inflammatory cytokines, while microglia clears up toxic debris. Moreover, the inflammation event itself directly activates radial glial cells through cysteinyl leukotriene signalling (*8*). Subsequent neurogenesis quickly replaces the damaged neurons.

A successful regeneration consists of not only the activation of stem cells, but also incorporation into the existing circuit. While the details of successful neuronal integration into the adult zebrafish circuitry have not been examined to date, several factors have been identified. They could be proliferation factors that recruit NSCs, or permissive factors that allow the development of NSCs into long lasting neurons. Wnt and Notch signalling are known thus far to be involved in radial glia proliferation and neurogenesis following TBI: Wnt induces proliferation, while the RG-repressing Notch indirectly allows proliferation through its own decrease upon injury (*2*). As well, the *cxcr5* gene expression in RG is shown to permit its differentiation into neurons (*9*).

Differences also lie in the migration of newborn neurons to the injury site. For adult spinal cord injury in mammals, the failure of axons to navigate to the injury site may underlie the absence of neuronal replacement (*10*). Whereas for adult zebrafish, Fgf signalling induces radial glia to form a "glial bridge" that allows for newly formed axons to migrate over to the injury site. RG progenitors thus act as a navigation guide for their own derived neurons in the injury response (*11*). It is noteworthy that mice do show Fgf signalling during embryonic development, but it is down regulated after birth. When mouse astrocytes are treated with Fgf, they show the same potential to form a glial bridge (*11*). In addition of Notch1, connective tissue growth factor a (ctgfa) expression in and around radial glia helps the bridging and migration process following spinal cord injury in adult zebrafish (*12*). Though there is no evidence of ctgf playing a similar role in adult mice, it does promote gliogenesis in embryos (*13*) suggesting a conserved mechanism.

Regeneration in adult mouse mammalian CNS

One crucial difference between the zebrafish and the mice in their regenerative capacity is the absence of neurogenic radial glial cells in adult mice. Mammals have radial glia that originate from NE during embryonic CNS development, but the radial glia NSCs subsequently differentiate into intermediate progenitor cells (IPCs) which then give rise to astrocytes and oligodendrocytes (*14*). Astrocytes are developed from GFAP+ cells that lose their radial characteristic and become more differentiated (*15*). They still share the most morphological similarities with radial glia out of all mammalian glia types, but specialize in maintaining homeostasis at the cost of regenerative function. However, introduction of brain-derived neurotropic factor (BDNF) has shown to induce adult neurogenesis in areas including the striatum and septum of the lateral and third ventricles, as well as the thalamus and hypothalamus that were not expected to show such activity (*16*), and astrocytes have been shown to generate neurons upon stimulation *in vitro*, though fail to do so *in vivo* (*17*). This restriction may therefore be in part contributed by the microenvironment of the mammalian brain.

Regenerative neurogenesis in mice does occur in the dorsal subgranular zone (SGZ) of the hippocampus and the ventral subventricular zone (SVZ) of the lateral ventricles. Unlike the rest of the brain, astrocytes in these areas actively regulate differentiation and integration of new neurons (*18*) . Successful neurogenesis here is thought to be regulated by a variety of signalling factor in common with the zebrafish such as Wnt, Shh, Notch, BMP, neurotrophin and neurotransmitters (*19*). The NSC population comprises of Type B astrocytes in the SVZ and Type 1 (also known as radial glia-like) cells in the SGZ before differentiating into neuroblasts (*19*).

Interestingly, the extent of NSC proliferation and neuron maturation is somewhat dependent on the extent of TBI (*20*). But in contrast to zebrafish, even after integration of the new neurons into the brain circuit, synapses remained immature in morphology (*21*) or shows altered morphology compared to surrounding neurons with unclear functional impacts in the long run (*22*).

Unlike the zebrafish, the response of adult mice following TBI in brain regions outside of the SVZ and SGZ does not, save for the olfactory bulb, result in neuronal regeneration. Instead, intense inflammation and glial scarring are observed in complete contrast to the zebrafish. Although reactive astrocytes—astrocytes activated specifically following TBI—have the potential to be multipotent NSCs *in vitro*, the non-permissive environment *in vivo* prevents them from realizing this ability (*7*). What actually happens is that, in response to injury, NSCs proliferate and differentiate into neural progenitor cells (NPCs) that migrate from the SVZ (and the SVZ only) to the lesion site, just like injuries in the SVZ/SGZ. The proliferation factors associated include the rapamycin signaling pathway activation (*23*), Notch 1 (*24*). Chemokines expressed by macrophages and microglia attract NPCs to the injury site (*25*). The same signalling is not found in zebrafish. However, newborn SVZ neurons do not persist long nor mature where they need to be, that is, at the lesion site. This is thought to be due to extrinsic factors at the lesion site outside of the stem cell niche limiting SVZ differentiation. Surviving SVZ cells all end up becoming glial cells, not neurons that are needed to replace cell loss (*26, 27*).

There are several observable differences between the zebrafish and the mouse response to CNS injury. Unlike in zebrafish, the mammalian inflammatory response alone initiates gliosis, secondary tissue damage and lesion cavity expansion (*28*). Immediately following TBI, reactive astrocytes are mass recruited around the lesion site and promote extracellular matrix (ECM) protein deposition in forming the glial scar. However, astrogliosis at this stage serves to preserve tissue and repair the blood-brain barrier around the lesion site (*29*). Furthermore, recent research has demonstrated that astrocyte scar formation may actually support neuronal regrowth but only under artificial supply of axon-specific growth factors (*30*). While the early inflammation response activates both the pro-inflammatory M1 and the anti-inflammatory M2 immune cells, only the M1 response remains over time while the M2 deteriorates (*31*). Circulating macrophage and microglia then contribute to secondary tissue damage: Microglia releases pro-inflammatory neurotoxic and cytotoxic molecules such as cytokines and nitric oxide. Following the acute phase, neuroinflammation persists and spreads to regions surrounding the lesion site. The characteristic glial scar is the result of accumulation of astrocytes, extracellular protein deposition, persistence of leukocytes and inhibition of axonal regeneration around the lesion site, all leading to permanent scarring. There appears to be no benefit associated with the chronic response: it simply results in progressive brain deterioration, immune cell infiltration, and pro-inflammatory cytokines that suppress neurogenesis (*32*). Studies that aim to control the chronic response has shown to limit degeneration and improve functional recovery, but improvements are limited to the female mice (*33*). Interestingly, where inflammation can be avoided, axons have demonstrated an ability to extend even amidst degenerating white matter until they reach into the lesion site. This indicates that rather than universally hostile to regeneration, the reactive glial matrix at the lesion site itself appears to be the major barrier to neuronal growth (*34*). However, even in a dystrophic growth cone, the neuronal endings remain dynamic in their motility (*35*).

What stops growth cones at the site of the scar? Deposition of ECM debris during scarring mechanically blocks the axons, but there are also signals that actively inhibit them, in accordance with the assumption that it is the microenvironment around the lesion site that prevents neurogenesis. Several CNS myelin-derived proteins including the Nogo family, MAG, OMgp all work through the Nogo-66 receptor (NgR) to suppress neurogenesis (*36*). However, targeting Nogo does not increase neurogenesis despite improving functional recovery (*37*). In addition, reactive astrocytes release chondroitin sulphate proteoglycans (CSPGs) which inhibit axon growth. Even the function of these signalling factors differs between the mice and the zebrafish. In zebrafish, Nogo is actually growth permissive due to lacking a receptor domain necessary for growth inhibition (*38*), while CSPGs can guide optic nerve regeneration (*7*). And whereas *cxcr5* is responsible for radial glia differentiation into neurons in specific niches, the same gene in mice enhances SGZ cell proliferation but suppresses NPC population (*39*). Moreover, rho kinase, a molecule that inhibits neuron survival in mice (*40*) does not seem to work the same way in zebrafish besides aiding in neuronal development. Another inhibitory factor in mice is Olig2 which suppresses *Pax6*, a gene able to convert astrocytes into neurons *in vitro*. Suppression of Olig2 can lead to neurogenesis *in vivo* (*17*).

Evolutionary considerations

Similarities between SGZ/SVZ in mouse and neurogenic niches in the lateral areas of the dorsal/ventral telencephalon in zebrafish have been proposed (*5, 6, 41*) regarding their common function (*42*), neuroanatomy (*43*) or neuronal migration (*44, 45*), but not investigated in detail. A question is whether the vertebrate brain is by default permissive for neuronal regeneration while mammals have lost this capacity or somehow inhibited this

function; or it is by default inhibitory, but zebrafish have found a way to overcome this mechanism. Given the functional similarities between astrocytes and RG, and considering mechanisms retained in the mouse embryo but not the adult, the former scenario could be more likely. In this case, then, the course of mammalian evolution may eventually have selected against regeneration except for certain brain regions such as the hippocampus.

Besides the obvious advantage that adult neurogenesis confers to the organism in recovery from injuries, mice studies have also demonstrated the adaptive role of a neurogenic hippocampus in facilitating learning by optimizing new information storage (*46*). Neural networks in learning encounter the problem known as catastrophic interference, which is a dilemma between plasticity and stability of existing circuits. Interference of the existing circuitry may lead to loss of both old and new information. Neurogenesis in the hippocampus may have served as a strategy to resolve catastrophic interference by providing new neurons that store novel information without interfering with the existing circuit (*47*). On the other hand, neurogenesis may also aid learning by modifying the existing circuit, thereby clearing less relevant older memories to prevent them from interfering with new ones (*48*). Hippocampal neurogenesis is thus positively correlated with forgetting/new learning and negatively correlated with retention, and as such, mammals in adulthood generally decrease neurogenesis levels to resist changes to memory formation (*49*). For zebrafish, however, where survival largely depends on detecting chemical and visual cues in the aqueous environment rather than complex learning, neural plasticity is more exemplified in chemical and visual processing centers of the brain (*50*). In both scenarios, the adult neurogenesis response enhances the processing of novel information in an enriched environment. However, this may not always be the case for zebrafish; studies have shown that deprivation and novelty impact plasticity not as opposing factors, but both contribute in a stage-specific manner that is relative to the environmental context throughout time (*51*).

Even ignoring circuit interference, disadvantages of adult regenerative neurogenesis also exist. For mammals, recent discovery shows that the neurogenic burst following TBI actually depletes finite NPC storage in the hippocampus, leading to future decline in even basal rates of neurogenesis, but also increases susceptibility to chemical seizures (*52*). Perhaps, regular neurogenesis in zebrafish may render it immune to this disadvantage, yet robust neurogenic activity also has its downsides, namely brain tumour if improperly regulated. While tumour incidences are among one of the lowest in the brain (*53*), cancerous cells rise predominantly around the SVZ where neurogenesis is prominent. Less research has been done on tumour development in zebrafish focusing on its relationship to adult neurogenesis, however, overexpression of the certain genes that lead to tumours in mammals such as *KRAS* do not necessarily induce the same in zebrafish, suggesting different regulators of brain tumours across species (*54*).

Even the glial scar has proved to be of more value than it appears. Glial scarring in the early stage following TBI is integral to preserving tissue functionality around the lesion site (*29*). It may be that scarring to stop bleeding was more important in mammals' survival. For its part, zebrafish bypasses scar formation altogether by rapid replacement through neurogenesis following cell death (*55*). The same occurs in developing mammals until the radial glia are substituted by astrocytes, which may be a trade-off for specialized homeostasis at the cost of ready regeneration. Another possibility is that complete neuronal regeneration in adults may simply deplete too much energy for mammals. Given the complexity of the mammalian brain, rebuilding synaptic connections without disrupting the original circuit may involve a more complicated process that cost too much in energetics to be fully functional; whereas if partial repair ends up being more detrimental, discarding neurogenesis altogether may have been preferable. However, the consequences of temporary induction of neurogenesis following TBI are not yet clear. It is therefore suggested that more attention be drawn to potential adverse side-effects of overriding the inhibition that the mammalian brain has imposed on its own regenerative response.

Conclusion

The regenerative capacity difference between adult zebrafish and mice is in part contributed by inhibitory microenvironmental factors in the mammalian CNS which might limit an otherwise potentially neurogenic glia population repopulate the injured region. This inhibition may have evolved as an adaptive response to detrimental effects associated with neurogenesis. Given that the long term success of artificially inducing NSC proliferation remains ambiguous, future research that follows the survival and integration of newborn neurons as well as the fate of NSC populations post CNS injury could better characterize the possible roles that adult neurogenesis might play in mammals.

Competing interests

The author declare that she has no competing interests.

References

1. C. Kizil, J. Kaslin, V. Kroehne, M. Brand, *Dev Neurobiol* **72**, 429 (2012).
2. A. Alunni, L. Bally-Cuif, *Development* **143**, 741 (2016).
3. K. Johnson, *et al.*, *Glia* **64**, 1170 (2016).
4. J. Kaslin, V. Kroehne, J. Ganz, S. Hans, M. Brand, *Development* **144**, 3388 (2017).

5. J. Ganz, J. Kaslin, S. Hochmann, D. Freudenreich, M. Brand, *Glia* **58**, 1345 (2010).
6. B. Adolf, *et al.*, *Dev. Biol.* **295**, 278 (2006).
7. V. Kroehne, D. Freudenreich, S. Hans, J. Kaslin, M. Brand, *Development* **138**, 4831 (2011).
8. N. Kyritsis, *et al.*, *Science* **338**, 1353 (2012).
9. C. Kizil, *et al.*, *Neural Dev* **7**, 27 (2012).
10. M. Kerschensteiner, M. E. Schwab, J. W. Lichtman, T. Misgeld, *Nat. Med.* **11**, 572 (2005).
11. Y. Goldshmit, *et al.*, *J. Neurosci.* **32**, 7477 (2012).
12. M. H. Mokalled, *et al.*, *Science* **354**, 630 (2016).
13. F. A. Mendes, *et al.*, *PLoS ONE* **10**, e0133689 (2015).
14. A. Kriegstein, A. Alvarez-Buylla, *Annu. Rev. Neurosci.* **32**, 149 (2009).
15. N. Kishimoto, K. Shimizu, K. Sawamoto, *Disease Models & Mechanisms* **5**, 200 (2012).
16. V. Pencea, K. D. Bingaman, S. J. Wiegand, M. B. Luskin, *J. Neurosci.* **21**, 6706 (2001).
17. A. Buffo, *et al.*, *Proc. Natl. Acad. Sci. U.S.A.* **102**, 18183 (2005).
18. H. Song, C. F. Stevens, F. H. Gage, *Nature* **417**, 39 (2002).
19. A. M. Bond, G. L. Ming, H. Song, *Cell Stem Cell* **17**, 385 (2015).
20. X. Wang, X. Gao, S. Michalski, S. Zhao, J. Chen, *J. Neurotrauma* **33**, 721 (2016).
21. H. Nakatomi, *et al.*, *Cell* **110**, 429 (2002).
22. L. E. Villasana, G. L. Westbrook, E. Schnell, *Exp. Neurol.* **261**, 156 (2014).
23. X. Wang, P. Seekaew, X. Gao, J. Chen, *eNeuro* **3** (2016).
24. X. Wang, X. Mao, L. Xie, D. A. Greenberg, K. Jin, *J. Cereb. Blood Flow Metab.* **29**, 1644 (2009).
25. R. J. Gordon, A. L. McGregor, B. Connor, *Mol. Cell. Neurosci.* **41**, 219 (2009).
26. K. Yoshiya, *et al.*, *J. Neurotrauma* **20**, 1147 (2003).
27. E. H. Chang, *et al.*, *Front Neurosci* **10**, 332 (2016).
28. M. T. Fitch, C. Doller, C. K. Combs, G. E. Landreth, J. Silver, *J. Neurosci.* **19**, 8182 (1999).
29. J. R. Faulkner, *et al.*, *J. Neurosci.* **24**, 2143 (2004).
30. M. A. Anderson, *et al.*, *Nature* **532**, 195 (2016).
31. A. Kumar, D. M. Alvarez-Croda, B. A. Stoica, A. I. Faden, D. J. Loane, *J. Neurotrauma* **33**, 1732 (2016).
32. S. A. Acosta, *et al.*, *PLoS ONE* **8**, e53376 (2013).
33. Ert .
34. S. J. Davies, D. R. Goucher, C. Doller, J. Silver, *J. Neurosci.* **19**, 5810 (1999).
35. V. J. Tom, M. P. Steinmetz, J. H. Miller, C. M. Doller, J. Silver, *J. Neurosci.* **24**, 6531 (2004).
36. K. C. Wang, *et al.*, *Nature* **417**, 941 (2002).
37. D. J. Shepherd, S. Y. Tsai, T. E. O'Brien, R. G. Farrer, G. L. Kartje, *Front Neurosci* **10**, 467 (2016).
38. H. Abdesselem, A. Shypitsyna, G. P. Solis, V. Bodrikov, C. A. Stuermer, *J. Neurosci.* **29**, 15489 (2009).
39. M. J. Stuart, F. Corrigan, B. T. Baune, *J Neuroinflammation* **11**, 31 (2014).
40. N. Bye, K. J. Christie, A. Turbic, H. S. Basrai, A. M. Turnley, *Exp. Neurol.* **279**, 86 (2016).
41. J. Kaslin, J. Ganz, M. Brand, *Philos. Trans. R. Soc. Lond., B, Biol. Sci.* **363**, 101 (2008).
42. C. Broglio, *et al.*, *Brain Res. Bull.* **66**, 277 (2005).
43. C. Salas, C. Broglio, F. Rodriguez, *Brain Behav. Evol.* **62**, 72 (2003).
44. C. A. Byrd, P. C. Brunjes, *Ann. N. Y. Acad. Sci.* **855**, 274 (1998).
45. H. Grandel, J. Kaslin, J. Ganz, I. Wenzel, M. Brand, *Dev. Biol.* **295**, 263 (2006).
46. G. Alexander, R. Ingo, K. Gerd, *Hippocampus* **26**, 261 (2016).
47. W. Laurenz, R. M. J., K. Gerd, *Hippocampus* **16**, 329 (2006).
48. P. W. Frankland, S. A. Josselyn, *Neuropsychopharmacology* **41**, 382 (2016).
49. K. G. Akers, *et al.*, *Science* **344**, 598 (2014).
50. B. W. Lindsey, S. Di Donato, J. Kaslin, V. Tropepe, *Eur. J. Neurosci.* **40**, 3591 (2014).
51. B. W. Lindsey, V. Tropepe, *Dev Neurobiol* **74**, 1053 (2014).
52. E. J. Neuberger, B. Swietek, L. Corrubia, A. Prasanna, V. Santhakumar, *Stem Cell Reports* **9**, 972 (2017).
53. B. A. Kohler, *et al.*, *J. Natl. Cancer Inst.* **103**, 714 (2011).
54. S. Konefal, M. Elliot, B. Crespi, *Front Neuroanat* **7**, 21 (2013).
55. E. V. Baumgart, J. S. Barbosa, L. Bally-Cuif, M. Gotz, J. Ninkovic, *Glia* **60**, 343 (2012).

Examining estradiols neuroprotective abilities and mechanisms of action in cerebrovascular accidents and neurodegenerative conditions

Sukanthatulsee Uthayabalan

Abstract
Estrogens are known for playing essential roles in the body. These hormones exert crucial protective actions when faced with neural damage. Numerous studies have provided a deep understanding of these unique actions that go far beyond the scope of reproduction and reproductive regulation. Through various mechanisms, delivery routes, dosage levels, and with the age and health status of the individuals receiving the treatment in mind, the hormone can be used in protecting against neural death. This review examines the discoveries that comprise the current body of knowledge regarding estrogen as a neuro-protector against cerebrovascular accidents (CVA, stroke) and neurodegenerative diseases. These findings have great implications for improving the quality of life in the aging population. They provide insight into the impact of hormones on the protection of neural tissues, and prompt discussion between members of the scientific community, ensuring that future clinical studies utilize methods that will maximize the quality of the obtained results.

Keywords: Neuroprotection; Estrogen; Estradiol; E2; Stroke; Neurodegeneration; Neural death

Résumé
Les estrogènes sont connus pour les rôles essentiels qu'ils jouent dans le corps. Ces hormones exercent des actions protectrices cruciales face aux dommages neuronaux. De nombreuses études ont fourni une profonde compréhension de ces actions uniques qui vont bien au-delà de la portée de la reproduction et la régulation de la reproduction. En tenant compte des divers mécanismes, itinéraires de livraison, niveaux de dosage, l'âge et l'état de santé des personnes recevant un traitement, l'hormone peut être utilisée comme protection contre la mort neuronale. Cet article examine les découvertes qui composent l'ensemble de connaissances actuelles en ce qui concerne les estrogènes en tant que neuro-protecteurs contre les accidents vasculaires cérébraux (AVC) et les maladies neurodégénératives. Ces résultats ont de grandes implications pour l'amélioration de la qualité de la vie pour la population vieillissante. Ils donnent un aperçu de l'impact des hormones sur la protection des tissus neuronaux et initient une discussion entre les membres de la communauté scientifique, veillant à ce que les futures études cliniques utilisent des méthodes qui maximisent la qualité des résultats obtenus.

Mots Clés: Neuroprotection; Estrogène; Estradiol; E2; ACV; Neurodégénérescence; Mort neuronale

Introduction

Estrogens are known as compounds that impact the regulation of the reproductive system; however, the roles of estrogens are not limited to this function (*1*). Estrogens possess potent protective factors in the context of many physiological systems, especially the nervous system. They protect against neural damage caused by cerebrovascular accidents (CVAs) and neurodegenerative diseases through specific mechanisms and pathways (*2, 3*). Improving the understanding of the effects of estrogens will play a great role in modulating neurodegenerative conditions and in combatting the negative effects of CVAs.

Estrogen is a common steroidal sex hormone in women. Four natural estrogens are biosynthesized: estrone (E1), estradiol (E2), estriol (E3), and estetrol (E4) (*4, 5*). E1 has a hydroxyl group at the C3 position, and a ketone group at the C17 position (*5*). It is an agonist of the estrogen receptors ERα and ERβ but is considered to be a

Correspondence: tulsy21@yahoo.ca
Department of Biology, University of Ottawa, 30 Marie Curie, K1N 6N5, Ottawa, Canada

weak estrogen (*4*). E3 consists of 3 hydroxyl groups and is produced in large amounts only during pregnancy (*5*). E4 has four hydroxyl groups, is produced mainly during pregnancy by the fetal liver and is closely related to E3 (*5*). Finally, E2, the strongest form of estrogen, is produced during the menstrual cycle and before pregnancy or menopause. It has two hydroxyl groups at the C3 and 17β positions, as well as three double bonds on the phenolic A ring. This is the best estrogen to provide neuroprotective effects and can attenuate damage to neural tissue in animal models (*5*).

The discovery of three types of estrogen receptors (ER) which were traditionally thought to function as ligand-activated transcription factors (*6*) has caused a need to explore new mechanisms that may exist for estrogen action. Two classes of ERs exist: nuclear ERs (ERα and ERβ), which are members of the nuclear receptor family of intracellular receptors; and membrane ERs (mERs) (including GPER, GPR30 and ER-X), which are mostly G protein-coupled receptors (*7*). Estrogens produce their cellular actions, by binding these receptors. Gaining an understanding of the specific receptors and their corresponding actions allows for selective induction of the receptor pathway during treatment regimes. In this review, we examine the potential neuroprotective effects of E2 during the course of neurodegenerative diseases and CVAs. By examining these effects and the distinction between receptor/ non-receptor mediated mechanisms, it is possible to accumulate a greater body of knowledge regarding the clinical usage of E2 for treatment plans.

Basic actions of estradiol

E2 directly modulates cell death by acting on the neurochemical systems that are implicated in cognitive decline conditions, such as Alzheimer's Disease (AD), and in CVAs, such as ischemic stroke. Indirectly, it decreases cell aging by antagonizing the effects of oxidants and other neurotoxic compounds (*8*). E2 plays a key role in influencing various aspects of memory and cognition in healthy post-menopausal women (*6*). Most importantly, increased E2 levels delay the onset and progression of the form of cognitive decline that is typically associated with neurodegenerative diseases (*7*). Heightened levels of E2 play a large role in diminishing the harmful effects of acute-traumatic injuries associated with CVA while promoting neurogenesis (*7*).

Evidence of Estrogen-Induced Neuroprotection

Until recently, the majority of *in vivo* studies that investigated the mechanisms of injury in CVA and neurodegenerative diseases utilized males as models, assuming that any conclusions could be applied to females. Because females possess greater amounts of natural E2 compared to males, gender and E2 levels within the body play critical roles in protecting against neurodegeneration and CVA. Specifically, males have a minimum serum E2 concentration of 50 pmol/L (*9*). In females, serum E2 levels fluctuate depending on the menstrual cycle. The lowest level of serum E2 exists at the end of luteal phase (*10*). Here the minimum serum E2 concentration is 70 pmol/L (*10*). Even at the lowest natural levels, E2 appears in higher quantities in females than males. Studies indicate that due to these differences, females can better combat the harmful effects of the aforementioned conditions (*10, 11*). There are distinctions in the occurrence rate and outcome of neurodegeneration/CVA between the genders. Premenopausal women are at a reduced risk of experiencing an ischemic stroke compared to men (*8*). This disparity diminishes once these women are postmenopausal, indicating that E2 levels play a role in modulating age-related conditions of the brain. E2 has neuroprotective factors that diminish the effects of ischemic brain injury and neurodegeneration. Female rats that were given physiological doses of E2, sustained $\sim$50% less infarctions than males and ovariectomized female rats, after ischemia induced by transient middle cerebral artery occlusion (MCAO) (*6*). Additionally, mice expressing the mutant human Alzheimer precursor protein (βAPP) showed reduced behavioural changes, delayed progression of neurodegeneration and a greater neural survival rate following the onset of a neurodegenerative disease when E2 was administered in early stages (*6*).

A large range of concentrations of E2 (105–1012 M), different neurotoxic stimuli (glucose deprivation, oxidative stress, physical injury) and various culturing methods (primary neuronal cells, mixed neuron/explant cultures) have been used to test treatments (*5*). The dose administered is crucial as there is a high sensitivity to natural E2 levels (*12*). One study demonstrated neuroprotection (in the form of reducing ischemic injury and the progression of neurodegeneration) with acute pharmacological (1 mg/kg1) doses of E2 in male rats, but, identical doses in females failed to have any effect. Similarly, lower physiological doses were effective in reducing both ischemia and cognitive decline in ovariectomized female rodents, but similar doses in un-ovariectomized females failed (*12*). Here, naturally occurring E2 creates a tolerance. E2 administered to models with naturally high levels of the hormone must be increased for effects to be seen. However, administering the same dose of E2 to males or ovariectomized females is effective as natural E2 levels in these models are already low and thus, a tolerance is not present (*12*). This implies that precise doses based on sex, age, and natural E2 levels in the body are needed to see results. Moreover, these treatments were administered before and after CVA and the onset of neurodegeneration (*6*). Results showed that to see results, E2 should be administered in its lowest physiological concentration before a CVA. In the case of neurodegeneration,

administration of the lowest physiological dosage in the earliest stages of onset is critical (*6*).

Mechanisms of Estrogen Action

E2 protects the brain in adults by altering the ability of neurons to survive post-trauma. E2 acts on other cell types, such as vascular endothelial cells and microglia, through either estrogen receptor (ER)-dependent or independent mechanisms. The mechanism used depends upon the area of the brain involved in neuroprotection while the pathway of E2 action is influenced by the dose administered (*13*).

Non-Genomic

Some E2 receptors associate with the cell membrane and are rapidly activated by exposing the cell to E2. Pharmacological levels of E2 bypass cellular (cytosolic) ERs and act through membrane ERs. These receptors associate with cell membranes by attachment to caveolin-1, a scaffolding protein in plasma membranes, and form complexes with G proteins, striatin, receptor tyrosine kinases, and non-receptor tyrosine kinases (Src) (*14*). Through striatin, the membrane bound ER can lead to increased levels of Ca^{2+} and nitric oxide (NO) (*14*), eliciting antioxidant effects. Through the receptor tyrosine kinases, signals are sent to the nucleus through the mitogen activated protein kinase (MAPK/ERK) pathway and phosphoinositide 3-kinase (PI3K/AKT) pathway, producing changes in cell function (*10*).

Genomic

In the absence of hormone attachment, E2 receptors (ERα and ERβ) are located in the cytosol. E2 binding to its receptor leads to downstream events including migration of the receptor from the cytosol into the nucleus, receptor dimerization and binding of the receptor to estrogen response elements (ERE) on DNA. The DNA/receptor complex then recruits proteins (DNA Polymerases) that are responsible for the transcription of downstream DNA into mRNA (*14*). Finally, a change in cell function results (*14*). Here, physiological levels of E2 protect the brain through mechanisms dependant upon cytosolic ERs.

Receptor-Mediated Neuroprotection

Membrane (Classical) Estrogen Receptors (ER)

E2 classically exerts its effects via a nuclear membrane ER mechanism. E2 enters the cell by passive diffusion and binds to the nuclear ER. Following a series of activation steps, the E2-ER complex associates with the estrogen response element (ERE) and functions as an enhancer for ERE-containing genes (*14, 15*). E2 induction of ERE-containing genes contributes to the neuroprotective effects of the hormone. To evaluate the role of membrane ERs as mediators of E2 neuroprotection in a model of global ischemia, ICI 182 780, a competitive membrane ER antagonist antagonist of E2, was delivered intracerebroventricularly (ICV) during the early post-ischemic period (at 0 and 12 hours after reperfusion) (*13*). Results revealed that the antagonist, ICI 182,780, reduced E2-elicited neuroprotection (*13*). When E2 was administered alone, the hormone promoted neuronal survival (*6*). When the membrane ER was antagonized, E2 could not bind to it at the nuclear membrane of neuronal cells by attaching to membrane proteins. Thus, signals were not sent to the nucleus through the MAPK/ERK and Pl3K/AKT pathways, preventing changes in cell function and reducing neuroprotection in damaged cells.

Additionally, the membrane ER, GPR30's role in mediating estrogen signaling and neuroprotection in the hippocampus following global cerebral ischemia GCI was examined. An E2 conjugate, E2-BSA, which exerted rapid regulation of kinase activation and neuroprotection in the hippocampal CA1 region of ovariectomized adult rats was used (*16*). GPR30 was knocked out by bilateral administration of antisense (AS) oligodeoxynucleotides every 24 hours for 4 days. On the fourth day, a GCI was performed. E2-BSA (10 μM in 5 μl 0.9% saline) was administered bilaterally via ICV injection 60 minutes before induction of GCI (*16*). E2-BSA treatment resulted in neuroprotection, indicated by a significant increase in surviving neurons in the CA1 region in the GPR30-active control group. GPR30 knockout greatly reduced the neuroprotective effect of E2-BSA in the CA1 region of the experimental group, after GCI. Finally, administration of the GPR30 agonist, G1, with E2-BSA exerted a strong neuroprotective effect against GCI-induced neuronal cell death in the CA1 region in both groups (*16*). The study demonstrates the importance of membrane receptors that act in membrane ER-based neuroprotection. Knocking out GPR30 with AS prevents E2-BSA from binding to the cell membrane entirely, increasing GCI-induced neuronal cell loss.

Estrogen Receptor (ER) α and Estrogen Receptor (ER) β

In the central nervous system (CNS), although ERs (alpha and beta) co-express in some regions, others show selective expression (ERα in the ventromedial hypothalamic nucleus and subfornical organ, ERβ in the cerebral cortex/hippocampus), indicating that expression of ER in the brain is subtype-specific (*6*). These subtypes undergo ligand activation. This leads to the formation of a receptor dimer with high affinity for specific DNA sequences called estrogen response elements, (EREs) within promoters of target genes (*17*). One investigation used homozygous ERα and ERβ-knockout mice to determine the efficacy of E2 and concluded that ERα played a key role in protecting against neuronal injury in

animals undergoing MCAO (*18*). The results showed that deletion of ERα in mice eliminates the neuroprotective effect of E2 in all regions of the brain, while the capability of E2 was preserved for neuroprotection against this brain injury in the absence of ERβ (*18*). The results denote that ERα is a critical mechanistic link in mediating the protective effects of E2 in brain injury.

Additionally, physiological levels of E2 cannot delay the progression of cognitive decline or protect against ischemic stroke in ERα knock-out mice (*19*). This finding stresses ERα's critical role in mediating E2's effects. Gollapudi and Oblinger's studies show that PC12 cells (derived from rat adrenal medulla) transfected with the full-length rat ERα respond to the protective effects of E2 while cells transfected with vector DNA alone do not, further cementing the theory that ERα is a crucial mechanism that mediates the neuroprotective effects of physiological levels of E2 (*20*). To evaluate the role of ERα vs ERβ, subtype-selective agonists were administered daily for 2 weeks before and 7 days after ischemia (*13*). Both propyl pyrazole triol (PPT, ERα-agonist) and WAY 200070-3 (ERβ-agonist) promoted the survival of nearly all CA1 pyramidal neurons in approximately 50% of the animals (*13*), suggesting that E2 acts through both ERα and ERβ to protect CA1 neurons, though ERα may be a more commonly used receptor.

Another study showed that within 24 hours of MCAO, ERα is dramatically up-regulated and E2 pretreatment prevents injury-induced down-regulation of ERβ in the cerebral cortex (*21*). These findings suggest that any form of brain injury or degeneration causes increased responsiveness of the injured region to E2. This induces actions that are specific to each subtype of the receptor. Normally, high levels of ERα are only expressed in the cerebral cortex (CC) during neonatal development (*22*). Following this stage, the expression of ERα in the CC is minimal. Post-injury, the substantial increase in ERα caused by up-regulation causes an increase in estrogen in the area of injury, evoking a hormonal state that is similar to a neonatal brain (*22*). Following injury, this process then promotes neurogenesis and re-differentiation of the cortex, similar to the process in a neonatal (*19*).

Due to the presence of ERβ and injury-induced up regulation of ERα, the expression of the anti-apoptotic gene, bcl-2, is increased in the ischemic penumbra (area impacted by ischemic event), the CC, and basal ganglia (area impacted by neurodegenerative diseases). E2 affects the expression of genes that are involved in regulating apoptosis and in activating ERs, leading to enhanced neuronal viability (*11,22*). Estrogen's ability to exert any receptor-mediated neuroprotection correlates with differential expression of ERα and ERβ mRNA in the CC.

Non-Receptor-Mediated Neuroprotection

While many E2 analogues require membrane or cellular receptors, unique derivatives function without receptor-mediation. These analogues rapidly decrease N-methyl-D-aspartate (NMDA)-induced currents, reducing excitatory cell death caused by neurodegeneration or CVA (*22*). To examine non-receptor mechanisms of neuroprotection in CVAs, cytotoxicity was induced in HT-22 (mouse hippocampal) cells by 10 mmol/L glutamate. A novel non-receptor estrogen analogue (ZYC3) was added immediately before the exposure to glutamate and then an ischemia/reperfusion injury was induced by temporary MCAO. ZYC3 did not bind to mER, ERα or ERβ (*23*). The infarct volume was significantly reduced to 122.4$\pm$17.6 in ZYC3 groups, compared with 252.6$\pm$15.6 mm in the ovariectomized group (*23*). This occurs because ZYC3 increases cerebral blood flow in both sides of the brain within 30 minutes after reperfusion during MCAO, preventing cell death. In neurodegeneration, E2 influences members of the nitric oxide synthase family to induce vasodilatory actions on cerebral blood vessels, improving blood flow to compromised brain regions. These unique analogues of E2 are potent antioxidants and inhibit lipid peroxidation through the C3 hydroxyl group located and the phenolic A-ring of E2 and through the nitric oxide synthase family (*10, 24*). The reduction of perioxidation permits the reduction of overall cell death caused by neurodegeneration. This implies that non-receptor mechanisms of E2 neuroprotection are beneficial for neuroprotection against oxidative stress injuries as well as CVA related damage.

Future Directions and Questions to Consider

With newfound knowledge regarding estrogen, it may be possible to utilize natural/synthetic compounds to prevent neural death and to delay the onset of neurodegenerative diseases. Studies show that serum estrogen levels are inversely correlated with ischemic stroke damage in intact animals. Treatment of intact female mice with an anti-estrogen receptor compound, ICI182,780, greatly enhances stroke infarct size (*10*). This emphasizes the possibilities for treatment and prevention with E2. In future therapies for individuals coping with AD or ischemic stroke, E2 could be utilized to attenuate neural necrosis. These therapies could be utilized to alleviate the troublesome symptoms in post-menopausal women while reducing risks of cerebro-vascular disease. Questions that arise are plentiful because of the novel actions of E2. It is important to consider the availability of E2 therapies, whether or not neuroprotective actions of E2 are reversible, the window of opportunity for administration of treatment where E2 is most effective, whether or not the positive effects will endure if treatment is discontinued and the duration for which this would occur. These

potential limitations must be overcome with experimentation prior to distribution of treatments, in order to amplify positive results.

Conclusion

E2 is a complex and powerful hormone that produces favourable results in treating CNS injuries, as a protective agent. E2 attenuates the extent of injury incurred by increasing the resilience of the brain via receptor-mediated/receptor-independent mechanisms in both oxidative stress, and CVA-induced injuries. While many studies have come up with breakthrough results, limitations still exist. Further research must be conducted in order to fully understand the molecular mechanisms of E2 action. Challenges for the future include i) understanding how E2 therapy in men will impact feminization, and ii) combatting negative effects of high levels of E2 such as thrombosis, which can lead to severe cardiovascular problems. Combining various types of biosynthetic estrogens and therapy methods (e.g. oral, transdermal) may aid in administering controlled doses of the hormone, reducing side effects. This form of therapy can even provide an opportunity to use two different therapeutic agents at very low doses for additive or synergistic effects (e.g. E2 with an agonist) to improve the overall therapeutic outcomes. Despite limitations, E2 maintains the hope for successful neuroprotection in different CNS injuries. Current findings may lead to utilizing estrogens to target specific tissues for therapy, further eliminating unwanted side effects. In the future, acquiring a better understanding of E2 and its workings will facilitate the development of innovative therapies, significantly impacting the aging population by improving coping ability and quality of life.

Competing interests
The author declares that she has no competing interests.

References

1. S. Suzuki, C. M. Brown, P. M. Wise, *Front Neuroendocrinol* **30**, 201 (2009).
2. P. S. Green, J. W. Simpkins, *Int. J. Dev. Neurosci.* **18**, 347 (2000).
3. M. Fiocchetti, P. Ascenzi, M. Marino, *Front Physiol* **3**, 73 (2012).
4. L. M. Garcia-Segura, I. Azcoitia, L. L. DonCarlos, *Progress in neurobiology* **63**, 29 (2001).
5. N. Raghava, B. C. Das, S. K. Ray, *Neurosci Neuroecon* **6**, 15 (2017).
6. L. Zhao, T. W. Wu, R. D. Brinton, *Brain Res.* **1010**, 22 (2004).
7. S. Pozzi, V. Benedusi, A. Maggi, E. Vegeto, *Ann. N. Y. Acad. Sci.* **1089**, 302 (2006).
8. R. Norbury, *et al.*, *Exp. Gerontol.* **38**, 109 (2003).
9. D. B. Dubal, P. M. Wise, *Endocrinology* **142**, 43 (2001).
10. D. W. Brann, K. Dhandapani, C. Wakade, V. B. Mahesh, M. M. Khan, *Steroids* **72**, 381 (2007).
11. V. I. Alexaki, *et al.*, *FASEB J.* **18**, 1594 (2004).
12. L. D. McCullough, P. D. Hurn, *Trends Endocrinol. Metab.* **14**, 228 (2003).
13. A. M. Etgen, T. Jover-Mengual, R. S. Zukin, *Front Neuroendocrinol* **32**, 336 (2011).
14. P. M. Wise, S. Suzuki, C. M. Brown, *Dialogues Clin Neurosci* **11**, 297 (2009).
15. C. Behl, *Nature reviews. Neuroscience* **3**, 433 (2002).
16. H. Tang, *et al.*, *Mol. Cell. Endocrinol.* **389**, 92 (2014).
17. I. Paterni, C. Granchi, J. A. Katzenellenbogen, F. Minutolo, *Steroids* **90**, 13 (2014).
18. R. D. Spence, *et al.*, *Proc. Natl. Acad. Sci. U.S.A.* **108**, 8867 (2011).
19. D. G. Stein, *Trends Neurosci.* **24**, 386 (2001).
20. L. Gollapudi, M. M. Oblinger, *J. Neurosci. Res.* **56**, 471 (1999).
21. J. W. Simpkins, M. Singh, C. Brock, A. M. Etgen, *Neuroendocrinology* **96**, 119 (2012).
22. A. L. Mize, R. A. Shapiro, D. M. Dorsa, *Endocrinology* **144**, 306 (2003).
23. R. Liu, *et al.*, *Stroke* **33**, 2485 (2002).
24. Q. Wang, R. Santizo, V. L. Baughman, D. A. Pelligrino, C. Iadecola, *Stroke* **30**, 630 (1999).

Expressing the randomity of events – An analysis of random number generation with given distributions

Carl Zhou

Abstract In cases where it is necessary to generate random numbers that obey specific distributions, some of those distributions can be expressed as mathematical functions while others cannot. This is especially the case for epidemiological, medical, and pharmaceutical investigations, where more accurate methods, utilising actual distribution (from survey and experimental data) to generate random numbers may be required. In this study, three methods are analyzed to demonstrate simple computation examples. These methods include: inverse transform, acceptance-rejection, and Monte-Carlo simulations. Their applications are explored from a data analysis point of view. Additionally, this article discusses a flexible and practical approach of statistical measures optimization, which approximates the solution by fitting the statistical measures.

Keywords: Pseudo-random; Random number generator; Specified distribution; Monte Carlo simulation

Résumé Dans les cas où il est nécessaire de générer des nombres aléatoires qui obéissent à des distributions spécifiques, certaines distributions peuvent être exprimées sous forme de fonctions mathématiques, alors que d'autres ne peuvent pas l'être. Ceci est le cas pour les enquêtes épidémiologiques, médicales et pharmaceutiques, où on exige parfois des méthodes plus précises qui utilisent la distribution actuelle (à partir des données expérimentales et d'enquêtes) afin de générer des nombres aléatoires. Cette étude explore trois méthodes afin de démontrer des exemples de calculs simples. Ces méthodes comprennent la transformée inverse, la méthode du rejet et les simulations de Monte-Carlo. Leurs applications sont explorées à partir des analyses de base de données. En outre, cet article traite d'une approche flexible et pratique l'optimisation des mesures statistiques, qui estime la solution en ajustant les mesures statistiques.

Mots Clés: Pseudo-aléatoire; Générateur de nombres aléatoires; Distribution spécifiée; Simulation Monte-Carlo

1 Introduction

Random numbers, or stochastic numbers, are often necessary for experimentation, that is, to describe stochasticity in studies by generating random numbers instead of performing mass data collection. Generally, random numbers have three uses: (i) Sampling. e.g. sampling a population representatively, or randomly distributing laboratory animals into experimental groups, for example; (ii) Optimizing model parameters. e.g. Monte-Carlo method (*1*); (iii) Simulating population or events. e.g. simulating the initial genetic status of a population, in which the selection, genetic cross, and mutations are all random. It can also be applied to queuing and resource storage scenarios, which often require cost estimations by performing simulations based on generated random numbers.

Correspondence: czhou027@uottawa.ca
Interdisciplinary School of Health Sciences, University of Ottawa, 25 University Private, K1N 7K4, Ottawa, Canada

Since the 1950s, a number of studies have presented methodologies of generations based on computation mathematics and related technology. Because a mass of random numbers is only made by computers, discussions of the methodology can be reviewed in two stages. In the computer's early years, Marsaglia, Tausworthe, Fishman, and Lewis systematically presented the theoretical analyses, which indicated the technical feasibility and laid the theoretical foundations for generating random numbers in the 1960s and 1970s (*2–5*). Since then, the use of statistical simulations has accelerated due to the development of computer technology and its wide applications (*6*). Many researchers discussed and developed realistic approaches for various experiments (e.g. Rubenstein, Devroye, Ripley, Dagpunar, Law, and Kelton) (*7–11*). Most studies introduce approaches in detail for generating random numbers on several popular distributions (e.g. Aiello et al., Deng and Lin, Ferguson et al., L'Ecuyer, Luby, Marsaglia and Zaman, Niederreiter

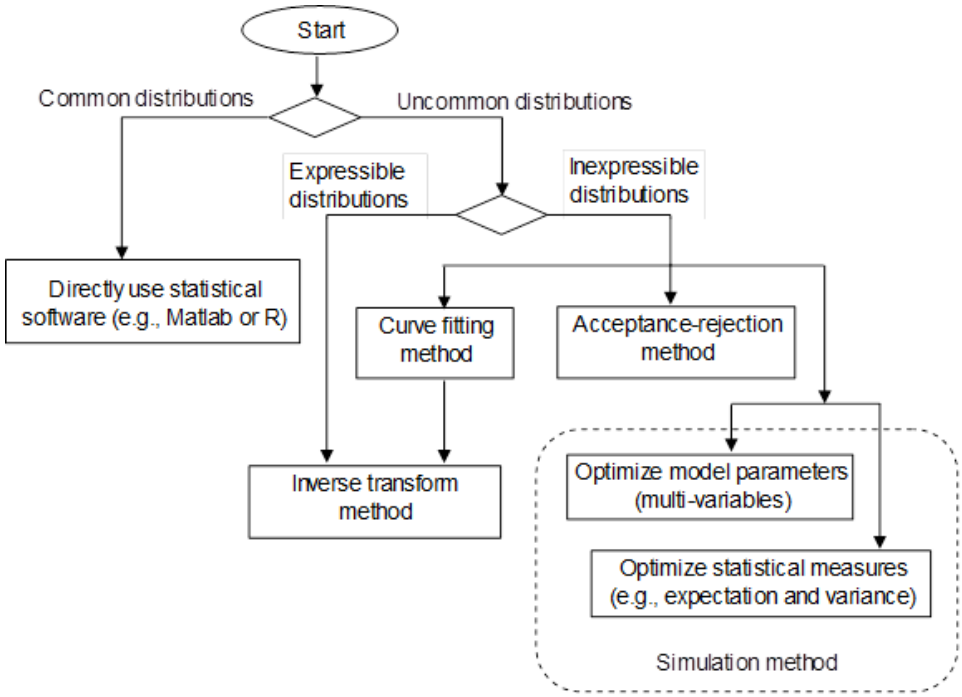

Figure 1: Method selection flow chart for constructing random number generators that obey different distributions. Diamonds denote logical judgement, rectangles indicate methods or processes, dotted boxes mean type of method and arrow lines illustrate the selection of methods.

and Shparlinski, Ross) (*12–19*). To describe various practical problems, however, not all distributions can be easily expressed by mathematical analytic formulas. When performing data analysis, there is the frequently asked question of how to generate random numbers with the actual distributions. Especially for epidemiological, medical, and pharmaceutical experiments, the need for precision might require the use of actual data distributions collected from surveys, investigations, and experiments to generate random numbers.

With regards to the aforementioned needs for realising stochasticity, an analysis of different approaches to generate random numbers is presented. These approaches include inverse transform, acceptance-rejection, and Monte-Carlo simulations. As a powerful tool for the application of simulation methods, the sampling technique is introduced and illustrated for solving the problems that have no analytical solutions. In other words, this article derivates algorithms, which generate random numbers based on several different calculations (Figure 1). The study objectives are to: (1) provide an overview of three principal approaches for generating random numbers that describe the stochasticity of events based on practical observations, and (2) analyze the random number generator based on inexpressible distributions and its accuracy and efficiency for applications.

2 Existing Distributions Provided by Statistical Software

Theoretically, random numbers are generated through physical phenomena, such as coin tossing, dice rolling, roulette, etc. These random numbers are called true random numbers and they are relatively difficult to create via computer. However, in practical application, the use of pseudo-random numbers is often sufficient. These number series appear to be random numbers, but they are actually generated through a repeatable computation using the computer (*20–22*). Utilizing pseudo-random numbers with uniform distribution, many statistical software packages can generate random numbers subjected to various distributions. For example, Matlab can generate random numbers subjected to the distributions of normal (randn), Beta (betarnd), binomial (binornd), chi-square (chi2rnd), exponential (exprnd), F (frnd), and numerous other function forms. If a desired distribution cannot be constructed using a statistical software, further calculations or transformations are required to generate these random numbers. The following sections summarize some approaches that can be used. These methods all use the most basic pseudo-random number generator.

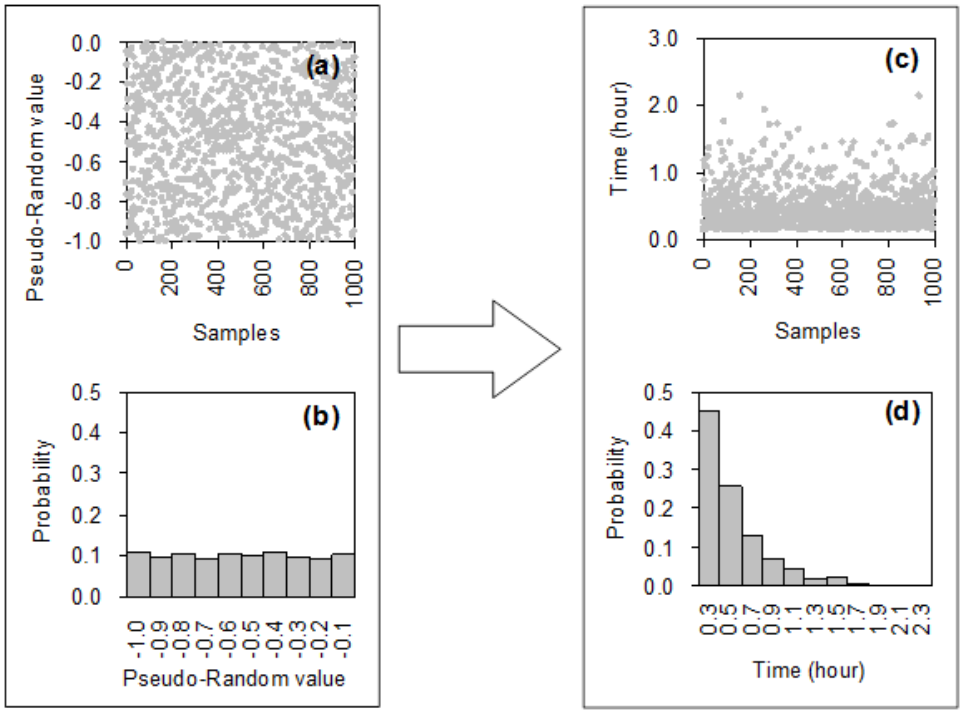

Figure 2: Diagram of the transformation from uniform distribution x to exponential distribution y. (a) and (b) illustrate all 1000 sample values x generated by uniform distribution; (c) and (d) show the converted random data complying with y.

3 Random Generator Based on Expressible Distributions

In some cases, the required distribution can be expressed with a formula. This allows for easy mathematical processing. A commonly used approach is called the inverse transform method, which includes two steps that are briefly outlined as follows.

Step 1: Assume $X[0,1]$ obeys uniform distribution $u(x)$ and its cumulative probability distribution function $U(x)$. $Y[ay,y]$ obeys the desired distribution $h(y)$ and its cumulative probability distribution function $H(y)$. Then we solve $U(x)$ and $H(y)$, and let $U(x) = H(y)$, i.e. $\int_{ax}^{x} u(t)dt = \int_{ay}^{y} h(t)dt$, where x and y are two random variables, and ax and ay are initial values. Note that there is a one-to-one correspondence between x and y. Because the left side of the equation is equal to x, we obtain $x = H(y)$.

Step 2: Solve the inverse function of x to y based on $U(x) = H(y)$. The inverse function is $y = H - 1(x)$. Therefore, we can generate random number y using x.

The following is a calculation example. Survey data suggests that three newborns are delivered at a hospital per hour on average. In order to simulate (not only to calculate) the number of newborns delivered in the next hour, a set of dummy data is required to represent the delivery of a newborn after time T. Let us assume that the dummy data meets the exponential distribution

$$e^{-kt} \text{ or } ra^{-kt} \tag{1}$$

Here we will use the latter to demonstrate the approach (let the parameters be $r = 2.0$, $a = 2.7$, $k = 3.0$).

According to the example scenario, set: Uniform random number x's probability density function is

$$p(x) = \begin{cases} 1, & if 0, \leq x \leq 1 \\ 0, & otherwise. \end{cases} \tag{2}$$

Its cumulative probability is $U(x) = \int_0^x p(x)dx$. The desired probability density function is

$$p(y) = \begin{cases} ra^{-ky}, & y \geq 0 \\ 0, & y < 0 \end{cases} \tag{3}$$

where y denotes the time in hours when no babies are born. Its cumulative probability is $H(y) = \int_0^y p(y)dy$. Since $p(x)$ and $p(y)$'s cumulative probabilities are equal, we have

$$\int_0^x dx = \int_0^y ra^{-ky}dy \tag{4}$$

Table 1: Observation of a doctor's time spent with patients.

Time (minute)	Number of Patients	Probability
10	26	0.250
11	24	0.231
12	20	0.192
13	17	0.164
14	10	0.096
15	6	0.058
16	1	0.010
Total	104	1.0

The number of patients (observed data) is 104 ($n = 104$).

Solving it, we get $x = -(ra^{-ky})/(k \log a)$. Its inverse function can then be derived as

$$y = -[\log(-kx) + \log(\log a) - \log r]/(k \log a)(1) \quad (5)$$

This is the random number generator that meets the distribution (ra^{-kt}). Figure 2 displays the transformation from uniform distribution x to exponential distribution y. As demonstrated for this simulation, when T is 0.5 hours, the probability of no newborns delivered is 0.273. In other words, the probability of at least one newborn delivered is 0.727 in this time.

4 Random Generator Based on Inexpressible Distributions

4.1 Observation-based distributions

4.1.1 Curve fitting

There will often be some need for curve fitting in many practical applications. We hope to generate random numbers according to the probability distribution of the actual sample. These distributions derived from observed samples vary greatly, and they often cannot be expressed using existing function forms. In these cases, a suitable function can be chosen, such as a polynomial function, to fit the actual distribution. Then, we can use the inverse transform method to derive the distribution curve. It is important to note that since the inverse function of second- and higher-order polynomials is very complex, it may be difficult to find a solution. Therefore, solving these inverse functions require optimization by computer. In the following paragraph, the example of queuing for a walk-in clinic will be used to demonstrate how to solve such problems.

Example: According to survey data, the distribution representing a doctor's time spent with patients is neither Poisson nor negative exponential distribution, as shown in Table 1 and Figure 3. Time cost calculation depends on this distribution; we need to generate random numbers to simulate the possible visitation times of a number of patients (e.g. 300 patients). The derivation of the distribution is presented as follows by fitting the curve and solving its inverse function.

Let uniform random number x's probability density function be

$$p(x) = \begin{cases} 1, & 0 < x \leq 1 \\ 0, & otherwise \end{cases} \quad (6)$$

Its cumulative probability is $U(x) = \int_0^\infty p(x)dx$. The observation data probability function is

$$p(y) = -0.00263y^2 + 0.02690y + 0.24863 \ (10 \leq y \leq 16) \quad (7)$$

where y denotes doctor's time for each patient (Figure 3). Its cumulative probability is

$$H(y) = \int_0^y p(y)dy \quad (8)$$

where $H(y)$ is equal to 1. Since $\int_0^\infty dx$ equals 1, let $\int_0^\infty dx = \int_0^y p(y)dy$. We have

$$x = -0.000876667y^3 + 0.01345y^2 + 0.24863y = 2.95463 \quad (9)$$

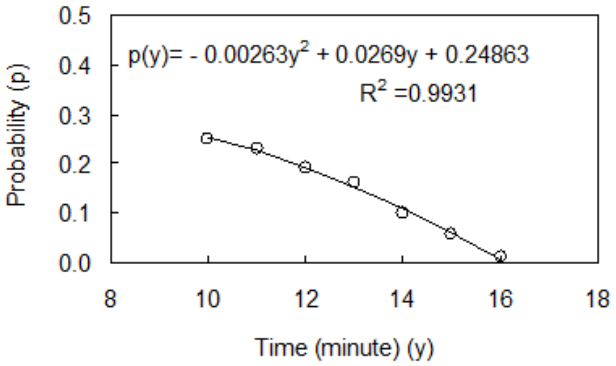

Figure 3: The distribution representing a doctor's time spent with patients based on observed data. The circles denote the time samples ($n = 7$), and the solid line displays the fitting curve based on the regression function $p(y)$.

The inverse function of $x = f(y)$ is hard to express in analytical form. We can solve it through programmed optimization algorithms. The idea is to first generate 300 random numbers x $(0 \leq x \leq 1)$, then find a y for every x that is $10 \leq y \leq 16$, until the precision of $x - x \leq 0.001$ (or $x - x = minimum$) is satisfied, where x is the x that

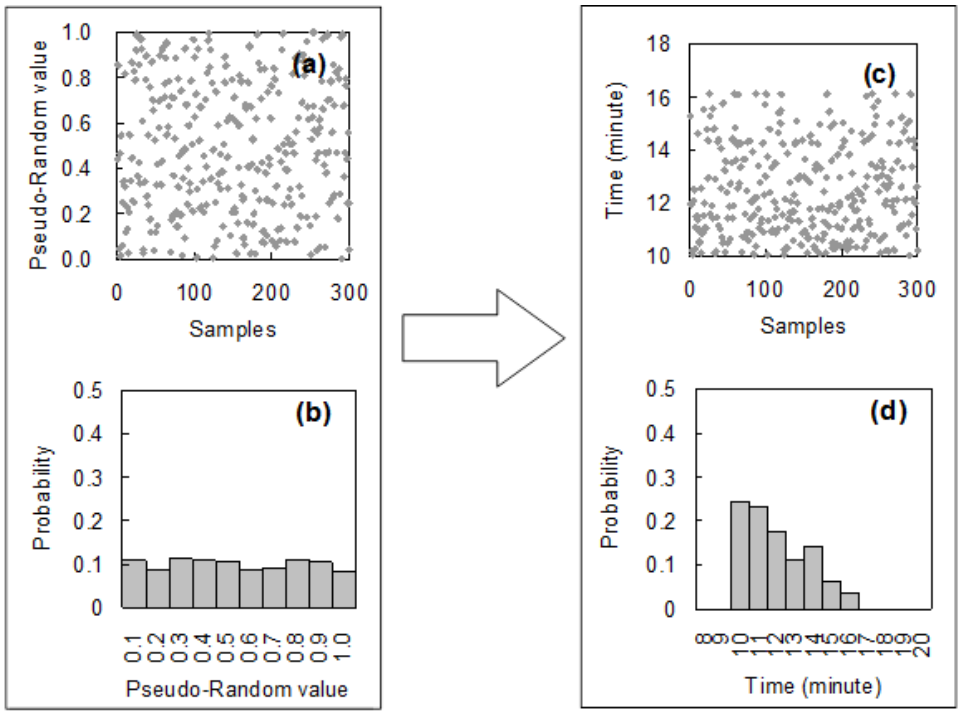

Figure 4: An example of random number generation under a specified probability density function. (a) and (b) illustrate all 300 sample values generated by uniform distribution; (c) and (d) denote the converted random data complying with the specified distribution shown in Figure 3.

has met the accuracy of the polynomial. After 300 x's have been fitted, we obtain all y values corresponding to x (Figure 4).

The solution presented above shows that the resultant random numbers distribution is close to the survey data distribution (Figure 4). Clearly, good curve-fitting increases the accuracy of the distribution, while poor fitting will not yield a satisfactory estimate. If higher precision is required to match the two distributions (survey data and random numbers), the following method (the acceptance-rejection approach) is a very practical option.

4.1.2 The acceptance-rejection technique

The acceptance-rejection technique is simple to understand. It can be expressed visually by a two-dimensional area composed of x and y covered with randomly distributed dots. If the envelope of a given distribution curve or probability density function is placed in this area, and the dots above the line are rejected while the remaining dots are accepted, then they will become the random numbers we need (Figure 5). Ross suggested a judgement approach, which may be summarised as follows (*23*):

Step 1. Specify P to include enough random numbers p, having uniform probability density function.

Step 2. Specify Q to include enough random numbers q, having uniform probability density function.

Step 3. Generate p and q concurrently as a random pair. p is the x coordinate, while q is y coordinate.

Step 4. Specify a probability density function $f(x)$.

Step 5. Compare the q of each point with the function $f(x)$.

Step 6. Reject the points if $q > f(x)$. Accept the remaining points.

For example, we have the sampling results of a survey for the heights of men with different education levels in a city. The probability density of the survey results cannot be expressed by a function. How can we produce a large random number set (500) that complies with this survey probability? The survey distribution curve obtained is the solid black line in Figure 5; this example generated 3000 random numbers. The grey crosses above the black line are rejected random numbers (2500), and the circles below and on the line are the accepted random numbers (500).

4.2 Assumption-based multiple variables and distributions

In some cases, the required distribution does not come from observational results, but from our subjective judgment. This is often the case in parameter optimization, especially for parameterizing complex models, such as process-based models. If optimization of multiple parameters is needed, then it is necessary to generate random numbers in a multidimensional space. In other words, the

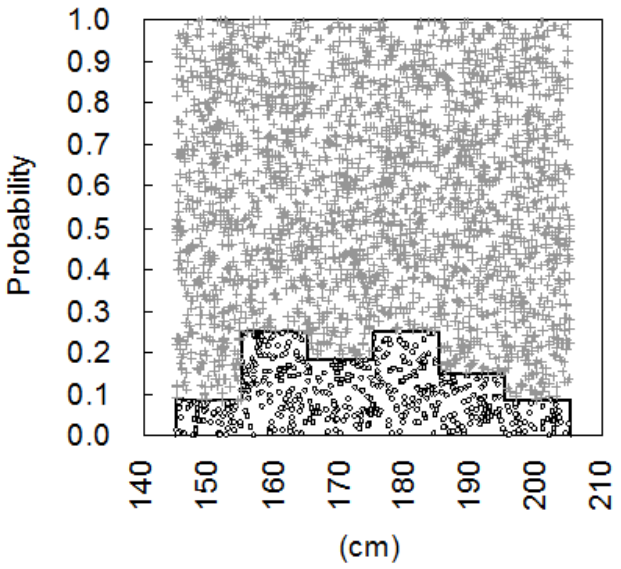

Figure 5: An example for generating random numbers using the acceptance-rejection method. The circles and crosses are accepted and rejected random data, respectively.

acceptance-rejection method is still used, but when the number of dimensions is greater than two, the time cost will be huge. In the interest of saving time, it may be necessary to use an effective algorithm, e.g. the Metropolis-Hastings algorithm (*24, 25*), to search for optimal parameters and to achieve rapid convergence. This is the application of Markov Chain Monte Carlo (MCMC) method (*26*). Here we employ exhaustion to illustrate this random number generator.

For example, the empirical equation for predicting male children's height, weight, and lung capacity in a specific city is

$$y = 0.01(b \times w - a \times h) - 0.1352 \tag{10}$$

where y is lung capacity, h is height, w is weight. a and b are undetermined parameters. Observed data is shown in Table 2. Now we parameterize this equation using statistic simulation instead of multiple regressions. Assume a ranges from 0.0 to 1.0, and b ranges from 0 to 10.0. Assume the distribution of these two parameters is uniform (Figure 6).

The algorithm can be summarized as follows:

Step 1. Generate a pair of random numbers (a, b) within a predetermined range. Substitute them into Equation 7.

Step 2. Obtain y based on observed h and w.

Step 3. Compare calculated y to measured y and go to Step 1 until residual error sum becomes minimal.

Table 2: Observation of male children's height (h), weight (w), and lung capacity (y).

No.	h	w	y	No.	h	w	y
1	145.8	34.5	2.3	16	155.4	39.1	2.5
2	159.6	48.0	3.0	17	144.8	33.0	2.5
3	137.7	29.9	2.0	18	154.4	42.6	2.3
4	152.2	44.3	2.8	19	157.1	38.5	2.5
5	160.4	40.2	2.8	20	147.7	31.4	1.5
6	168.4	49.1	2.9	21	157.8	37.2	2.0
7	153.2	32.0	1.7	22	154.1	35.2	2.0
8	153.6	41.5	2.7	23	154.4	32.4	1.7
9	150.0	39.9	2.0	24	147.6	34.2	2.5
10	133.4	32.5	1.8	25	171.1	41.8	2.7
11	161.9	45.9	2.7	26	134.9	27.3	1.3
12	144.9	32.0	1.8	27	152.1	35.7	1.8
13	156.8	37.5	2.7	28	146.8	37.8	2.2
14	161.1	37.7	2.0	29	155.1	32.4	1.7
15	150.7	33.6	2.2	30	154.1	36.2	2.0

The number of children (observed data) is 30 ($n = 30$). The units are cm (h), kg (w), and litre (y).

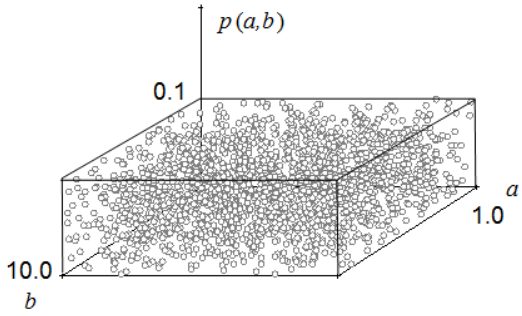

Figure 6: Two-dimensional distribution of parameters a and b in Equation 7. The circles represent all random pairs that include coordinate values a and b. Random numbers were generated to consist of 2000 pairs in this example. A point ($a = 0.4558$, $b = 8.0766$) was found within the distribution as an optimal parameter a and b.

This is an example of generating random numbers in a two-dimensional distribution (Figure 6). In this way, some parameter pairs can be solved. One of the pairs is solved as $a = 0.4558$, $b = 8.0766$. They are close to the optimal parameters. As the sample increases, the accuracy can be improved.

4.3 Parameter-based distributions

In model or parameter optimization, we may be required to obtain several random numbers. The function form of the distribution may not be required, but the sta-

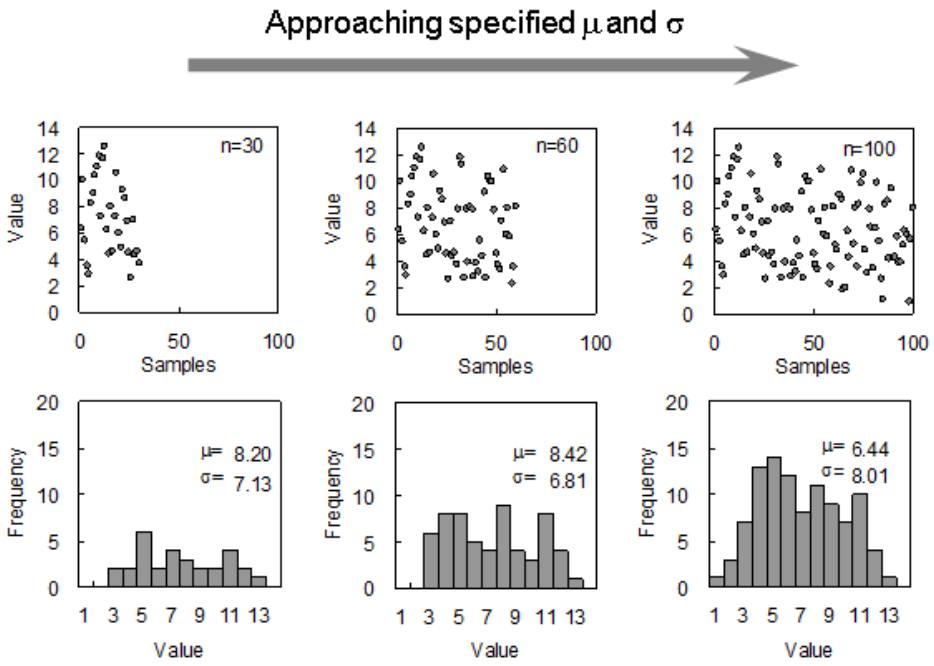

Figure 7: A generation of random data on a specified normal distribution ($\mu = 65$, $\sigma = 80$). The relative differences are less than 1.0% for both specified mathematical expectation (μ) and variance (σ). The dots denote generated numbers.

tistical measures of distribution must be specified, e.g. at least the mathematical expectation (μ) and variance (σ^2) or standard deviation (σ). Optimization of statistical measures is needed in these cases. The algorithm can be designed to generate random numbers by the Monte-Carlo simulation method. The simulation progresses dynamically step by step. While samples are generated adequately, the statistical measures of distribution approach the specified values (*27*). When the residual error between the random number and specified value reaches an acceptable low level, the simulation can end.

For example, the steps below demonstrate how to fit the two statistical measures by generating 100 random number sets ($\mu = 6.5$, $\sigma = 8$; Figure 7).

Step 1. Generate two random numbers near μ.

Step 2. Generate the next random number, calculate the μ and σ of the three random numbers, and compare them with the specified value.

Step 3. If the error does not meet the acceptable level, e.g. 2.0 for μ and 1.5 for σ, then abandon this random number. Generate the next random number, repeat Step 3.

Step 4. If the error is accepted and meets the acceptable level, accept this random number. Put the accepted random numbers in the set. Generate the next random number and repeat Step 3 until we have 100 accepted random numbers ($n = 100$).

Figure 7 illustrates the state of simulation when n is 30, 60, and 100. μ and σ are constantly approaching the specified value, finally reaching the relative error of less than 1.1% ($\mu = 6.43$, $\sigma = 8.01$). As more random numbers are generated, the accuracy of the resulting distribution will increase.

5 Summary

Three main methods for constructing random number generators, i.e. inverse transform, acceptance-rejection, and Monte-Carlo simulations, have been analyzed in this study by demonstrating applicable and simple computation experiments. As Section 3 explained, a random generator is easily realized for widely used distributions in study experiments. In practice, however, the distributions from observed data may not be close to the common forms. To generate random numbers that obey these practical distributions, the approach application depends on different cases. When selecting an appropriate approach, the issues of accuracy and efficiency are often considered. For the curve fitting method, polynomials can theoretically fit any continuous function of probability density, but their inverse functions may not be derived easily, especially for the inverse functions of fourth order polynomials. The approximate solutions of an inverse function are available by utilizing the numerical method with consideration to both accuracy and efficiency. Similarly, the accuracy and efficiency should still be balanced

in the acceptance-rejection method. If the dimension is more than three, searching for an optimal solution becomes a challenge. In that case, coding experiments using Matlab or R would be necessary to finding an appropriate polynomial to decrease computational time. Briefly, random number generation under inexpressible distributions is an issue that we encounter in the applications of statistical simulation. This analysis suggests that this issue has flexible and diverse solutions, and always requires a balance between accuracy and efficiency. The selection of methods is illustrated in Figure 1. If the distribution density can be regressed with an expression, the approaches of curve fitting and inverse transform are suitable for building a random number generator. The merit of this method is convenience, and the demerit is that the use is limited by the form of distribution functions. In the cases of distributions that show irregular forms, the acceptance-rejection approach is a realistic option. Additionally, this approach generates random numbers strictly according to the given distribution curve (Figure 5); therefore, the accuracy is higher than the curve fitting method. As for some special purpose experiments such as the construction of assumption distributions or parameter-based distributions, the simulation methods can be flexibly utilized for various applications.

Competing interests

The author declares that he has no competing interests.

Acknowledgements

I am grateful to the two anonymous reviewers and the corresponding editor for their insightful comments and very helpful suggestions.

References

1. L. Kelvin, *The London, Edinburgh, and Dublin Philosophical Magazine and Journal of Science* **2**, 1 (1901).
2. G. Marsaglia, *Commun. ACM* **6**, 37 (1963).
3. R. C. Tausworthe, *Mathematics of Computation* **19**, 201 (1965).
4. G. S. Fishman, *Principles of Discrete Event Simulation* (John Wiley & Sons, Inc., New York, NY, USA, 1978).
5. P. A. W. Lewis, G. S. Shedler, *Naval Research Logistics Quarterly* **26**, 403 (1979).
6. B. Efron, R. Tibshirani, *Science* **253**, 390 (1991).
7. R. Y. Rubinstein, *Simulation and the Monte Carlo Method* (John Wiley & Sons, Inc., New York, NY, USA, 1981), first edn.
8. L. Devroye, *Non-Uniform Random Variate Generation(originally published with* (Springer-Verlag, 1986).
9. B. D. Ripley, *Stochastic Simulation* (John Wiley & Sons, Inc., New York, NY, USA, 1987).
10. J. Dagpunar, *Principles of random variate generation*, Oxford science publications (Clarendon Press, 1988).
11. A. M. Law, D. M. Kelton, *Simulation Modeling and Analysis* (McGraw-Hill Higher Education, 1999), third edn.
12. W. Aiello, S. Rajagopalan, R. Venkatesan, *Journal of Algorithms* **29**, 358 (1998).
13. L.-Y. Deng, D. K. J. Lin, *The American Statistician* **54**, 145 (2000).
14. N. Ferguson, B. Schneier, T. Kohno, *Cryptography Engineering: Design Principles and Practical Applications* (Wiley Publishing, 2010).
15. P. L'Ecuyer, *Annals of Operations Research* **53**, 77 (1994).
16. M. G. Luby, L. Michael, *Pseudorandomness and Cryptographic Applications* (Princeton University Press, Princeton, NJ, USA, 1994).
17. G. Marsaglia, A. Zaman, *Ann. Appl. Probab.* **1**, 462 (1991).
18. H. Niederreiter, I. E. Shparlinski, *Monte Carlo and Quasi-Monte Carlo Methods 2000*, K.-T. Fang, H. Niederreiter, F. J. Hickernell, eds. (Springer Berlin Heidelberg, Berlin, Heidelberg, 2002), pp. 86–102.
19. S. Ross, *Introduction to Probability Models* (Elsevier Science, 2006).
20. D. H. Lehmer, *Proceedings of the Second Symposium on Large Scale Digital Computing Machinery* (Harvard University Press, Cambridge, United Kingdom, 1951), pp. 141–146.
21. M. Greenberger, *J. ACM* **8**, 163 (1961).
22. W. H. Payne, J. R. Rabung, T. P. Bogyo, *Commun. ACM* **12**, 85 (1969).
23. S. M. Ross, *Simulation, Fourth Edition* (Academic Press, Inc., Orlando, FL, USA, 2006).
24. N. Metropolis, A. W. Rosenbluth, M. N. Rosenbluth, A. H. Teller, E. Teller, *The Journal of Chemical Physics* **21**, 1087 (1953).
25. W. K. Hastings, *Biometrika* **57**, 97 (1970).
26. S. Asmussen, P. Glynn, *Stochastic Simulation: Algorithms and Analysis*, Stochastic Modelling and Applied Probability (Springer New York, 2007).
27. G. Givens, J. Hoeting, *Computational statistics*, Wiley series in probability and statistics (Wiley-Interscience, 2005).

Investigating graphene oxide permeable reactive barriers for filtering groundwater contaminated from hydraulic fracturing

Étude des barrières réactives perméables à l'oxyde de graphène pour filtrer les eaux souterraines contaminées par la fracturation hydraulique

Zifeng An, Konrad Grala, Aakanx Panchal and Kunjan Trivedi

Abstract

Hydraulic fracturing, or fracking, is a method of natural gas extraction which involves pumping a brine solution into the ground to create a fracture that will allow natural gas to rise. One of the major concerns surrounding this method of natural gas extraction is that wastewater enters the groundwater supply, thereby contaminating it. This wastewater contains toxic materials such as heavy metal ions, radionuclides and other salts and organic compounds in high concentrations. Some of these materials are carcinogenic and thus a concern to human life and the environment. The current solution involves the use of a zerovalent iron (ZVI) permeable reactive barrier (PRB) to filter out these toxic substances. However, it causes more fouling due to the accumulation of mineral precipitates and therefore is not very effective. A recent development in nanotechnology may allow us to develop a superior water filter to prevent groundwater contamination. Therefore, a novel PRB is suggested: featuring the use of solid graphene oxide (GO), a nanomaterial with a superior sorption ability is proposed as a replacement for the system. The proposed experiment will test the filtration capability of the GO-PRB as compared to the traditional ZVI-PRB. By emulating the process of groundwater contamination and flow using common materials found in fracking wastewater, we can determine how much more effective the GO-PRB is than the ZVI-PRB.

Résumé

La fracturation hydraulique est une méthode d'extraction de gaz naturel qui consiste à pomper une solution de saumure dans le sol pour créer une fracture qui permettra au gaz naturel de monter. L'une des principales préoccupations entourant cette méthode d'extraction du gaz naturel est que les eaux usées pénètrent dans l'eau souterraine et la contaminent. Cette eau usée contient des matières toxiques telles que des ions de métaux lourds, des radionucléides et d'autres sels et composés organiques à des concentrations élevées. Certains de ces matériaux sont cancérigènes et donc préoccupants pour la vie humaine et l'environnement. La solution actuelle implique l'utilisation d'une barrière réactive perméable (BRP) en fer zéro valent (FZV) pour filtrer ces substances toxiques. Cependant, elle n'est pas très efficace puisqu'elle provoque plus d'encrassement dû à l'accumulation de précipités minéraux. Un développement récent en nanotechnologie peut nous permettre de développer un filtre à eau supérieur pour empêcher la contamination des eaux souterraines. Par conséquent, une nouvelle BRP est proposée qui utilise l'oxyde de graphène solide (OG), un nanomatériau doté d'une capacité de sorption supérieure est proposé comme remplacement pour le système. L'expérience proposée testera la capacité de filtration de la GO-BRP par rapport à la FZV-BRP traditionnelle. En imitant le processus de contamination et d'écoulement des eaux souterraines à l'aide de matériaux communs trouvés dans les eaux usées de fracturation, nous pouvons déterminer à quel point la GO-BRP est plus efficace que la FZV-BRP.

*McMaster University, Hamilton, Ontario, Canada
Université McMaster, Hamilton, Ontario, Canada

†Lower division / Division inférieure
‡1st place / 1ère place

Novel hybrid biofilm system using synthetically engineered curli fibres

Nouveau système de biofilm hybride utilisant des fibres de curli synthétiques

Harshini Ramesh, Keerthana Pasumarthi, Maggie Hou and Jennifer Lee

Abstract

Hydraulic fracturing, a popular mining technique, generates heavy metal contamination in nearby freshwater aquifers. This poses a threat to both the surrounding ecosystems and human health if exposed. Existing methods of heavy metal removal can produce additional hazardous byproducts. This proposal presents the use of a hybrid biofilm filter containing graphene and curli fibres with metal binding sites. Curli fibres are amyloid fibrils found on the extracellular biofilm of *Escherichia coli (E coli.)*. Through the use of plasmid vectors, *E. coli* will be engineered to produce secreted curli fibres with metal-binding residues. The stability and cohesive properties of the curli fibres augments the adherence to the graphene scaffolding, thus allowing for generation of a hybrid biofilm. With the filtration design and various experimental controls proposed, this model is ready for empirical proof of concept and subsequent quantitative optimization.

Résumé

La fracturation hydraulique, technique d'extraction populaire, génère une contamination par les métaux lourds dans les aquifères d'eau douce situés à proximité. Cela constitue une menace à la fois pour les écosystèmes environnants et pour la santé humaine. Les méthodes actuelles d'élimination des métaux lourds peuvent produire des sous-produits dangereux supplémentaires. Cette proposition présente l'utilisation d'un filtre à biofilm hybride contenant du graphène et des fibres de curli avec des sites de liaisons métalliques. Les fibres de curli sont des fibrilles amyloïdes retrouvées sur le biofilm extracellulaire *d'Escherichia coli (E coli.)*. Grâce à l'utilisation de vecteurs plasmidiques, l'*E. coli* sera manipulé pour produire des fibres de curli sécrétées avec des résidus de liaison aux métaux. La stabilité et les propriétés cohésives des fibres de curli augmentent l'adhérence à l'échafaudage de graphène, permettant ainsi la génération d'un biofilm hybride. Avec la conception de la filtration et les différents contrôles expérimentaux proposés, ce modèle est prêt pour la validation empirique du concept et l'optimisation quantitative subséquente.

*McMaster University, Hamilton, Ontario, Canada
Université McMaster, Hamilton, Ontario, Canada

†Lower division / Division inférieure
‡2nd place / 2ème place

Taking the hydro out of hydrofracturing: Application of ultra-light weight proppants to cryogenic liquid nitrogen as a fracturing fluid

Élimination de l'hydroélectricité par hydrofracturation : application d'agents de soutènement ultra-légers à l'azote liquide cryogénique comme fluide de fracturation

Amna Ahmed, Amna Majeed and Teresa Zhu

Abstract

In the last decade, hydraulic fracturing has rapidly gained popularity worldwide, emerging as the leading method of natural gas extraction in the United States. However, the practice remains controversial due to its contribution to greenhouse gas emissions and the contamination of freshwater used in fracturing fluids. Although waterless fracturing fluids have been developed, including those using N_2, CO_2, oil, and alcohol, their application has been limited largely due to reduced fracturing power. Recent research has demonstrated that cryogenic nitrogen may prove a viable alternative, if this issue is properly addressed. Addition of durable, lightweight proppants is one way to increase fracturing power. This study aims to investigate the effect of proppant addition on the fracturing capabilities of cryogenic nitrogen. Three ultra-lightweight proppants will be combined with liquid nitrogen and fracturing power will be measured using triaxial stress tests. This novel approach has not yet been explored and will open more avenues of research into sustainable and efficient fracturing using cryogenic nitrogen.

Résumé

Au cours de la dernière décennie, la fracturation hydraulique a rapidement gagné en popularité dans le monde entier, devenant la principale méthode d'extraction du gaz naturel aux États-Unis. Cependant, cette pratique reste controversée en raison de sa contribution aux émissions de gaz à effet de serre et à la contamination de l'eau douce utilisée dans les fluides de fracturation. Bien que des fluides de fracturation sans eau aient été mis au point, y compris ceux utilisant du N_2, du CO_2, de l'huile et de l'alcool, leur application a été limitée en grande partie en raison de la réduction du pouvoir de fracturation. Des études récentes ont démontré que l'azote cryogénique peut s'avérer une alternative viable, si cette question est correctement traitée. L'ajout d'agents de soutènement durables et légers est un moyen d'augmenter le pouvoir de fracturation. Cette étude a pour but d'étudier l'effet de l'ajout d'un agent de soutènement sur les capacités de fracturation de l'azote cryogénique. Trois agents de soutènement ultra-légers seront combinés avec de l'azote liquide et le pouvoir de fracturation sera mesuré à l'aide de tests de résistance triaxiaux. Cette approche novatrice n'a pas encore été explorée et ouvrira davantage de pistes de recherche sur la fracturation durable et efficace à l'aide d'azote cryogénique.

*University of Toronto St. George, Toronto, Ontario, Canada
Université de Toronto St. George, Toronto, Ontario, Canada

†Lower division / Division inférieure
‡3rd place / 3ème place

The effects of radium-226 in cattle and predicted impacts of cancer

Les effets du radium-226 sur les bovins et les effets prévus du cancer

Nayha Eijaz, Bhairavei Gnanamanogaran, Paras Kapoor and Saranya Naraentheraraja

Abstract

Hydraulic fracturing is a controversial method of natural gas extraction that has gained its fair share of critics. Although research has been conducted on the environmental impact of fracking, research concerning naturally occurring radioactive materials (NORM) has been scarce. Radionuclides are known to bioaccumulate in the environment and can have toxic effects on humans. This study aims to examine the extent of biomagnification of radium-226 in soil, crops and animals. Fluid samples from areas near fracking sites will be compared with samples from non-fracking sites via gamma spectroscopy.

Homogenized samples of soil and crops will be analyzed by gamma spectroscopy while milk and cattle meat samples will undergo alpha spectroscopy. This will provide a clear image of the process of bioaccumulation and magnification of radionuclides in the environment as a byproduct of fracking.

Résumé

La fracturation hydraulique est une méthode controversée d'extraction de gaz naturel qui a gagné sa juste part de critiques. Bien que des recherches aient été menées sur l'impact environnemental de la fracturation hydraulique, les recherches sur les matières radioactives naturelles (MRN) sont rares. Les radionucléides se bioaccumulent dans l'environnement et peuvent avoir des effets toxiques sur les êtres humains. Cette étude vise à examiner l'ampleur de la bioamplification du radium-226 dans le sol, les cultures et les animaux. Les échantillons de fluides provenant des zones proches des sites de fracturation seront comparés à des échantillons provenant de sites non fracturés par spectroscopie gamma.

Les échantillons homogénéisés de sol et de cultures seront analysés par spectroscopie gamma tandis que les échantillons de viande et de lait des bovins subiront une spectroscopie alpha. Cela fournira une image claire du processus de bioaccumulation et de grossissement des radionucléides dans l'environnement en tant que sous-produit de la fracturation hydraulique.

*University of Toronto Scarborough, Toronto, Ontario, Canada
Université de Toronto Scarborough, Toronto, Ontario, Canada

†Upper division / Division supérieure
‡1st place / 1ère place

Reducing volatile organic compound emissions with a biofilter inoculated with synthetically engineered *Escherichia coli*

Réduire les émissions de composés organiques volatiles avec un biofiltre inoculé avec l'*Escherichia coli* synthétiquement modifié

Mihai Dumbrava, Cindy Kao, Daniel Lee and Inmo Sung

Abstract

Various byproducts of fracking, such as methane gas, benzene, and other Volatile Organic Compounds (VOCs), have become a target for studies on health and environmental damage. These compounds are released during natural gas and petroleum extraction, and from the toxic residual water created from the fracking process. Although the long-term effects of some of these chemicals have yet to be determined, the elevated levels present in neighboring communities have been shown to cause an increase in the prevalence of acute respiratory, neurological, and reproductive diseases. In order to reduce the levels of these harmful airborne pollutants, we propose the creation of a biofilter inoculated with genetically engineered bacteria designed to metabolize VOCs and convert them into safer end products.

Résumé

Divers sous-produits de la fracturation, tels que le méthane, le benzène et d'autres composés organiques volatiles (COV), sont devenus la cible d'études sur les dommages pour la santé et l'environnement. Ces composés sont libérés lors de l'extraction du gaz naturel et du pétrole, ainsi que par l'eau résiduelle toxique créée par le processus de fracturation. Bien que les effets à long terme de certains de ces produits chimiques n'aient pas encore été déterminés, les niveaux élevés présents dans les communautés avoisinantes provoquent une augmentation de la prévalence des maladies respiratoires, neurologiques et de reproduction. Afin de réduire les niveaux de ces polluants atmosphériques nocifs, nous proposons la création d'un biofiltre inoculé avec des bactéries génétiquement modifiées conçues pour métaboliser les COV et les convertir en produits finaux plus sécuritaires.

*University of Western Ontario, London, Ontario, Canada
Université de Western Ontario, London, Ontario, Canada

†Upper division / Division supérieure
‡2nd place / 2ème place

Optimization of reverse osmosis flowback water treatment using halotolerant microbes naturally enriched in fractured shales

Optimisation du traitement de l'eau de reflux par osmose inverse à l'aide de microbes halotolérants naturellement enrichis en schistes fracturés

Mark Cahalan, David Moskal, Cimon Song and Jianhan Wu

Abstract

Flowback water recovered after hydraulic fracturing operations poses a serious environmental concern due to the sheer quantity produced and its toxic chemical composition. Traditional methods of wastewater treatment cannot be used for flowback water treatment due to its high concentration of non-biodegradable dissolved solids. Consequently, alternative technology has been developed to address this problem. Reverse osmosis (RO) treatment is one such example. However, guar gum gelling agents found in flowback water impede membrane permeability and water flux rate of RO, consequently decreasing the efficiency and practicality of this desirable, environment-friendly technology. Previously, a biological solution using activated sludge to degrade guar gum prior to RO treatment was attempted with limited success due to the inhibitory effects of hypersalinity (characterized by high total dissolved solids content) on microbial activity. To solve this problem, several recently discovered strains of bacteria and archaea found to be naturally enriched in fractured shales may be utilized through genetic modification to degrade guar gum under hypersaline conditions. These microbes are naturally halotolerant and thrive under hypersaline conditions, making them prime targets for genetic modification targeting various chemical additives in flowback water. Here, we provide a proof of concept model using these microbes to selectively target guar gum degradation to improve the efficiency of RO treatment.

Résumé

L'eau de reflux récupérée après les opérations de fracturation hydraulique pose un sérieux problème environnemental en raison de la quantité produite et de sa composition chimique toxique. Les méthodes traditionnelles de traitement des eaux usées ne peuvent pas être utilisées pour le traitement de l'eau de reflux en raison de sa forte concentration de solides dissous non biodégradables. Par conséquent, une technologie alternative a été développée pour résoudre ce problème. Le traitement par osmose inverse (OI) en est un exemple. Cependant, les agents gélifiants de guar trouvés dans l'eau de reflux entravent la perméabilité de la membrane et le débit de flux d'eau de l'OI, diminuant par conséquent l'efficacité et l'aspect pratique de cette technologie écologique. Auparavant, une solution biologique utilisant des boues activées pour dégrader la gomme de guar avant le traitement d'OI a été tentée avec un succès limité en raison des effets inhibiteurs de l'hypersalinité (caractérisée par une teneur élevée en solides dissous) sur l'activité microbienne. Pour résoudre ce problème, plusieurs souches de bactéries et d'archées récemment découvertes et naturellement enrichies en schistes fracturés peuvent être utilisées par modification génétique pour dégrader la gomme de guar dans des conditions hypersalines. Ces microbes sont naturellement halotolérants et prospèrent dans des conditions hypersalines, ce qui en fait des cibles privilégiées pour la modification génétique ciblant divers additifs chimiques dans l'eau de reflux. Ici, nous fournissons un modèle de preuve de concept utilisant ces microbes pour cibler sélectivement la dégradation de la gomme de guar pour améliorer l'efficacité du traitement d'OI.

*McMaster University, Hamilton, Ontario, Canada
McMaster University, Hamilton, Ontario, Canada

†Upper division / Division supérieure
‡3rd place / 3ème place

ACKNOWLEDGEMENTS

The University of Ottawa Science Undergraduate Research Journal would like to thank all of its authors and faculty reviewers who have made this issue possible.

In addition, the journal was supported through contributions from our generous sponsors :

- Office of the Vice-President, Research
- Office of Undergraduate Research
- Faculty of Science
- Science Students' Association (SSA - AÉS)
- Kaplan Test Prep

This year also saw the launch of a 4-workshop course entitled "Learn, Write, Publish" taught by four mentors who graciously offered their research experience in teaching students the basics of literature review and ultimately writing in-depth review articles. To Dr. Benjamin W. Lindsey, Dr. Lisa D'Ambrosio, Carl Farah, and Patrick M. D'Aoust, we thank you.

The initiation of OSURJ was a monumental task, requiring expertise from many individuals at uOttawa. We would like to thank Jeanette Anne Hatherill, the scholarly communication librarian, who helped implement the Open Journal Systems submission program and publish this issue electronically. We would also like to thank Teslin Sandstrom, Danny Jomaa, and Laura Forrest of the University of Ottawa Journal of Medicine (UOJM) for their guidance in the setup of the journal.

Lastly, with the successful publication of this issue, we would like to express our gratitude to our faculty advisors, Dr. Kathy-Sarah Focsaneanu, Dr. Tuan Bui, Dr. Michael Jonz, and Dr. John Basso, all of whom provided countless hours of guidance and mentorship.

REMERCIEMENTS

Le Journal étudiant de recherche scientifique de l'Université d'Ottawa (JRSUO) voudrait remercier tou.te.s ses auteur.e.s et réviseur.e.s de la Faculté qui ont rendu cette édition possible. De plus, le journal a été soutenu par les contributions de nos généreux parrains :

- Cabinet du vice-recteur de la recherche
- Bureau de la recherche au premier cycle
- Faculté des sciences
- Association des étudiants en sciences (SSA - AÉS)
- Kaplan Test Prep

Cette année nous avons débuté une série de quatre ateliers, nommée « Apprendre, écrire, publier ». Ils étaient enseignés par quatre mentors qui ont gracieusement offert leur expérience dans la recherche en enseignant aux étudiants les bases de la revue littéraire et pour finir, en les dirigeant vers l'écriture des articles de revues approfondis. Nous remercions mille fois Dr. Benjamin W. Lindsey, Dr. Lisa D'Ambrosio, Carl Farah et Patrick M. D'Aoust.

L'initiation du JRSUO fut un travail monumental, qui a nécessité la compétence de nombreux individus à l'Université d'Ottawa. Nous voudrions remercier Jeanette Anne Hatherill, la bibliothécaire responsable de la communication savante, qui a aidé à mettre en oeuvre le programme de soumission Open Journal Systems, pour la publication électronique de cette édition. Nous voudrions aussi remercier Teslin Sandstrom, Danny Jomaa et Laura Forrest du Journal médical de l'Université d'Ottawa (JMUO) pour leurs conseils dans l'organisation de notre journal.

Dernièrement, en publiant notre édition, nous aimerions exprimer notre gratitude à nos conseillers pédagogiques, Dr. Kathy-Sarah Focsaneanu, Dr. Tuan Bui, Dr. Michael Jonz et Dr. John Basso, qui ont tous fourni d'innombrables conseils de mentorat.